

Materials Advances

Accepted Manuscript

This article can be cited before page numbers have been issued, to do this please use: M. S. Islam, S. Kundu, M. Samsunnahar, T. Khandaker, A. B. M. Ibrahim, M. A. M. Anik, Md. K. Hasan and M. S. Hossain, *Mater. Adv.*, 2025, DOI: 10.1039/D5MA00786K.



This is an Accepted Manuscript, which has been through the Royal Society of Chemistry peer review process and has been accepted for publication.

Accepted Manuscripts are published online shortly after acceptance, before technical editing, formatting and proof reading. Using this free service, authors can make their results available to the community, in citable form, before we publish the edited article. We will replace this Accepted Manuscript with the edited and formatted Advance Article as soon as it is available.

You can find more information about Accepted Manuscripts in the [Information for Authors](#).

Please note that technical editing may introduce minor changes to the text and/or graphics, which may alter content. The journal's standard [Terms & Conditions](#) and the [Ethical guidelines](#) still apply. In no event shall the Royal Society of Chemistry be held responsible for any errors or omissions in this Accepted Manuscript or any consequences arising from the use of any information it contains.

1

2

Carbon Gel Materials: Synthesis, Structural Design, and Emerging
Applications in Energy and Environmental Technologies

3

4

Md Shariful Islam^{1#}, Shreyase Kundu^{1#}, Mst Samsunnahar^{1#}, Tasmina Khandaker², Ahmed B.M. Ibrahim^{3,4}, Md Al Amin Mia Anik¹, Md. Kamrul Hasan¹, Muhammad Sarwar Hossain^{1*}

5

6

¹Chemistry Discipline, Khulna University, Khulna-9208, Bangladesh

7

8

²Department of Chemistry, Khulna Khan Bahadur Ahsanullah University, Khulna-9100, Bangladesh.

9

10

³Department of Chemistry, College of Science, Imam Mohammad Ibn Saud Islamic University (IMSIU), Riyadh 11623, Saudi Arabia.

11

12

⁴Department of Chemistry, Faculty of Science, Assiut University, Assiut 71516, Egypt

13

14

*Correspondence: sarwar@chem.ku.ac.bd

15

16

These authors contributed equally to this work.

17

18

Abstract

19

20

21

22

23

24

25

26

27

28

29

30

31

Carbon-based gel materials have become a flexible class of porous materials with great promise for sustainable material innovations, energy storage, and environmental remediation. The synthesis methods, structural categories, and multipurpose uses of carbon gels, such as aerogels, xerogels, cryogels, and hydrogels, are all well covered in this review. These materials are appropriate for a variety of applications due to their special qualities, which include high surface area, hierarchical porosity, electrical conductivity, and mechanical tunability. Recent developments in green synthesis techniques employing precursors generated from biomass are highlighted, as is the creation of hybrid systems that combine metal oxides, graphene, and carbon nanotubes to improve mechanical strength, conductivity, and catalytic activity. A critical analysis of how different drying and carbonization methods affect pore structure, stability, and performance is conducted. Carbon gels' uses in fuel cells, lithium-ion/sodium-ion batteries, supercapacitors, and water treatment are discussed, with an emphasis on how their structural characteristics affect their adsorption and electrochemical properties. The analysis also examines the increasing interest in hydrogels based on graphene and gels made from biomass as environmentally friendly and sustainable substitutes for energy systems. Despite impressive advancements, problems with mechanical robustness, pore structure management, and cost-effective large-scale production still exist. In order to create next-generation carbon gel materials for worldwide energy and

environmental solutions, future prospects are examined with a focus on combining green chemistry, functionalization methods, and innovative composite designs.

Keywords: Carbon-based gels; Sustainable materials; Hierarchical Porosity; Energy storage application.

1. Introduction

Industrialization and rapid technological advancement have significantly raised human living standards, but they have also made global problems like water scarcity, pollution, and energy shortages worse. These issues are interrelated because water treatment uses a lot of energy and energy production uses a lot of water resources [1]. With over 1.6 billion people without access to clean water and over 1.3 billion without power, the situation is expected to get worse as a result of industrialization, urbanization, and climate change [2]. In addition, conversion inefficiencies result in the loss of over half of the energy generated, and industrial and agricultural water pollution exacerbates environmental and health issues[3]. To address these pressing issues, there is a growing need for integrated, sustainable solutions. Although renewable energy sources like solar, wind, and biomass have potential, the creation of effective energy storage technologies is necessary for them to succeed. Likewise, access to clean water, especially in areas with water scarcity, depends on sophisticated water purification systems. In this regard, materials based on multifunctional carbon have drawn interest due to their excellent conductivity, chemical stability, and adaptability. Applications for materials like graphene, fullerenes, carbon nanotubes, and activated carbon in energy storage, catalysis, and water treatment are being investigated more and more, despite obstacles including high production costs and environmental concerns [4-6]. Because of these drawbacks, scientists are working harder to create more affordable, sustainable, and scalable carbon-based materials. Carbon-based gel materials, such as hydrogels, xerogels, carbon aerogels, and cryogels, have shown great promise [7]. These enormous specific surface areas of gels, three-dimensional porous networks, and adaptability in terms of both chemical and physical properties for a variety of uses are what define them. Carbon gels, particularly carbon aerogels, have received a lot of attention due to their extremely high porosity (often exceeding 90-99%), high electrical conductivity, and lightweight structure. Because of these properties, they are suitable for high-performance applications such as environmental remediation, energy storage devices, sensors, electromagnetic shielding, and catalysis [8].



Sol-gel methods, which involve the polymerization of organic precursors such as resorcinol and formaldehyde or other phenolic chemicals, are commonly used to create carbon gels [9]. A stiff carbon framework is produced by drying and carbonizing the resultant organic gel. The unique benefit of this synthesis method is that it gives precise control over the textural and structural properties of the final product. Variables including the carbonization temperature, solvent type, catalyst content, pH, drying conditions, and precursor concentration can all be changed to alter the distribution of pore sizes, surface area, and electrical conductivity. Aerogels, cryogels, and xerogels are among the several gel morphologies that can be produced by the drying method that is employed, such as ambient drying, freeze-drying, or supercritical drying. Among these, carbon aerogels are notable for their exceptional porosity and low density, which are achieved by preserving the original nanostructure of the wet gel [10]. Historically, Pekala and associates created carbon aerogels by carbonizing organic resorcinol-formaldehyde gels in the late 1980s [11]. Numerous precursor systems and synthesis techniques have since been investigated. The use of sustainable and renewable precursors to make carbon gels, like lignin, cellulose, tannins, and other compounds derived from biomass, has grown in importance in recent years. These biomass-based carbon gels help the broader goals of sustainable material development by offering a sustainable alternative to petroleum-based resins. Additionally, the addition of nanostructured carbon additives like graphene oxide (GO), reduced graphene oxide (rGO), and carbon nanotubes (CNTs) to gel matrices has opened up new possibilities for producing hybrid carbon gels with enhanced mechanical, electrical, and electrochemical properties [12].

Carbon-based gels are increasingly being used as electrodes for fuel cells, lithium-ion batteries (LIBs), sodium-ion batteries, and supercapacitors in the field of energy conversion and storage [13]. Their high surface area and conductive framework allow for rapid electron and ion transport, even though the open pore structure provides ample space for electrolyte access and ion diffusion. Carbon aerogels have shown to be effective electrodes for electric double-layer capacitors due to their remarkable cycle stability and high capacitance. They can also be utilized as catalyst supports in fuel cells and as active materials in hybrid capacitors due to their ability to contain metal oxides or nanoparticles. By removing organic contaminants, heavy metals, and colors from water by adsorption and catalytic degradation, carbon gels have proven effective in environmental applications. Their robustness ensures mechanical and chemical durability under a variety of treatment conditions, and their high surface area and adjustable surface functions enable the



selective collection of contaminants [14]. Carbon gels have also been studied as efficient adsorbents for cleaning up oil spills due to their inherent oleophilicity and hydrophobicity. They are able to absorb hydrocarbons from aqueous solutions in a selective manner as a result.

Materials made of carbon gel are sufficiently adaptable to be used in sensors and analytical instruments. Because of their high conductivity and surface reactivity, carbon gels can be used in electrochemical sensors to detect gases, biomolecules, and pollutants. Their porosity network enables rapid signal transduction and analyte diffusion, increasing sensitivity and response time. Additionally, advancements in carbon gel functionalization have opened the door to their use in biosensors and wearable electronics. Despite its promising characteristics, a number of barriers currently prevent carbon-based gel materials from being widely used. Among the primary obstacles are the need for environmentally friendly and scalable production techniques, the high expense and time commitment of supercritical drying procedures, and the difficulty of precisely controlling pore structure during synthesis. To solve these problems, a multidisciplinary approach involving materials science, chemical engineering, and environmental science is required. Future research should focus on developing sustainable synthesis processes, constructing hybrid systems that integrate carbon gels with other functional materials, and producing bio-based precursors.

The overarching aim of the present work is to provide a comprehensive and critical review of carbon-based gel materials, with particular focus on their synthesis, structural tuning, functionalization, and application potential across diverse fields such as energy storage, catalysis, gas separation, environmental remediation, and biomedicine. Unlike earlier reviews that primarily focused on the general properties or isolated applications of aerogels, xerogels, or hydrogels, this work emphasizes the integrative perspective-linking their fundamental structure-property relationships with practical performance outcomes. Special attention is given to their role in supercapacitive energy storage, where recent advancements in novel electrolyte materials are discussed in parallel with electrode design strategies to underline the interdependent nature of device performance. Furthermore, the review extends its scope to include hybrid and composite systems, particularly those integrating 2D frameworks such as MXenes, COFs, MOFs, HOFs, and Prussian blue analogs, which are increasingly explored for next-generation energy and environmental technologies [15-20]. By consolidating state-of-the-art findings, identifying current limitations, and projecting future research needs, this work aims to serve as both a reference and a



roadmap for researchers and engineers, ultimately guiding the translation of carbon-based gels from laboratory research to scalable, sustainable, and industrially relevant applications. The growing research interest in carbon-based gel materials is evident from the increasing number of publications over the past decade. As shown in **Figure 1**, studies in this field have risen steadily from fewer than 15 articles in 2015 to nearly 70 in 2024, highlighting their expanding role in energy and environmental applications. This sharp upward trend underscores the timeliness and relevance of the present review.

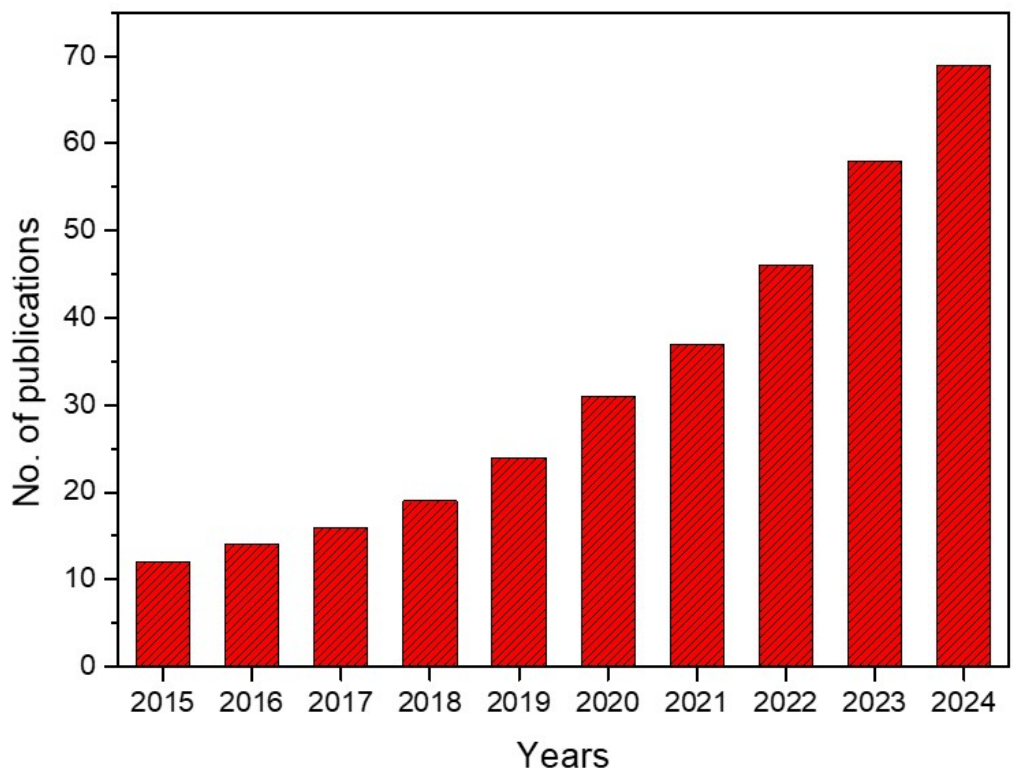


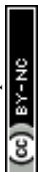
Figure 1. Publication trend (2015–2024) in the field of carbon-based gel materials. Data retrieved from Google Scholar (search keywords: “Carbon based gel”; accessed 15 August).

2. Classification of Carbon-based gels

Carbon gels are porous materials typically synthesized through sol-gel polymerization of organic monomers (e.g., resorcinol-formaldehyde) or renewable biomass precursors, followed by drying and carbonization. Their classification is largely determined by the drying method and resulting structural characteristics. Carbon aerogels, produced via supercritical or freeze-drying, retain an open, highly porous network that supports rapid mass and charge transfer-ideal for high-

performance electrochemical devices. Xerogels, obtained by ambient drying, often suffer pore collapse from capillary forces, lowering surface area and porosity, but remain useful in applications where ultra-low density is unnecessary. Cryogels, generated by freeze-drying aqueous gels, possess interconnected macropores that promote fluid transport and thermal insulation [21]. The catalyst ratio (resorcinol-to-catalyst, R/C) governs gelation kinetics and network density: higher ratios accelerate crosslinking, yielding denser microporous frameworks that boost electric double-layer capacitance but restrict large-molecule diffusion; lower ratios slow gelation, producing larger meso/macropores that enhance adsorption of bulky species yet reduce volumetric capacitance. Biomass type also shapes pore architecture. Cellulose-rich feedstocks favor mesoporosity for fast ion transport in supercapacitors, whereas lignin-rich sources promote microporosity for gas storage and selective adsorption. Biomass with inherent minerals can serve as in-situ templates, modifying pore geometry without external additives. Drying technique critically influences structural preservation. Freeze-drying maintains mesoporosity by avoiding capillary collapse; supercritical CO₂ drying produces interconnected micro-mesoporous networks with exceptionally high surface area; ambient drying, while cost-effective, risks shrinkage and reduced conductivity. These structure-property links are central to optimizing carbon gels for targeted adsorption and electrochemical applications.

A hallmark of carbon gels is their hierarchical porosity, combining micropores (<2 nm), mesopores (2–50 nm), and macropores (>50 nm), enabling efficient adsorption and ion diffusion. These features, however, are highly sensitive to synthesis parameters. This multiscale porosity enhances the efficiency of carbon gels in adsorption-based applications such as gas storage and water purification by encouraging the transit of molecules into the material's interior. Additionally, by promoting efficient charge storage and quick ion transit, hierarchical porosity raises power and energy densities in electrochemical devices like batteries and supercapacitors [22]. Another significant characteristic of carbon gels is their modifiable surface chemistry. Functional groups like hydroxyl, carboxyl, and carbonyl groups are added during synthesis or post-synthetic modification to increase adsorption selectivity. Specific interactions with target molecules are made possible by these groups. Furthermore, doping carbon gels with heteroatoms such as phosphorus, nitrogen, sulfur, or boron can significantly enhance their electrical structure, conductivity, and catalytic activity. For instance, because nitrogen-doped carbon gels enhance



electron mobility and generate new active sites, they have shown remarkable performance in supercapacitors and oxygen reduction processes (ORR) [23]. Carbon-based gels can be broadly classified into three types: aerogels, xerogels, and cryogels, depending on the drying technique employed. Figure 2 shows the distinct surface area and porosity characteristics of each variation, which influence their applications in energy storage, environmental remediation, and catalysis.

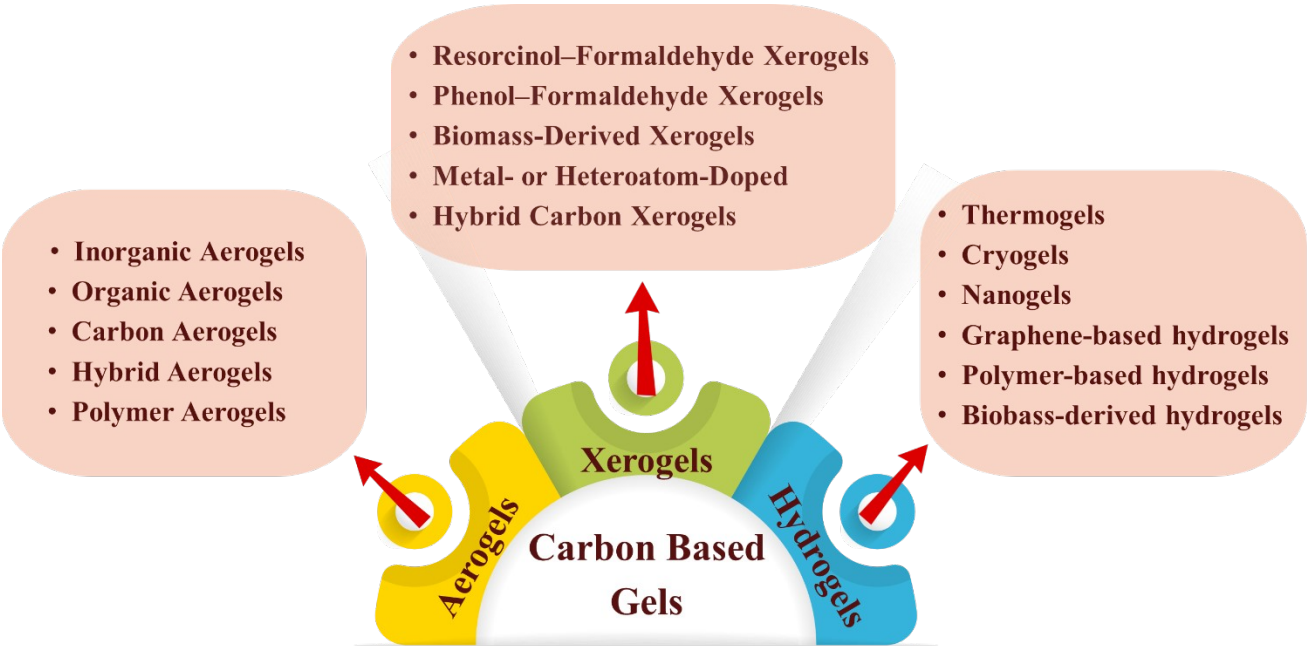


Figure 2. Classification of carbon-based gel materials based on structure and composition

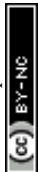
2.1. Aerogel

Aerogels are extremely porous materials created by substituting a gaseous phase for the water portion of hydrogels or comparable wet gels while maintaining their fine, linked microstructures [24]. This process results in an ultralight structure where 90% to 99% of the volume is air, giving aerogels their remarkably low densities, ranging from 1000 kg/m³ down to as little as 1 kg/m³, in some cases even lesser than the density of air [25]. These structural characteristics lead to unique physical properties such as ultralow thermal conductivity, low sound velocity, and a minimal dielectric constant, along with high specific surface areas and tunable density and refractive index [26, 27]. These characteristics make aerogels appropriate for a wide range of uses, including as thermal insulators, chemical sensors, catalytic supports, and even space technology components. Aerogels are also well-known for having nanometer-sized pores, high porosity, and superior light

transmittance, which makes them perfect for usage in transparent materials and sound insulation. The two primary processes in the traditional synthesis of aerogels are the gelation stage, in which a solvent penetrates the gel network, and the drying stage, in which the solvent is eliminated without causing the structure to collapse. Recent developments concentrate on producing more robust aerogels using affordable techniques like freeze-drying, despite the fact that early techniques relied on supercritical drying, which uses a lot of energy and produces aerogels with low mechanical strength. These newer aerogels are developed using materials such as carbon nanofibers [28], graphene, nanocellulose [29], and epoxy-clay [30]. Aerogels can be broadly categorized into four principal types based on their chemical composition: inorganic aerogels (such as silica and alumina), organic aerogels, carbon-based aerogels, and hybrid aerogels [31]. Their combination of low density ($0.004 - 0.500 \text{ g/cm}^3$), large pore volumes, and high surface areas makes them promising materials in supercapacitors [32, 33], stretchable electronics [34], lithium-ion batteries [35], and artificial muscles [36]. Although their internal structure rather than particular chemical components defines aerogels, they can be created from a variety of precursor materials, such as organic, mineral, and composite sources [37]. The structure and density of aerogels are influenced by the precursor's molecular weight, molecular structure, and concentration. Low precursor concentrations often yield fragile networks prone to volumetric shrinkage during solvent exchange or supercritical drying, whereas higher concentrations produce denser, more interconnected frameworks, altering porosity and surface area [38]. $\text{H}_2\text{O}/\text{Na}_2\text{SiO}_3$ molar ratios from 83.3 to 333.3, finding that lower silicate concentrations prolonged gelation (1 min to 6 h) due to reduced particle collision frequency. Increasing the ratio to 166.6 enlarged colloidal particles, increasing pore size and reducing shrinkage, though excessive dilution again raised bulk density from network collapse.

2.1.1 Inorganic Aerogels

Silica gels represent the first class of mineral gels to be synthesized via acid-catalyzed processes. Increasing the concentration of acid catalysts accelerates hydrolysis and condensation reactions during gel synthesis, producing smaller pores and a more compact network structure. Such modifications in pore architecture can significantly alter the aerogel's adsorption characteristics and impact its electrochemical behavior. Catalysts are commonly used to control the hydrolysis and condensation reaction rate, which leads to different microstructures. During the preparation of inorganic aerogels, the hydrolysis reaction kinetics can be accelerated by adding an acid or a base



226 catalyst, and the condensation reaction kinetics can be accelerated by adding a base catalyst [39].
227 Indeed, the ultimate structure of hydrolyzed silica is influenced by the pH level of the solution.
228 Silica particles rearrange into a linear chain structure with limited crosslinking when the pH is low.
229 This gives rise to a highly porous and weak gel structure and may result in redispersion in the
230 solution. At higher pHs, crosslinking between the chains increases, and the network becomes more
231 branched, which leads to a higher density and stronger gel structure. Although naturally occurring
232 organic gels are now more commonly found, the sol-gel technique enables the transformation of
233 almost any metal or semiconductor oxide into a gel. The most researched mineral aerogels are
234 silica-based ones, which are followed by titanium, zirconium, tin, aluminum, vanadium,
235 chromium, iron, tantalum, molybdenum, and niobium-based ones. Furthermore, binary or ternary
236 oxide aerogels can be created. However, these kinds of aerogels are typically quite delicate because
237 of their ceramic composition [40]. The goal of ongoing research is to improve the mechanical
238 stability, especially by creating composites of these materials. Recent research emphasizes
239 significant progress in carbon nanostructure-silica aerogel composites and their incorporation as
240 three-dimensional nanoporous fillers within polymer-based nanocomposites.

241 2.1.2 Organic Aerogels

242 Organic aerogels are synthesized from organic raw materials that form robust polymeric networks
243 through covalent carbon-carbon (C–C) bonds. Among the most widely used organic systems for
244 producing these aerogels are resorcinol-formaldehyde and melamine-formaldehyde compounds.
245 These organic compounds are usually condensed in an alkaline aqueous environment as part of the
246 synthesis process. Sodium hydrogen carbonate serves as a catalyst to speed up the reaction,
247 whereas sodium hydroxide is frequently used as the basic media [41]. The melamine-formaldehyde
248 reaction route is depicted in Figure 3 and affects the final aerogel's density. The synthesis of
249 aerogel is not directly related to all of the other investigations, even if they all add to our
250 understanding of material chemistry and applications[42, 43].

251



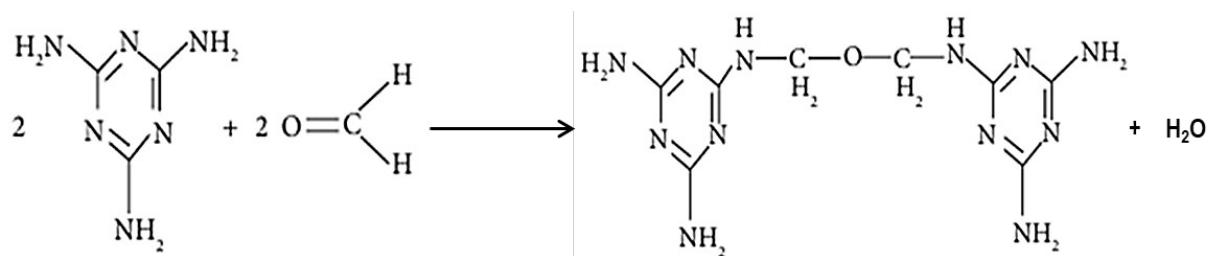


Figure 3. Melamine-formaldehyde aerogels synthesized via a polycondensation reaction, enabling tunable density. Reproduced from reference [44] with permission from Elsevier, copyright 2017.

2.1.3 Carbon Aerogels

A gas phase usually fills the interior spaces of carbon aerogels, which are made of nanostructured porous carbon. The pyrolysis of organic aerogels at temperatures higher than 500°C is a commonly used synthesis technique. The organic aerogel is converted into a conductive carbon aerogel by this high-temperature process, but its surface area and pore structure are preserved [45]. Carbon aerogels, owing to their distinctive properties of high porosity, thermal and structural stability, and intrinsic electrical conductivity, are well-suited for diverse applications such as catalyst supports, adsorption of oils and organic solvents, and energy storage devices [46]. Notably, carbon aerogels are among the lightest materials available, exhibiting densities as low as 0.16 mg cm⁻³ [47]. Because carbon aerogels are porous and lightweight, they may also be made to be electrically conductive, which makes them perfect for use in electrical and electrochemical devices including supercapacitors, batteries, and conductive catalyst supports. Carbonizing organic gels in a non-oxidizing environment, like nitrogen or argon, is the conventional method for creating these materials. Precursors generated from biomass, such as proteins, sugars, or polysaccharides, are used in more contemporary techniques under aqueous gelation and self-assembly conditions. The ultralow density and remarkable conductivity of emerging carbon aerogels based on cutting-edge materials like graphene or CNTs further expand the possible uses of aerogel technologies.

2.1.4 Hybrid Aerogels

By combining both organic and inorganic (mineral) components, hybrid aerogels significantly expand the functional range of conventional aerogels. By adding organic materials to the silica surface, hybrid aerogels boost their hydrophobicity, which improves their resistance to water absorption. Additionally, the elasticity of the material is increased by the addition of organic



components, making it more flexible and resistant to mechanical stress. Hybrid aerogels are frequently created via the sol-gel technique, which turns a precursor gel into a solid network. This technique gives precise control over the properties of the material, including pore architecture and surface modifications. Hybrid aerogels are more useful for applications needing a balance between strength and flexibility since they are less brittle than traditional inorganic aerogels. Because of these properties, hybrid aerogels can be used in a number of applications, including sensors, insulation, and better composites [48].

2.1.5 Polymer Aerogels

Due to their higher mechanical durability and environmental stability compared to silica aerogels, polymer aerogels are beneficial for a wide range of applications, particularly in demanding settings like aerospace. Polymer aerogels are robust and stable even under more demanding conditions than silica aerogels, which are brittle and hygroscopic. The thermal conductivities and low volumetric shrinkage of these organic aerogels during processing are comparable to those of silica aerogels with comparable densities (about $14 \text{ mWm}^{-1}\text{K}^{-1}$ for aerogels with a density of 0.1 gcm^{-3}). Their mechanical properties are far better than those of silica aerogels, with compressive moduli ranging from 1 to 5 MPa [49].

Polymer-based aerogels come in a wide range of materials, including cellulose, resin, polyimide, and PVA. The structural and functional properties of these aerogels are greatly influenced by the kind of polymer utilized and the specific manufacturing conditions. Their structures include assemblies of colloidal nanoparticles, networks of nanofibrils or microfibrils, and even frameworks that resemble sheets. Furthermore, significant structural characteristics like pore size, morphology, and degree of ordering have a big impact on these materials' bulk performance. The structural diversity polymer aerogels allow them to be tailored for specific applications, improving their performance and versatility.

2.2 Xerogels

2.2.1 Resorcinol-Formaldehyde (RF) Carbon Xerogels

One of the most studied carbons xerogels is resorcinol-formaldehyde (RF) carbon xerogels, which are created when resorcinol and formaldehyde polycondensate in an alcoholic or aqueous media. They are attractive due to their large surface area, structural tunability, and simplicity of synthesis. Less branched structures are obtained at low pH values, which results in larger polymer particles.



On the other hand, at higher pH values, highly crosslinked and branched structures are obtained, which causes a more interconnected network with smaller polymer particles. Moreover, as a consequence of smaller particles and interconnected networks, the specific surface area of the aerogel increases. The carbon xerogel is created by pyrolyzing and drying the gel at temperatures ranging from 700 to 1000 °C in an inert environment, usually N₂ or Ar. Usually, the polymerization is catalyzed by a basic, such sodium carbonate. One of the characteristics that sets RF-based carbon xerogels apart is their changeable porosity. The microstructure can be modified by adjusting the resorcinol-to-catalyst (R/C) ratio, solvent content, pH, and aging time.

Higher R/C ratios provide finer, microporous networks, whereas lower ratios usually result in greater pore sizes and lower surface areas. Surface areas that are frequently cited vary from 400 to over 1000 m²/g. They typically have disorganized graphitic domains and amorphous carbon. Catalysis, supercapacitors, and adsorption (especially for CO₂ and metal ions) are just a few of the many uses for RF-derived xerogels. They are suitable for electrochemical devices due to their conductivity and stability at high temperatures, and they are ideal for aqueous-phase adsorption due to their hydrophilic nature and tunable pore network. One major advantage is that they can be further altered. RF xerogels can be doped with metals, nitrogen, or sulfur during or after production to alter their electrical and chemical properties, enhancing performance in specific applications such oxygen reduction reactions or energy storage devices [50, 51].

2.2.2 Phenol-Formaldehyde (PF) Carbon Xerogels

Although they employ phenol rather than resorcinol, phenol-formaldehyde (PF) based xerogels are structurally and synthetically comparable to RF xerogels. PF xerogels are appealing for large-scale applications because phenol is more affordable and accessible than resorcinol, despite being marginally less reactive. After condensation reactions catalyzed by bases or acids, PF xerogels undergo aging, drying, and pyrolysis. Depending on the synthesis conditions, the resultant carbon xerogels exhibit a varied pore network that ranges from microporous to mesoporous, as well as good thermal and chemical stability. PF xerogels have the advantage of having a more hydrophobic surface, which makes them ideal for applications like gas adsorption and organic contamination remediation that require less water affinity as well as for eliminating non-polar contaminants. Similar to RF xerogels, PF xerogels have disordered carbon domains and are physically



amorphous; but, because of variations in crosslinking density and polymerization kinetics, they may exhibit somewhat smaller surface areas (usually 300 – 800 m²/g) [52, 53].

The characteristics of PF xerogels can be greatly improved by activation or doping modifications. Chemical activation with substances like KOH or H₃PO₄ can increase surface area and produce ultra-micropores, which are beneficial for supercapacitor or hydrogen storage applications. Because of their adjustable electrical characteristics, PF xerogels have also been used in sensors and photocatalysis (when hybridized with metal oxides) [54]. Environmental effect is one important way that RF and PF xerogels differ from one another. Because it is more harmful, phenol requires safer handling and consideration of the environment. However, advances in green chemistry approaches are addressing these limitations by using bio-derived phenolic compounds.

2.2.3 Biomass-Derived Carbon Xerogels

The term biomass refers to a diverse range of materials originating from plants, animals, and marine organisms, all of which hold considerable promise as renewable and cost-effective carbon precursors. Plant-derived biomass primarily consists of carbohydrate polymers such as cellulose, hemicellulose, and lignin, whereas animal-derived biomass predominantly contains proteins and lipids [55, 56]. Carbon fibers and lignin-derived materials, sourced from abundant biomass, present significant potential for the sustainable fabrication of high-performance redox flow battery (RFB) electrodes. Advancing carbon materials for RFBs is essential, as they offer high electrical conductivity, excellent chemical stability, and cost-effectiveness. RFBs represent a relatively emerging large-scale energy storage technology, well-suited for addressing the variability and intermittency inherent to renewable energy generation sources such as wind and solar power [57]. Similarly, lignocellulosic biomass (LCB), composed primarily of cellulose, hemicellulose, and lignin, is considered particularly advantageous owing to its favorable structural and biochemical characteristics [58]. Because of their low cost, environmentally benign synthesis methods, and renewable nature, biomass-derived carbon xerogels are also receiving a lot of interest. Carbon-rich polymers like cellulose, lignin, chitosan, starch, and alginates- which include intrinsic functions like -OH, -NH₂, or -COOH that can be maintained or altered in the final carbon material- are commonly used to create these xerogels. Sol-gel polymerization, ambient or freeze-drying, and carbonization under inert circumstances are all part of the basic procedure. The green synthesis of biomass-derived xerogels and the possibility of customizing surface chemistry through precursor



selection are what make them appealing [59]. For example, chitosan-based xerogels are perfect for CO₂ collection and electrocatalysis since they naturally have nitrogen functionalities. Similarly, because of their aromatic component, lignin-derived xerogels can help with mesoporosity and high carbon yields.

The pore architectures of these xerogels vary, ranging from microporous to hierarchical porous networks, contingent on the post-treatment procedures and the gelling behavior of the biopolymer. Porosity can be further enhanced by additional activation stages, and their surface areas can vary from 200 to 800 m²/g. The main benefit is the sustainability and abundance of biomass, which complement waste valorization and the circular economy. Heavy metal adsorption, gas separation, supercapacitor electrodes, and electrocatalysis are some of the uses [60]. Additionally, certain studies emphasize its application in biosensing and medication delivery, especially when the final xerogel retains the biopolymer structure.

2.2.4 Metal or Heteroatom-Doped Carbon Xerogels

Doping carbon xerogels with metals (like Fe, Ni, and Co) or heteroatoms (like N, S, P, and B) greatly improves their physicochemical characteristics, making them suitable for use in energy conversion, environmental remediation, and catalysis. Doping can be accomplished via post-synthetic modification techniques such as pyrolysis or impregnation with dopant precursors, or it can be accomplished during the sol-gel synthesis. Because of their improved surface basicity, electrical conductivity, and active sites, heteroatom-doped xerogels- especially N-doped varieties- are widely used [61]. In the graphitic structure, nitrogen atoms can take the place of carbon atoms to generate graphitic, pyridinic, or pyrrolic nitrogen functionalities that enhance electrocatalytic activity, particularly in the ORR. Likewise, sulfur doping increases chemical reactivity and adds electron-donating characteristics. Doping with phosphorus and boron can alter the electron density and enhance energy storage performance. Because of the creation of active redox centers, metal-doped xerogels- such as those containing Fe, Ni, and Co- perform very well in Fenton-like catalysis, battery anodes, and supercapacitors [62].

The structure and porosity of the xerogels can also be influenced by the dopants; metal catalysts can occasionally encourage graphitization at lower carbonization temperatures. The surface areas of xerogels, which normally range from 400 to 1200 m²/g, vary greatly based on doping concentrations and activation techniques. Li-ion batteries, fuel cells, supercapacitors,



electrocatalysis, and pollutant degradation are a few examples of applications [63]. Doped xerogels are very appealing for cutting-edge technologies because of the multifunctionality made possible by the synergy between dopants and carbon frameworks.

2.2.5 Hybrid Carbon Xerogels

Composites known as hybrid carbon xerogels mix organic carbon matrices with inorganic or other nanomaterials to improve structural, electrical, or catalytic capabilities in a complementary way. Carbon-metal oxide, carbon-silica, carbon-graphene, and carbon-polymer composites are examples of common hybrid systems. Prior to drying and pyrolysis, they are usually created by co-gelling or in-situ incorporating secondary phases into a matrix obtained from biomass or resorcinol-formaldehyde. Metal oxides (such as TiO_2 , ZnO , and FeO_4) can be added to improve electrical conductivity, magnetic responsiveness, or photocatalytic activity. For instance, TiO_2 -carbon xerogel hybrids, which take advantage of both the surface area and the optical activity of xerogel of TiO_2 , are efficient in the photodegradation of dyes and contaminants. Silica-carbon composites are utilized for adsorption and separation and retain their structural integrity in challenging environments. In contrast, hybrids based on graphene or CNTs provide better electron transport and greater mechanical strength, which are advantageous for energy storage and sensing applications [63, 64].

High surface areas (500–1500 m^2/g) are usually retained by hybrid xerogels, which also show enhanced stability, hierarchical porosity, and multifunctionality. Depending on the embedding phase, the design flexibility enables customization of adsorption capacity, electrochemical activity, and thermal conductivity. Hybrid xerogels are used in gas storage and separation, magnetic separation, photo- and electro-catalysis, and electrochemical capacitors. Their adaptability results from the special blend of qualities that the organic-inorganic architecture bestows.

2.3 Hydrogels

Hydrogels are three-dimensional networks made of polymers that are linked together by physical or chemical bonds, allowing them to hold a lot of water inside. Owing to their distinctive physicochemical properties, hydrogels have found broad applicability across a wide range of fields [65], drug carriers [66], electrode materials [67], actuators [68], sensors [69], and adsorbents [70].



Hydrogels can be categorized based on a number of factors, such as their network structure (affine or phantom models), cross-linking type (covalent or non-covalent interactions), and provenance (natural or synthetic) [71]. The mechanical strength and stability of conventional hydrogels, which are often cross-linked using organic polymers, are frequently restricted, which limits their usefulness. But new developments have made it possible to create sophisticated hydrogels and hybrid systems with far better qualities. These next-generation hydrogels improve mechanical, electrical, and functional performance by including cutting-edge elements like carbon nanotubes, graphene, biomass-derived components, or functional nanoparticles [33], graphene-poly(N,N-dimethylacrylamide) composite hydrogels [65], graphene hydrogels, and polymer-clay nanosheet composite hydrogels. Carbonaceous nanofiber-based multifunctional hydrogels, for instance, exhibit increased functionality and better mechanical robustness. Because hybrid hydrogel structures exhibit noticeably improved mechanical qualities, their potential for a wide range of applications is increased. Hydrogels, also known as aqua gels, are networks of three-dimensional polymers that are insoluble in water but have a great capacity to absorb water, giving them a flexibility similar to that of natural tissues [72]. These materials have several uses in industries including medication delivery systems, wastewater treatment, and scaffolds for tissue engineering. They can be made from natural or synthetic polymers. Hydrogels are ideal for a variety of biological and environmental applications due to their remarkable ability to absorb large volumes of water.

2.3.1 Thermogels

A unique type of hydrogels known as thermogels behaves in a temperature-responsive manner, going through a Sol-gel transition at a particular temperature. Thermogels change between sol and gel phases in reaction to temperature changes, unlike non-thermoresponsive hydrogels, where gelation is mostly reliant on polymer concentration. This characteristic results from the polymer architecture's inclusion of both hydrophilic and hydrophobic regions, which have a significant impact on the gelation process. The kinetics of the sol-gel transition are strongly influenced by the temperature and molecular weight of these segments. As a result, the transition is controlled by both the inherent molecular properties of the polymer components and external heat stimuli. The capacity of temperature-sensitive hydrogels to form gels in situ at physiological temperatures has generated a lot of interest in biomedical applications, especially in controlled drug delivery



Open Access Article. Published on 21 August 2025. Downloaded on 9/5/2025 7:05:43 PM.
This article is licensed under a Creative Commons Attribution-NonCommercial 3.0 Unported Licence.

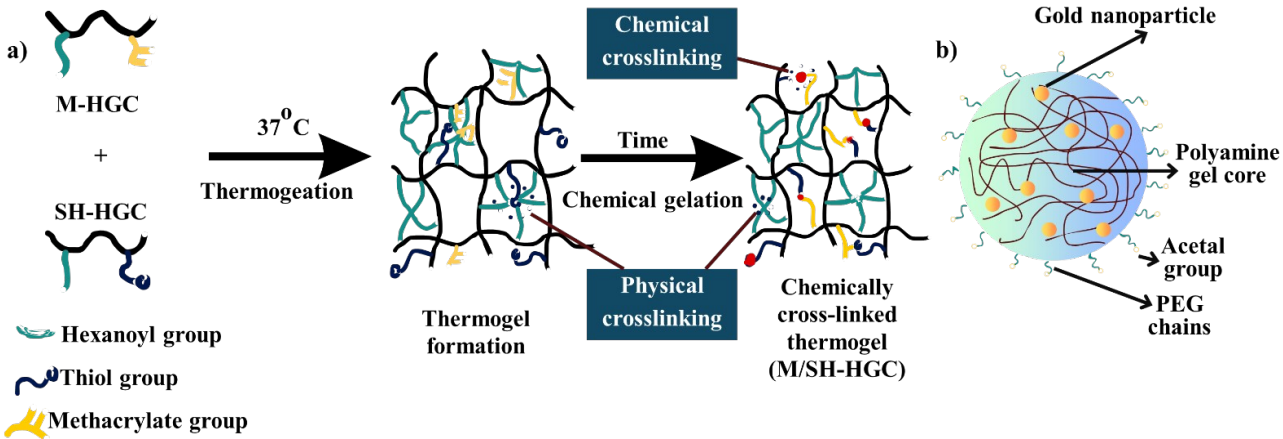


Figure 4. a) Illustration of the thermogel formation and cross-linking mechanism. (b) Diagram of a PEGylated nanogel encapsulating gold nanoparticles. Reproduced from reference [75] with permission from Elsevier, copyright 2023.

2.3.2 Nanogels

Using networks of cross-linked polymers, nanogels are three-dimensional hydrogel structures that can expand and hold large volumes of water without disintegrating in the surrounding aquatic environment. Because they can be made from natural or synthetic polymers, or their combinations, they provide a great deal of flexibility in customizing their characteristics for particular uses. Nanogels can have a range of characteristics, including varied softness, size, amphiphilicity, charge, degradability, and porosity, by modifying their chemical makeup. This enables the behavior of the gels to be fine-tuned in various settings. Although most nanogels are spherical, new synthetic techniques have made it possible to create nanogels in a variety of different shapes, increasing their usefulness for a range of applications. These innovations are evident in the work by Rolland et al., who demonstrated the fabrication of shape-specific nanobiomaterials [76], and Tagliazucchi et al., who explored how the aspect ratio and deformability of nanoparticles influence

their ability to extravasate through nanoscopic pores [77]. An example of a PEGylated nanogel incorporating gold nanoparticles is depicted in Figure 4 (b) [78].

2.3.3 Cryogels

The main components of conventional hydrogels are networks of hydrophilic polymers that have swelled with water; nevertheless, these materials frequently lack crucial characteristics like linked macroporosity and enough elasticity, which are necessary for particular biomedical applications. Cryogels, a special kind of hydrogel, have been created to get around these restrictions. Cryogels are created by a freeze-thaw process at extremely low temperatures, which results in the creation of intricately linked supermacroporous structures. Due to its ability to promote cell proliferation and provide effective nutrition and waste exchange, this unique architecture offers substantial advantages, especially in tissue engineering scaffolds. Cryogels are successfully used in wound healing, cell immobilization, purification systems, controlled drug delivery, biosensors, and bioseparation technologies in addition to tissue engineering. Figure 5 represents the formation mechanism of cryogel. The production of cryogels involves freezing the liquid within the wet gel and then drying it by sublimation under low pressure, a process that produces materials with high porosity, typically around 80%. Compared to aerogels, cryogels have a more macroporous structure and experience greater shrinkage. While aerogels dried using supercritical CO₂ show a more uniform structure with higher surface areas (as measured by BET), cryogels generally exhibit narrower pore size distributions, smaller BET values, and less shrinkage when compared to those produced by hot or vacuum drying techniques [79].



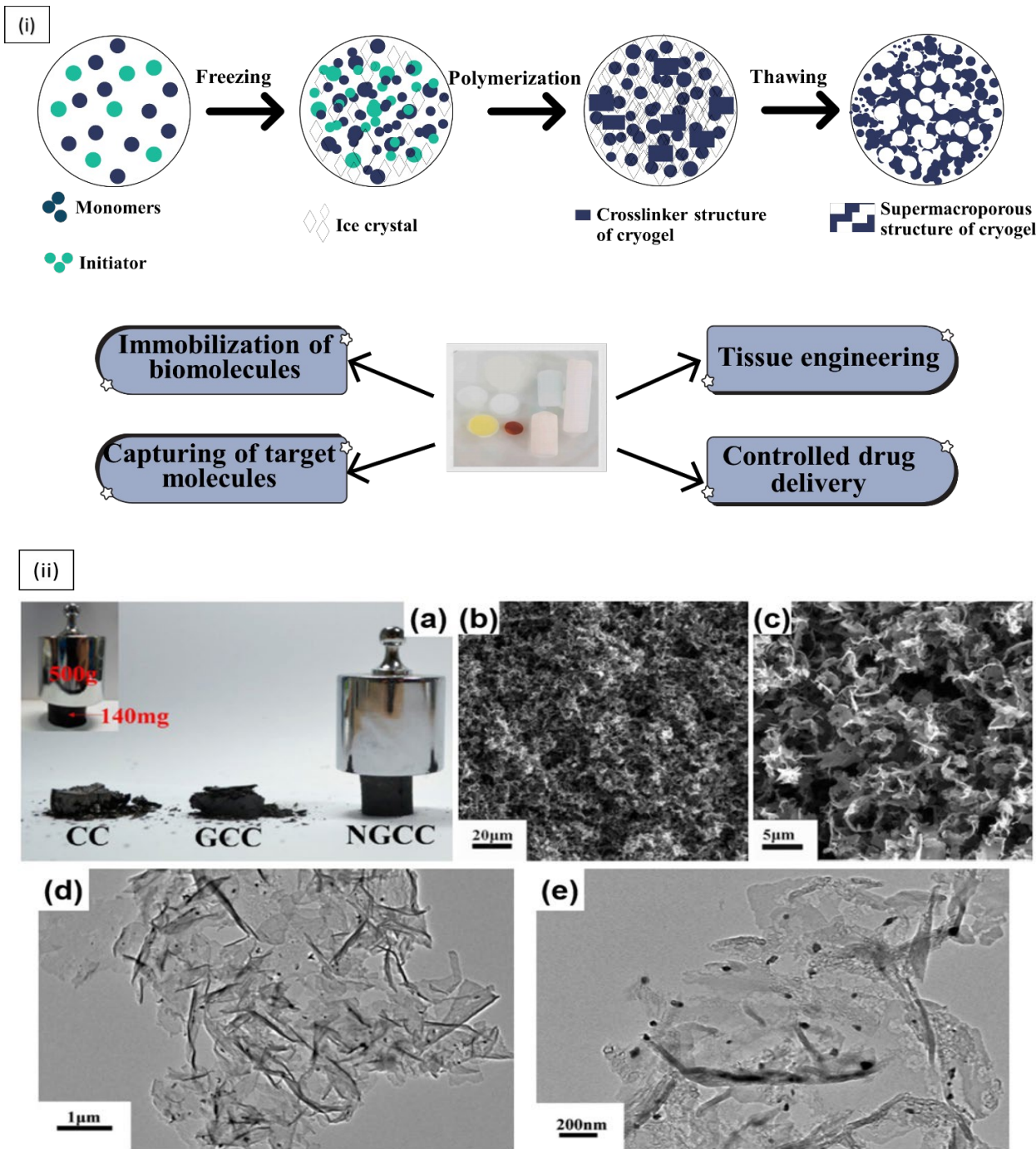


Figure 5. (i) Schematic of the cryogel formation process. (ii) (a) Photographs of carbon cryogel (CC), graphene/carbon cryogel (GCC), and Ni-doped graphene/carbon cryogel (NGCC), each weighing 90 mg, supporting a 200 g load. (Inset: A 140 mg NGCC monolith supporting a 500 g weight.) (b, c) SEM images and (d, e) TEM images of the Ni-doped graphene/carbon cryogel are also shown. Reproduced from reference [75, 80] with permission from Elsevier & ACS, copyright 2023 & 2013.

2.3.4 Graphene-Based Hydrogels

Graphene and its derivatives exhibit exceptional flexibility, electrical conductivity, and mechanical strength, making them highly suitable for diverse technological applications. Their outstanding chemical adsorption capacity, thermal stability, and superior electrical properties further enhance their utility. In the field of energy storage, engineers and researchers are particularly interested in graphene-based supercapacitors due to their remarkable durability, high power density, and ability to endure numerous charge-discharge cycles. The combination of high electrical conductivity of graphene, extensive specific surface area, thermal stability, and excellent mechanical and chemical resilience significantly improves the performance and reliability of supercapacitors [81, 82]. Moreover, graphene is a cutting-edge nanomaterial with a distinct two-dimensional layered structure, endowing it with exceptional mechanical, electrical, and thermal properties. These characteristics make it an ideal filler for enhancing the performance of polymer-based nanocomposites [83]. Given its remarkable properties, graphene has been extensively studied for its potential to enhance the performance of various materials, particularly in the development of nanocomposites. In contrast, hydrogels are polymeric networks characterized by moderate cross-linking and branching, forming three-dimensional structures capable of absorbing substantial amounts of water. These materials swell rapidly and exhibit soft, elastic, and biologically compatible properties [84]. When graphene is incorporated into hydrogels, it plays a dual role: acting as a gelator to help self-assemble the hydrogel structure, and as a filler to enhance the functionality of the hydrogel by blending with small molecules and macromolecules. These graphene-based hydrogels (GBHs) are designed to have multifunctional properties, which have been extensively studied for various applications.

Typically, two-dimensional materials such as graphene and graphene oxide are functionalized with hydroxyl, carboxyl, and epoxide moieties to create graphene-based hydrogels. These functional groups facilitate the incorporation of additional materials, such as metals, metal oxides, or heteroatoms (e.g., oxygen, nitrogen, and boron), through electrostatic interactions and hydrogen bonding [85]. The hierarchical three-dimensional structure of graphene hydrogels offers superior mechanical, electrical, and thermal properties compared to their 2-D forms, with better porosity and the ability to prevent agglomeration- a common challenge in utilizing two-dimensional graphene sheets [86]. The stability of the three-dimensional structure of these hydrogels is



maintained by various forces, including π - π stacking interactions, van der Waals forces, and hydrogen bonding, which prevent agglomeration, enhancing the overall performance of the material [87].

The synthesis of graphene-based hydrogels is predominantly classified into three main approaches: hydrothermal and solvothermal reactions, gel formation via cross-linking polymers, and template-based synthesis methods [88, 89]. Additionally, graphene hydrogels can be functionalized with noble metals to further enhance their properties, expanding their potential for use in diverse applications [90].

2.3.5 Polymer-based hydrogels

Polymers are macromolecules consisting of repeating subunits, playing a crucial role in numerous aspects of human life due to their versatility and wide range of applications. Among the various types of hydrogels, water-swollen polymer networks stand out due to their unique properties [91, 92]. These hydrogels can be synthesized from both synthetic and natural polymers and can be further enhanced by incorporating various functional materials into the polymer backbone, thereby imparting additional properties. Hydrogels can be classified based on their composition and the functionalities introduced within the polymer network. These classifications include non-conducting polymer hydrogels, which are primarily valued for their ability to absorb and retain large volumes of water; conducting polymer hydrogels, which incorporate conductive polymers for applications in bioelectronics and sensors; quantum-dot incorporated polymer hydrogels, offering distinctive optical properties suitable for imaging and diagnostics; and nanoparticle-polymer hydrogels, which combine the unique benefits of nanoparticles and polymers to create versatile materials with enhanced properties for applications in drug delivery, tissue engineering, and more [92].

2.3.6. Biomass-derived hydrogels

The use of biomass as a sustainable raw material for the development of advanced materials has garnered significant attention in scientific research. Numerous studies have highlighted the effectiveness of biomass in hydrogel synthesis. A notable example is provided by Wu et al., who synthesized spongy hydrogels from watermelon biomass composed of carbon nanospheres and



nanofibers. Watermelon biomass, especially the rind, can be converted into activated carbon with a well-developed porous architecture, which plays a crucial role in its adsorption and electrochemical characteristics. The pore size and distribution, governed by processing techniques such as alkali activation or plasma treatment, critically determine the material's efficiency in pollutant removal and its capacity for energy storage. In their approach, the soft segments of watermelon were subjected directly to hydrothermal treatment, during which the inherent carbohydrates underwent polymerization to form nanostructured materials. The resulting solid carbonaceous blocks exhibited interconnected networks of carbon nanospheres and nanofibers, with the monolith size controllable by adjusting the dimensions of the watermelon pieces (Figure 6 a-b) [93]. A one-step synthesis approach was used to create conducting polymer hydrogels with 2D structures, employing oxidative polymerization and non-covalent interactions. These hydrogels display reversible gel-sol transitions in response to external redox stimuli, particularly chemicals with electrode potentials above 0.8 V, highlighting their potential in electro-responsive applications (Figure 6c) [94]. Schematic representation shown in Figure 6d of a three-dimensional porous composite electrode consisting of silicon nanoparticles (Si NPs) embedded within a conductive polymer hydrogel. Each Si NP is individually coated with a conductive polyaniline layer and integrated into a porous hydrogel matrix. The polymer coating forms uniformly on the Si NPs through interactions between hydroxyl groups on the nanoparticle surface and phosphonic acid groups from the phytic acid cross-linker.

Cheng et al. reported the synthesis of carbon fiber hydrogels and aerogels derived from cotton, achieving an exceptionally high specific surface area of up to 2436 m²/g [95]. Cotton, composed predominantly of cellulose and possessing an intrinsic fibrous, hollow morphology, is a promising precursor for porous carbon materials with hierarchical pore architectures. Structural modification through activation- either chemical (e.g., KOH, ZnCl₂) or physical (e.g., steam, CO₂)- significantly influences functional performance: micropores contribute to elevated surface area, enhancing adsorption capacity and electric double-layer formation, whereas meso- and macropores promote efficient ion and molecule transport, thereby improving both electrochemical energy storage and pollutant removal efficiency. The cotton fibers were first carbonized to obtain carbon fiber (CF), which was then soaked in 2 M KOH. During high-temperature treatment, the KOH reacted with carbon, creating vacancies and enhancing porosity. This method preserved the original porous and



flexible nature of the cotton while converting it into a conductive fibrous aerogel (Figure 6e). Additionally, biopolymers such as bacterial cellulose and agarose have proven to be cost-effective and abundant biomass sources for hydrogel production [96-98]. Liang et al. prepared aerogels from bacterial cellulose (BC) synthesized by *Acetobacter xylinum* in a culture containing sucrose and coconut milk [99]. The wet bacterial cellulose (BC) pellicles were cryogenically sectioned using a frozen blade at -196°C , followed by freeze-drying at 50°C under a pressure of 0.04 mbar. Subsequently, the samples were pyrolyzed at 800°C in a nitrogen atmosphere and further subjected to nitrogen doping through a secondary heat treatment under an ammonia flow at $700-900^{\circ}\text{C}$, resulting in aerogels with enhanced functionalities [100].



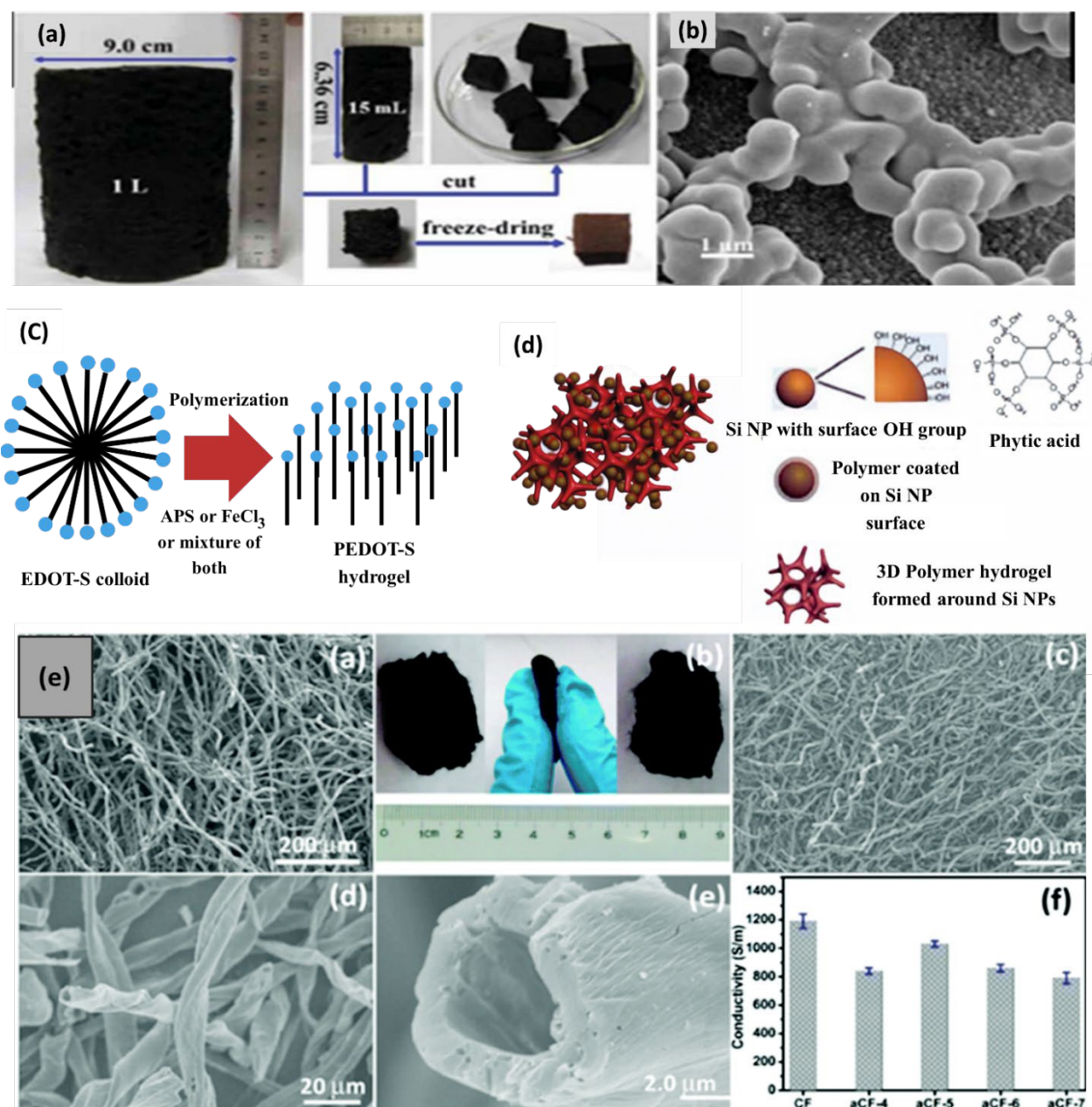


Figure 6. (a) Photographs of carbonaceous hydrogel monoliths in various volumes and the resulting carbonaceous aerogel block. (b) SEM image of the carbonaceous gels. (c) Schematic representation of the synthesis of conducting polymer hydrogels: an 3,4-ethylenedioxythiophene sulfonate (EDOT-S) colloidal solution containing spherical micelles transforms into a Poly(3,4-ethylenedioxythiophene) sulfonate (PEDOT-S) hydrogel with sheet-like structures upon addition of an oxidant (APS, FeCl_3 , or a combination) to initiate polymerization. (d) Illustration of a 3D porous SiNP/conductive polymer hydrogel composite electrode. (e) (a) SEM image of carbon foam



(CF). (b) Digital image of aCF-6 before and after manual compression. (c-e) SEM images of aCF-6 at various magnifications. (f) Electrical conductivity measurements of CF and aCF using a standard four-probe method. Reproduced from reference [100, 101] with permission from Royal Society of Chemistry & Materials Research Society, copyright 2019 & 2015.

3. Preparation of carbon gel

The preparation of carbon gels involves three key stages: polymerization, drying, and carbonization. In the polymerization step, network formation is strongly dependent on the precursor composition and catalyst concentration. A higher catalyst ratio promotes faster gelation and smaller pore formation, advantageous for high-capacitance applications, whereas a lower catalyst ratio creates looser networks with larger pores, improving mass transfer for adsorption of bulky contaminants. The selection of biomass type influences pore development during carbonization. Cellulose-derived gels generally yield a balanced micro-mesoporous network, beneficial for supercapacitors, while lignin-based gels favor micropores for gas storage and selective adsorption. Intrinsic minerals in certain biomass feedstocks can act as pore-forming agents, eliminating the need for external templating. The drying process determines how well the pore structure survives after gelation. Freeze-drying and supercritical drying preserve the open pore network, maintaining high surface area and connectivity, which is crucial for rapid ion transport. In contrast, ambient drying, though more cost-effective, can induce structural collapse due to capillary forces, reducing accessible surface area and lowering electrochemical performance [102].

Carbonization, typically under inert atmospheres, further develops the pore network while removing volatile components. Optimization of carbonization temperature is essential-moderate temperatures (700-1000 °C) enhance microporosity and surface area, while excessively high temperatures (>2000 °C) promote graphitization, improving conductivity but often at the expense of surface area. From an efficiency and applicability standpoint, industrial-scale synthesis benefits from precursor systems requiring minimal pre-treatment, catalyst ratios that balance pore structure control with cost, drying methods that preserve structure without excessive energy demand, and carbonization protocols tuned for the intended application (adsorption vs. electrochemistry).



The synthesized hydrogel undergoes curing in a controlled environment at temperatures between 60°C and 80°C to promote particle aggregation and strengthen internal bonding. Following this, solvent exchange is performed to remove residual water from within the material. The dried hydrogel is then subjected to carbonization at temperatures ranging from 300°C to 2500°C. This process removes remaining oxides and hydrogen-containing groups, converting the organic hydrogel into a carbon gel with a highly porous structure. The increase in carbonization temperature enhances the formation of mesopores and micropores, thereby boosting the specific surface area and total pore volume of the carbon gel. However, at temperatures above 1000°C, the pore volume begins to decline due to the structural collapse of the porous framework. To further functionalize the carbon gel, an oxidation step is introduced. Physical oxidation in air produces phenolic and carbonyl groups on the surface, while chemical oxidation using nitric acid generates carboxylic groups [103]. Physical oxidation typically occurs at higher temperatures than chemical methods and does not require a washing step. The entire synthesis process is visually summarized in Figure 7.

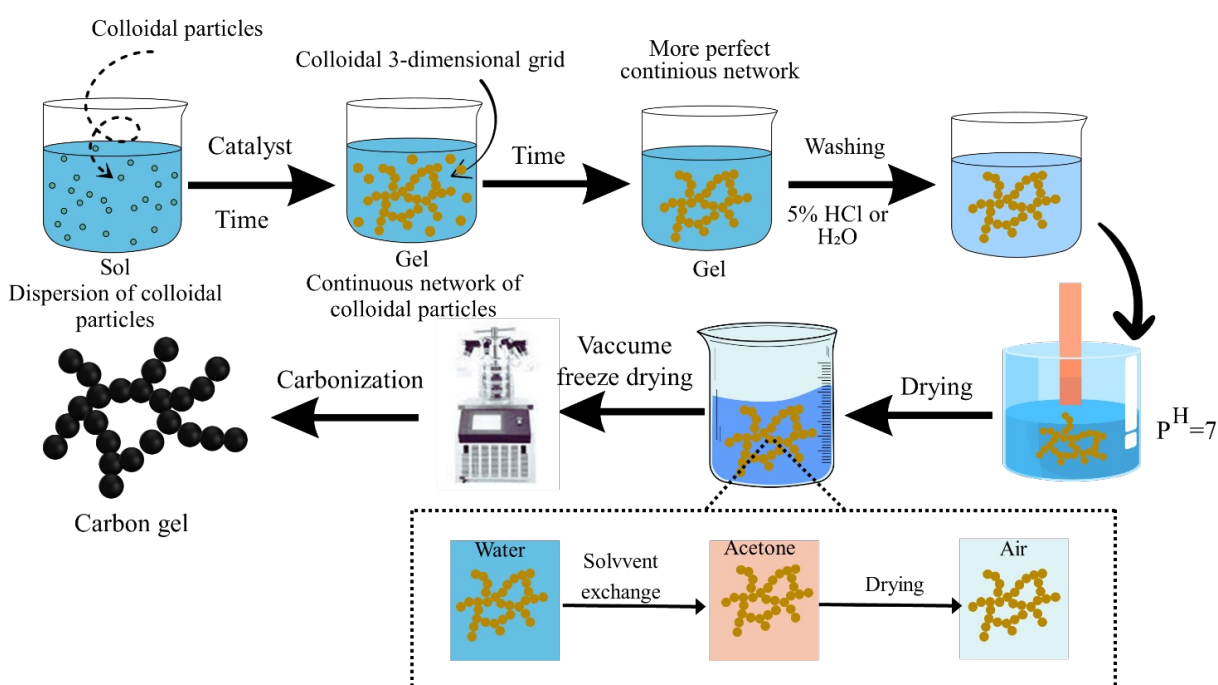


Figure 7. Process flow for carbon gel synthesis.

3.1. Preparation of aerogels



3.1.1 Gelation of precursors

The synthesis of carbon gels generally comprises three principal stages: polymerization, drying, and carbonization. During the polymerization phase, hydrogels are generated through molecular polymerization and crosslinking, involving three successive chemical transformations. Initially, hydroxymethyl groups ($-\text{CH}_2\text{OH}$) are introduced via addition reactions between aldehyde and hydroxyl functional groups. Following this, condensation reactions of hydroxymethylated resorcinol result in the formation of methylene ($-\text{CH}_2-$) and methylene ether ($-\text{CH}_2\text{OCH}_2-$) linkages. The final step encompasses extensive crosslinking and aggregation, culminating in the establishment of a three-dimensional hydrogel framework (Fig. 4). Basic catalysts, including sodium hydroxide (NaOH), sodium carbonate (Na_2CO_3), potassium carbonate (K_2CO_3), and calcium hydroxide ($\text{Ca}(\text{OH})_2$), are commonly utilized to promote the addition step by producing resorcinol anions with enhanced nucleophilic reactivity. In contrast, recent research has explored the use of acid catalysts to facilitate electrophilic addition reactions between formaldehyde and resorcinol [104]. Traditionally, organic carbon aerogels have been produced through the polymerization of resorcinol and formaldehyde in the presence of different catalysts [105]. In addition to the resorcinol-formaldehyde system, other aromatic-aldehyde combinations, including melamine-formaldehyde, phenol-formaldehyde, phenol-furfural, and cresol-formaldehyde, have been employed for the synthesis of organic aerogels. To aid in the fabrication of templated carbon aerogels, various templates- such as polymers, inorganic salts, and ceramic nanoparticles- have been incorporated during the polymerization process. The resulting aerogels typically exhibit well-defined pore size distributions, highly ordered porous architectures, and enhanced mechanical flexibility [106]. More recently, alternative precursors such as graphene, carbon nanotubes (CNTs), and biomass have been explored, providing more straightforward synthesis routes compared to traditional polymer-based methods [93, 107]. Various approaches, such as sol-gel processing, template-assisted methods, spacer-supported techniques, self-supporting strategies, and substrate-based fabrication, have been utilized to produce graphene aerogels [108]. CNT-derived aerogels hold great potential as electrically conductive materials due to their ability to crosslink via van der Waals forces, facilitating the formation of aerogels. However, the direct synthesis of CNT aerogels faces considerable challenges, such as the development of poorly structured 3D frameworks, mechanical instability, and restricted elasticity [109]. To address these



issues, the incorporation of surfactants to reduce CNT surface activity, along with the addition of polymer additives to strengthen the network, has been suggested [110]. Biomass serves as a promising precursor for carbon aerogels owing to its affordability, wide availability, and environmentally sustainable characteristics [111]. Moreover, hydrated biomass precursors, including watermelons and bacterial cellulose, eliminate the need for additional gelation steps [112, 113]. These hydrated biomass materials, containing more than 80 wt.% water, facilitate the creation of porous 3D structures through the straightforward sublimation of water during the preparation process.

3.1.2 Drying

The drying method employed significantly influences the textural properties of carbon aerogels. During drying, the solvent within the hydrogel is removed, leaving the solid matrix intact. To maintain the integrity of the porous structure-essential for optimal performance-drying must be carried out in a manner that prevents structural collapse. Common drying techniques for carbon aerogels include freeze drying, supercritical drying, and ambient drying, producing cryogels, aerogels, and xerogels, respectively. Although these methods yield distinct materials, the term 'aerogels' is often used broadly in the scientific literature to describe all such dried gel forms shown in figure 8 [114].

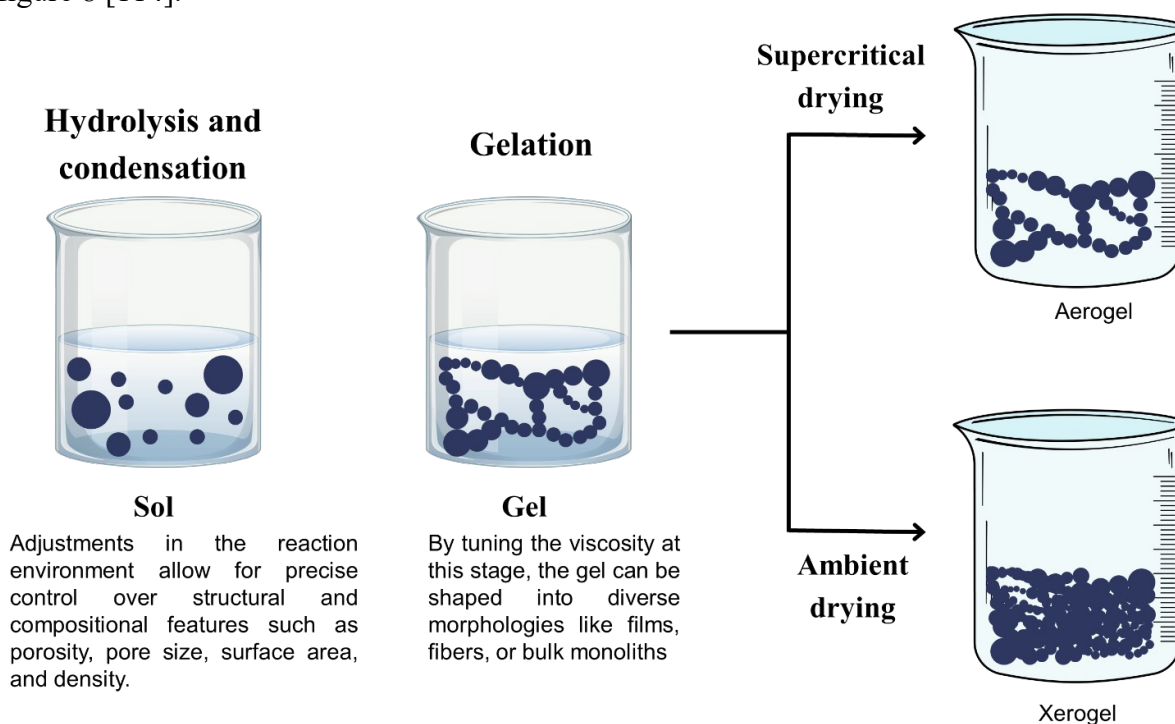
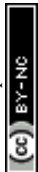


Figure 8. Schematic diagram showing the drying-based synthesis routes for aerogels and xerogels. Reproduced from reference [114] with permission from Wiley, copyright 2014.

3.1.2.1 Supercritical drying

In the supercritical state, the boundary between liquid and vapor phases vanishes, resulting in the elimination of surface tension at the solid-liquid-gas interface. This absence of surface tension prevents pore collapse during drying, thus maintaining the gel's porous architecture [115]. Among various drying techniques, supercritical drying is particularly effective in producing aerogels with highly porous and uniform microstructures [116]. This method maintains the nanoscale pore structure of aerogels by removing the solvent under supercritical conditions, thus preventing pore collapse from capillary forces. Consequently, it produces materials with high porosity, uniform pore size distribution, and a well-connected mesoporous network with minimal structural shrinkage. Aerogels prepared via supercritical drying exhibit improved electrochemical properties due to their enlarged surface area and enhanced ion transport, along with superior adsorption performance arising from preserved active site accessibility and efficient diffusion channels. However, its practical application is constrained by various factors, including the necessity for complete solvent exchange prior to drying. Incomplete replacement of the original solvent can negatively impact the final material's performance. Additionally, the supercritical drying process is complex and time-intensive, generates substantial solvent waste, and incurs high operational costs, which limit its feasibility for large-scale commercial production.

Barim et al. provided a representative example of this approach by synthesizing carbon aerogels through the polymerization of resorcinol and formaldehyde, subsequently dried under supercritical conditions to preserve the porous network [117]. Following the primary gelation stage, the hydrogel underwent successive solvent exchange steps using acetone. This was followed by supercritical extraction using carbon dioxide under conditions of 138 bar pressure and 323 K temperature. The resulting carbon aerogels exhibited high pore volumes and retained well-defined porous structures, free from collapse. Additionally, the robust and uniform pore architecture facilitated the formation of homogeneously distributed metal nanoparticles within the carbon matrix.



3.1.2.2 Freeze-drying

Freeze-drying is commonly utilized in the fabrication of porous carbon aerogels owing to its operational simplicity, low cost, and environmentally benign nature [118]. This technique involves initially freezing the solvent contained within the hydrogel, followed by its removal via sublimation under reduced pressure, thereby eliminating the liquid-vapor interface that might otherwise compromise the gel structure. The textural characteristics of the resulting aerogel, particularly its porosity, are significantly governed by the freezing kinetics and the concentration of precursors. Faster freezing rates result in the development of smaller ice crystals, yielding finer pore structures and enhancing the specific surface area of material. In contrast, lower precursor concentrations tend to favor the development of larger ice crystals, thereby affecting the overall pore morphology of the aerogel.

Vazhayal et al. showcased the utility of this method by fabricating carbon aerogels from waste tissue paper (WTP) and poly(vinyl alcohol) (PVA), targeting applications in CO₂ capture and electromagnetic interference (EMI) shielding [119]. Polymerization of waste tissue paper (WTP) and poly(vinyl alcohol) (PVA) was carried out at ambient conditions using hydrochloric acid as a catalytic agent. Post-molding, the hydrogel samples were extensively rinsed with deionized water and subjected to freeze-drying at 193 K under a vacuum below 1×10^{-5} bar. The resulting WTP-PVA-derived carbon aerogels exhibited a robust three-dimensional porous architecture, as evidenced by SEM imaging, and demonstrated significant microporosity, as verified through nitrogen adsorption-desorption isotherms.

3.1.2.3 Ambient pressure drying

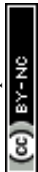
Ambient drying is increasingly recognized as a promising technique for the scalable fabrication of carbon aerogels, owing to its operational safety, procedural simplicity, and cost-effectiveness [108]. Despite these advantages, a major challenge associated with this method is the generation of significant capillary tension at the solid-liquid-vapor interface during the drying process. This capillary stress often results in structural shrinkage, which compromises the mechanical integrity of the final product. To mitigate this issue and maintain structural stability under ambient conditions, two principal strategies have been proposed [120]. The initial approach aims to lower



solvent surface tension to reduce capillary-induced stress during drying, commonly achieved via solvent exchange. Acetone is frequently employed in this process, which is typically conducted at 323 K for a period ranging from one to six days. Selecting an appropriate solvent is critical to ensuring minimal structural deformation and maintaining the integrity of the porous network [121]. The second approach aims to improve the mechanical robustness of the gel framework, allowing it to better resist the capillary forces encountered during the drying process. Feng et al. employed this strategy in the synthesis of resorcinol-formaldehyde (RF) aerogels dried under ambient conditions shows in fig. 7 [122]. In their study, poly(acrylonitrile) (PAN)/RF hydrogel composites were subjected to ethanol-based solvent exchange for seven days, followed by sequential oven drying- first at 323 K for three days and then at 373 K for one day. The resulting PAN/RF aerogels displayed more than 10% structural shrinkage and exhibited a relatively low micropore volume, highlighting the limitations of ambient drying despite its practical benefits.

3.1.3 Carbonization

Subsequent to drying, carbon aerogels generally undergo pyrolysis under an inert atmosphere- typically nitrogen (N_2) or argon (Ar)-at elevated temperatures between 773 and 2773 K, a process that significantly improves their mechanical stability [123]. Throughout the pyrolysis process, functional groups containing hydrogen and oxygen decompose into volatile species, thereby facilitating the development of a porous, carbon-enriched three-dimensional framework [124]. The microporous characteristics of the final aerogel are mainly governed by the conditions of the carbonization step, while mesoporous and macroporous features are largely determined by the initial synthesis and drying procedures [125]. The carbonization temperature significantly influences the physical and structural properties of the aerogels. For instance, when pyrolysis is performed at temperatures exceeding 1473 K, excessive densification of the carbon framework can occur, which markedly reduces the specific surface area [126]. At even higher temperatures, above 2273 K, complete graphitization of the carbon structure is achieved, leading to a substantial improvement in electrical conductivity [127]. Therefore, for applications such as electrochemical devices, it is essential to carefully optimize the carbonization temperature to balance the requirements for both high specific surface area and electrical conductivity [128]. Pyrolysis is typically redundant for inherently graphitic materials like graphene- or carbon nanotube (CNT)-based aerogels. To optimize their textural characteristics, carbon aerogels may undergo physical



or chemical activation using agents such as potassium hydroxide (KOH), sodium hydroxide (NaOH), carbon dioxide (CO₂), or steam (H₂O), which promote the development of surface area and porosity [129]. The essential methodology for synthesizing carbon aerogels represented in figure 9. Activation treatments are employed to enhance microporosity, resulting in a marked increase in specific surface area. Additionally, these treatments allow for fine-tuning of the surface characteristics, including pore volume and pore size distribution, thereby enabling the customization of carbon aerogels for targeted applications [130].

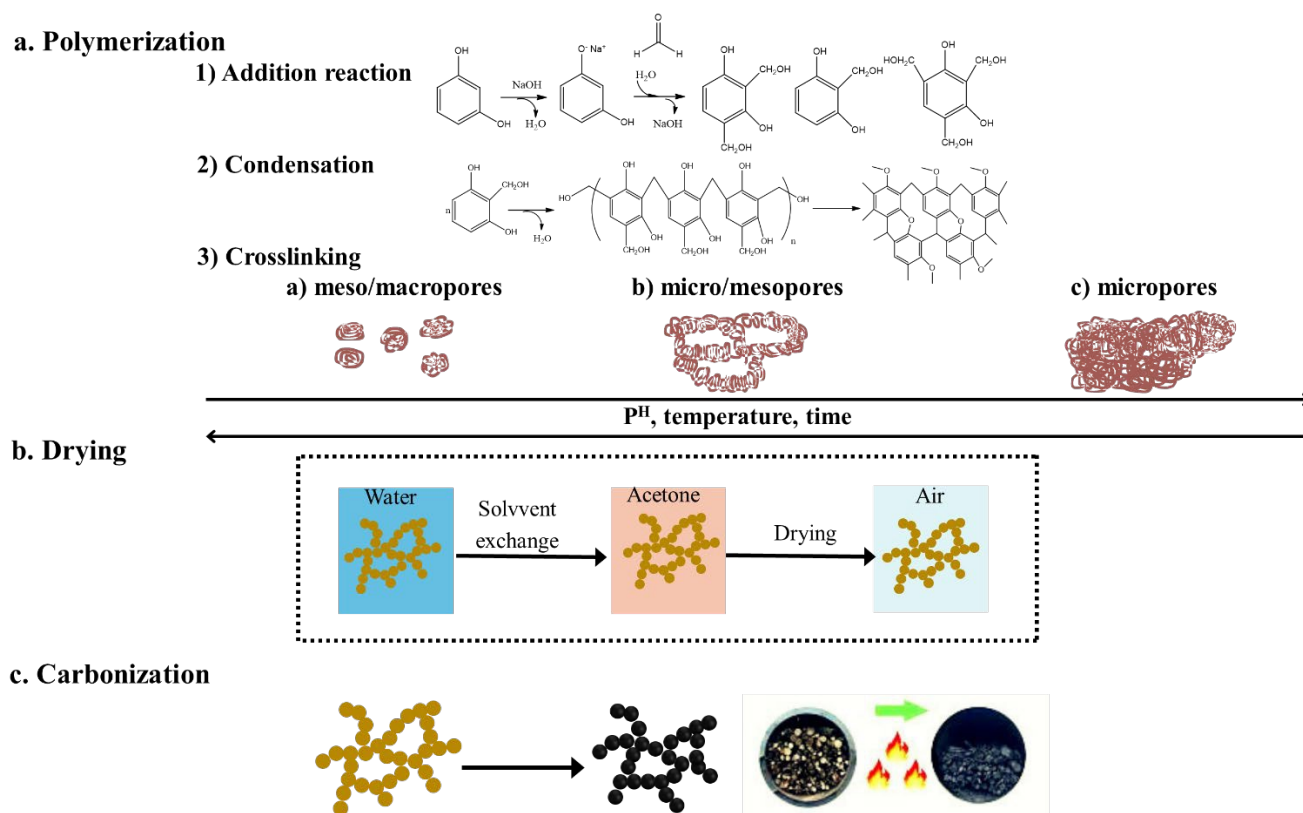


Figure 9. Core synthesis approach for carbon aerogels. Reproduced from reference [131] with permission from Elsevier, copyright 2016.

3.2 Preparation of Xerogels

An organic xerogel was prepared via the aqueous sol-gel polymerization of resorcinol and formaldehyde, catalyzed by sodium carbonate under basic conditions, based on the synthetic approach initially developed by Pekala et al. [11]. The synthesis employed specific molar ratios of resorcinol to catalyst (R/C = 1000 mol mol⁻¹) and resorcinol to formaldehyde (R/F = 0.5 mol



mol⁻¹), with a resorcinol concentration maintained at 0.5 g mL⁻¹. The components were thoroughly blended using magnetic stirring and subjected to a two-step thermal treatment. Initially, the mixture was kept at 30 °C for 26 hours to promote polymer formation, followed by a 48-hour curing phase at 85 °C in an electric oven to facilitate complete gelation and network development. The resulting gel was dried at 150 °C for 24 hours to form the organic xerogel. For carbonization, the xerogel was transferred to a quartz tube reactor (50 mm inner diameter, 1000 mm length) within a vertically aligned electric tube furnace (ARF-30K, Asahi Rika Co., Ltd., Japan). Under a continuous nitrogen stream (100 cm³ min⁻¹), the sample was initially heated from ambient temperature to 250 °C at a rate of 3.75 °C min⁻¹ and held for 2 hours, then further ramped to 800 °C at 4.17 °C min⁻¹ with an additional 2-hour dwell. Post-carbonization, the product was stored in a vacuum desiccator (VOS-210C, Tokyo Rikakikai Co., Ltd.) until further utilization.

To generate mesoporous carbon materials, the OTA (oxidation-thermal treatment-activation) method was applied to the carbon gel [132]. First, oxidation was carried out by heating the carbon gel in a quartz reactor under an air flow (50 cm³ min⁻¹) from room temperature to 350 °C, maintaining this temperature for 6 hours to introduce oxygen-containing functional groups. This was followed by thermal treatment at 1000 °C for 1 hour under a nitrogen atmosphere (50 cm³ min⁻¹), which removed the oxygen functionalities and generated unpaired electrons by disrupting chemical bonds, thereby enhancing surface reactivity.

$$\text{Burn-off (\%)} = \frac{W_i - W_f}{W_i} \times 100 \dots\dots\dots(1)$$

Finally, the sample was activated at 1000 °C for 1 hour in a carbon dioxide stream (50 cm³ min⁻¹), promoting the formation of abundant mesopores and micropores in the gel matrix. The activated carbon produced using the OTA method was labeled as CG OTAx, where "CG" denotes carbon gel and "x" indicates the activation time ranging from 1 to 3 hours. In contrast, samples activated by the conventional CO₂ method were labeled ACx, with "AC" representing activated carbon obtained at 1000 °C and "x" corresponding to activation times from 1 to 4 hours. The carbon burn-off during activation was quantified using Equation (1), where *W_i* and *W_f* represent the weights of the carbon gel before and after activation, respectively [133].

3.3 Preparation of Hydrogel

Hydrogels are three-dimensional polymeric structures characterized by their hydrophilic nature. Although they are commonly synthesized using hydrophilic monomers, hydrophobic monomers are occasionally incorporated to modulate specific physicochemical properties tailored to particular applications. These materials can be derived from both natural and synthetic polymers. Synthetic polymers, being inherently hydrophobic, exhibit greater chemical stability and mechanical strength compared to natural counterparts. While enhanced mechanical integrity contributes to increased durability, it also leads to a reduced degradation rate. As such, a careful balance between these opposing features is essential for optimal material performance [134]. Natural polymer-based hydrogels can also be engineered, provided the base polymers inherently contain suitable reactive functionalities or are chemically modified to include radically polymerizable groups.

Hydrogels are essentially three-dimensional networks formed by cross-linked hydrophilic polymers, characterized by their elasticity and capacity for substantial water uptake. The formation of these networks is commonly achieved through polymer cross-linking techniques, with one widely adopted approach being free-radical copolymerization or cross-linking polymerization. In this method, hydrophilic monomers interact with multifunctional cross-linking agents to establish the gel framework. Hydrogels may also be produced by cross-linking water-soluble linear polymers-originating from either synthetic or natural sources-through a variety of mechanisms, such as: (i) covalent bonding via chemical cross-linking reactions; (ii) irradiation-induced generation of polymer radicals that lead to inter-chain cross-linking; and (iii) physical interactions, including chain entanglements, electrostatic attractions, and crystallization phenomena [135].

A wide range of polymerization techniques- such as bulk, solution, and suspension polymerization- can be employed for the fabrication of hydrogels. These approaches allow for flexibility in designing hydrogels with specific forms and properties suitable for various applications. The hydrogel synthesis process fundamentally relies on three essential components: the monomer, the initiator, and the cross-linking agent. Proper management of these elements is crucial for controlling the exothermic nature of the polymerization reaction and for tuning the final characteristics of the hydrogel. Diluents, such as water or other aqueous solutions, are commonly



used during the synthesis of hydrogels. Following polymerization, it is essential to thoroughly wash the resulting hydrogel matrix to eliminate residual impurities. These include unreacted monomers, initiators, cross-linking agents, and by-products formed through side reactions (Figure 10).

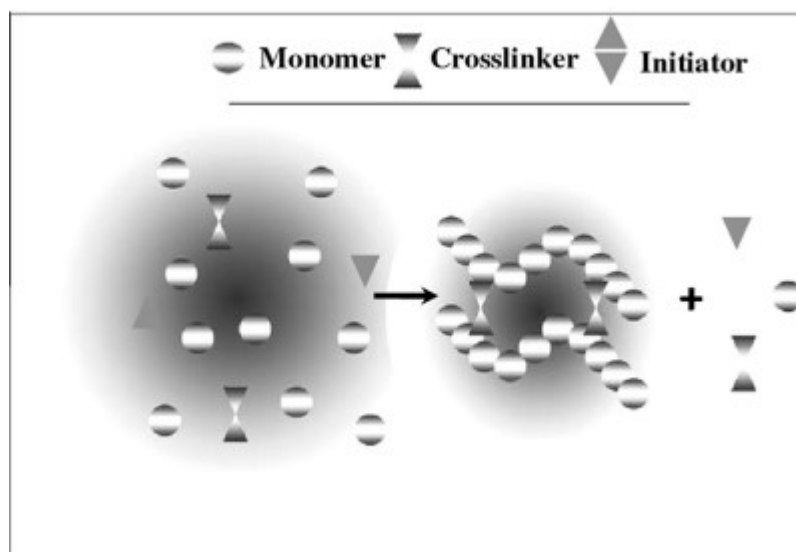


Figure 10. Schematic representation of the hydrogel synthesis process. Reproduced from reference [136] with permission from Asian Pacific Journal of Nursing and Health Sciences, copyright 2021.

Hydrogels composed of acrylamide, acrylic acid, and their salts have been produced through methods such as inverse-suspension polymerization and diluted solution polymerization, as detailed in prior studies [137]. In contrast, there has been limited research on the use of highly concentrated solution polymerization for acrylic monomers, with this method being mainly discussed in patent literature [138]. Notably, an acrylic acid–sodium acrylate superabsorbent hydrogel was successfully synthesized by Chen [139] through concentrated solution polymerization (43.6 wt%) using potassium persulfate as a thermal initiator. Hydrogels are generally prepared from polar monomers and, depending on their source materials, can be classified into three categories: those derived from natural polymers, synthetic polymers, or hybrid systems that combine both. From a preparative standpoint, hydrogels can be synthesized using several methods, including graft polymerization, cross-linking polymerization, network formation from water-soluble polymers, and radiation-induced cross-linking. A variety of hydrogel types are available, with many being lightly cross-linked copolymers of acrylate and acrylic acid, or grafted starch-acrylic acid polymers. These hydrogels are typically produced using techniques such as



inverse-suspension, emulsion, or solution polymerization, which are explained in further detail below. Hydrogels are characterized by their high-water absorption, enabled by hydrophilic moieties within their polymer networks. While increased water content enhances swelling capacity, it often reduces mechanical strength. Mechanical properties can be tuned by adjusting the degree of cross-linking: higher cross-linking improves strength but decreases elongation, making the gel more brittle. Copolymerization with hydrophobic monomers to form interpenetrating polymer networks (IPNs) or grafting to hydrophobic substrates can further enhance mechanical performance. Hydrogels can be engineered to mimic the transport and mechanical properties of natural soft tissues. For example, PET fibers incorporated into PHEMA/PCL semi-IPN hydrogels have been proposed for intervertebral disc prostheses, while PHEMA has been tested for fixing prostheses in the intramedullary cavity. Titanium dental implants have also been coated with poly(ethylene glycol diacrylate) hydrogels. Most hydrogels are unstable in both dried and swollen states; drying often induces cracks. This can be mitigated by incorporating hygroscopic salts or encapsulating the hydrogel in elastomeric layers. Recently, a double-hydrophobic coating-comprising a hydrophobic polymer and viscous oil applied via quenching-has been developed, forming a ~200 μm surface layer that effectively resists both swelling and drying damage [140].

3.3.1. Bulk polymerization

Bulk polymerization is one of the most straightforward techniques for synthesizing hydrogels, generally involving only the monomer and an initiator that is soluble within the monomer. The high concentration of monomer in this process accelerates both the polymerization rate and the degree of polymerization. However, the increased monomer concentration leads to a rise in viscosity as the reaction advances, along with significant heat generation. To manage these issues, the polymerization is often kept at relatively low monomer conversion rates, which helps to maintain thermal control and stability throughout the process [141]. Bulk polymerization of monomers produces a uniform, glassy, and transparent hydrogel matrix that is initially rigid. When this matrix is immersed in water, it absorbs the water, causing it to swell and transition into a soft, flexible hydrogel.



3.3.2. Solution Polymerization / Cross-linking

In solution copolymerization or cross-linking, ionic or neutral monomers are mixed with a multifunctional cross-linker in the presence of a solvent. The polymerization process is often initiated via thermal methods, UV light, or redox systems. A significant advantage of solution polymerization, compared to bulk polymerization, is the solvent's ability to act as a heat sink. This helps dissipate the heat produced during the reaction, providing better control over temperature. After polymerization, the hydrogels are thoroughly washed with distilled water to eliminate unreacted monomers, oligomers, cross-linkers, initiators, extractable polymers, and any other remaining impurities. If the water content during the polymerization process surpasses the hydrogel's capacity for equilibrium swelling, phase separation may occur, resulting in a non-uniform structure. Common solvents used in solution polymerization for hydrogels are water, ethanol, water-ethanol mixtures, and benzyl alcohol. After the gel forms, the solvent can be eliminated by immersing the hydrogel in water, which aids in swelling and cleaning the gel.

3.3.3. Suspension polymerization or inverse-suspension polymerization

Inverse suspension polymerization offers a practical approach for synthesizing hydrogel microspheres or powders, thus removing the necessity for mechanical size reduction post-synthesis. This method operates on a water-in-oil (W/O) emulsion system, distinguishing it from conventional suspension techniques that typically employ oil-in-water (O/W) dispersions. During inverse suspension polymerization, monomers and initiators are evenly distributed within a hydrocarbon phase to create a uniform dispersion. The characteristics-such as size and shape-of the resulting hydrogel beads are largely governed by variables including the monomer solution's viscosity, agitation speed and style, rotor design, and the nature of the dispersing agent employed [142]. Comprehensive discussions regarding the mechanisms and characteristics of hetero-phase polymerizations can be found in prior literature [143]. Because of the dispersion's thermodynamic instability, constant agitation is required to preserve uniformity. Additionally, a suspending agent with a low hydrophilic-lipophilic balance (HLB) is introduced to minimize the risk of phase separation and help stabilize the emulsion system.



3.4 Grafting to a Support

Hydrogels synthesized via bulk polymerization often exhibit limited mechanical strength due to their inherently weak structural framework. To enhance their mechanical performance, a common strategy involves grafting the hydrogel onto a more robust supporting surface. The direct polymerization of monomers onto the activated surface is made possible by this method, which starts the production of free radicals on the substrate surface. This procedure creates a hydrogel composite with improved mechanical reinforcement by chemically bonding the resultant polymer chains to the support. Grafting-based hydrogel synthesis has made use of a variety of polymeric supports, which significantly improves the material's structural stability and resilience [144]. The production of hydrogels from unsaturated monomers has been effectively initiated by high-energy ionizing radiation, such as electron beams [145] and gamma rays [146]. Free radicals are created directly on the backbones of polymers when aqueous polymer solutions are exposed to radiation. Furthermore, hydroxyl radicals are produced when water is radiolyzed, and these radicals then interact with the polymers to form macro-radicals.

Following their recombination across several chains, these reactive species can create covalent connections that create a three-dimensional, cross-linked hydrogel network. This method is frequently used to modify polymers such as poly(acrylic acid), poly(ethylene glycol), and poly(vinyl alcohol). Radiation-induced cross-linking has the important advantage of producing high-purity hydrogels without the need for chemical initiators, which lowers the possibility of contamination.

3.5 Contribution of Carbon Materials to the Mechanical Reinforcement of Hydrogels

Three-dimensional networks of polymers called hydrogels are well-known for their tremendous capacity to absorb water; nevertheless, their use is often limited by their low structural rigidity and poor mechanical resilience. Carbon-based compounds have become successful additions that greatly improve the mechanical performance of hydrogels in order to overcome this constraint [147]. One important way that carbon-based compounds improve mechanical performance of hydrogels by serving as reinforcing agents. High tensile strength and stiffness are just two of the remarkable mechanical properties of nanostructured carbons including graphene, carbon nanotubes, and carbon nanofibers. These materials provide structural reinforcement to the matrix



when embedded in hydrogel networks, improving its tensile strength, elasticity, and resistance to deformation. The strong covalent bonds that characterize the structure of the carbon nanostructures are primarily responsible for these improvements [148].

Furthermore, the increased cross-linking hydrogel network is facilitated by carbon-based elements. They increase the structural stability of the hydrogel by adding more crosslink sites through chemical or physical interactions with the polymer chains. This cross-linking improves the mechanical robustness of gel under a range of stress settings by increasing its resistance to compressive and shear pressures [100, 149]. Another process that contributes to improved mechanical behavior is the modification of the internal gel network. By causing structural reorganizations at the nanoscale, the addition of graphene sheets, or CNTs, creates a network that is more organized and interconnected. By promoting more effective load transfer and consistent stress distribution, this structural improvement improves the stiffness, toughness, and resilience of gel [150, 151].

Additionally, carbon-based fillers increase hardness and energy dissipation. Because of their rigidity, mechanical forces may be distributed throughout the hydrogel matrix in an efficient manner, minimizing localized stress concentrations and lowering the chance of structural failure. The hydrogels are therefore able to withstand higher strains without suffering catastrophic damage and exhibit enhanced fracture toughness [152, 153]. The electrical conductivity of hydrogels can be significantly increased by using conductive carbon-based elements such as graphene and CNTs in addition to mechanical support. These range of applications of composite hydrogels is expanded by this functional enhancement, which makes them perfect for next-generation technologies like tissue engineering scaffolds, soft actuators, and biosensing devices-fields where a blend of electrical sensitivity and mechanical robustness is essential [154-156]. As a result of a variety of effects, such as mechanical reinforcement, more cross-linking, structural refinement, greater toughness, effective energy dissipation, and increased electrical conductivity, carbon-based additions help to improve the mechanical properties of hydrogels. These enhancements enable hydrogels to exhibit superior strength, stiffness, and durability, broadening their applicability in fields requiring robust mechanical performance [156]. Figure 11 depicts how the incorporation of carbon-based nanomaterials and additional reinforcing agents contributes to the improved mechanical performance of hydrogels.



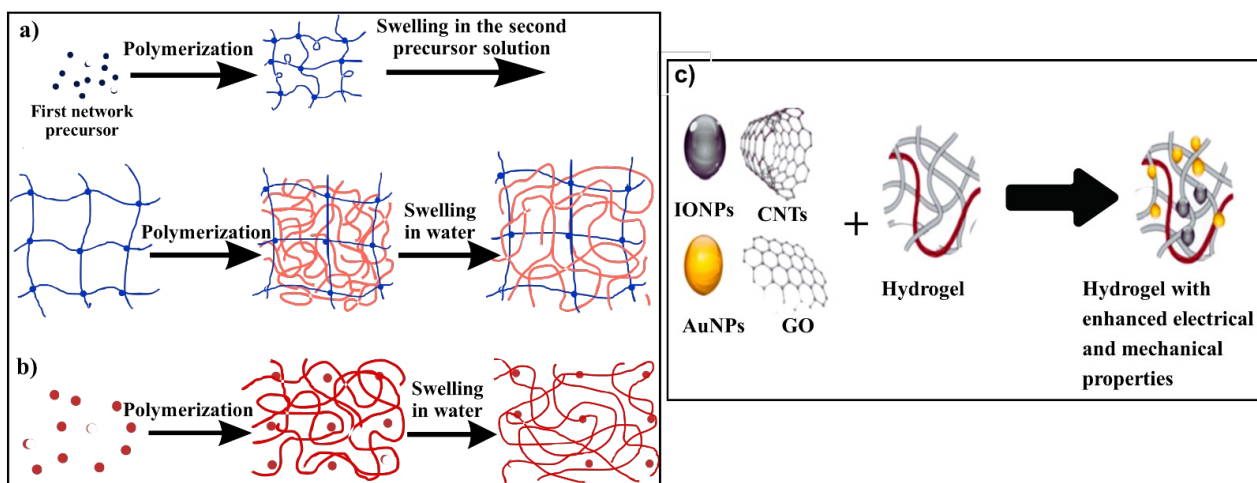


Figure 11. a, b) Mechanical properties of gel materials. (c) Enhancement of hydrogel mechanical strength via incorporation of carbon-based nanomaterials and other reinforcing agents. Reproduced from reference [75, 157] with permission from Elsevier & Royal society of chemistry, copyright 2023 & 2025.

3.6 Some other porous materials

In addition to carbon gels, several other advanced porous materials—including activated carbons, metal–organic frameworks (MOFs), and functionalized nanomaterials—have been extensively explored for applications in energy storage, catalysis, and environmental remediation. Each of these materials offers distinct advantages and limitations, and a comparative understanding can guide material selection for specific performance targets. Activated carbons remain the most commercially established option due to their low cost, abundant precursors, and high surface areas (often $>1000 \text{ m}^2/\text{g}$) [158]. They are highly effective in adsorption-based water purification and as electrode materials for supercapacitors. However, their pore structure is predominantly microporous, which can hinder electrolyte ion diffusion in high-power devices. Additionally, tailoring their surface chemistry often requires chemical activation or post-functionalization steps, which may increase environmental footprint.

MOFs are crystalline hybrid materials composed of metal nodes connected by organic linkers, offering precise control over pore size, topology, and chemical functionality. This tunability enables exceptional selectivity in gas separation, CO_2 capture, and catalysis. Nonetheless, their



high synthesis cost, complex processing, and limited thermal/chemical stability restrict their scalability for bulk applications. Furthermore, most MOFs have relatively low electrical conductivity, limiting their direct use in electrochemical devices without conductive additives. Functionalized nanomaterials, such as doped carbons, graphene derivatives, and surface-modified nanoparticles, allow for highly tailored surface chemistry to promote specific reactions or contaminant interactions. Nitrogen-, sulfur-, or phosphorus-doping, for instance, can enhance catalytic activity and conductivity in electrochemical applications. Despite their outstanding performance in targeted tasks, their synthesis often involves costly reagents, precise control over functionalization steps, and scalability challenges, making them more suited to high-value niche applications.

Carbon gels, by contrast, combine several advantages of these material classes. Their hierarchical pore structures-comprising interconnected micro-, meso-, and macropores-enable both high surface area and efficient mass transport, overcoming the diffusional limitations of microporous activated carbons. They can be synthesized from renewable biomass or synthetic monomers, offering flexibility in cost and sustainability. The surface chemistry of carbon gels can be readily tuned during synthesis or post-treatment, enabling tailored adsorption selectivity or enhanced electrochemical performance. While the production cost of carbon gels may exceed that of conventional activated carbon, their structural versatility, superior rate capability, and potential for sustainable, low-impact synthesis often justify their use in advanced applications such as high-rate supercapacitors, selective pollutant removal, and catalytic supports. Overall, the choice between carbon gels, activated carbons, MOFs, and functionalized nanomaterials depends on the desired balance between cost, structural properties, performance, and scalability, with carbon gels occupying a unique position where multifunctionality meets tunable design.

3.6.1 Scalable and Energy-Efficient Fabrication Methods

Recent advances in fabrication technologies have introduced energy-efficient and scalable approaches for producing porous carbon materials, including carbon gels, with improved control over porosity and reduced production costs. Among these, microwave-assisted activation, ultrasonic drying, and molten salt templating have attracted significant attention for their potential to enhance performance while lowering energy consumption [159]. Microwave-assisted activation



offers rapid and uniform heating by directly coupling microwave energy with the carbon precursor or activating agent. This method significantly shortens activation times-often from several hours to minutes-while enabling precise temperature control and uniform pore development. In addition to lowering energy use, microwave activation can produce well-distributed micro- and mesopores, enhancing adsorption kinetics and electrochemical accessibility in supercapacitors and capacitive deionization systems.

Ultrasonic drying is another energy-efficient technique that utilizes high-frequency sound waves to promote rapid solvent removal from wet gels. The acoustic cavitation effect disrupts capillary forces during drying, helping to preserve the gel's porous structure without the need for energy-intensive freeze-drying or supercritical drying. Ultrasonic drying can also be scaled for continuous production, making it particularly attractive for industrial applications where drying steps often represent a major cost factor. Molten salt templating uses salts such as NaCl, KCl, or eutectic mixtures as both heat transfer media and structural templates. During carbonization, the molten salt provides uniform thermal distribution and prevents pore collapse, while also creating interconnected meso- and macropores. After synthesis, the salts can be washed out with water, allowing for easy recovery and reuse, further reducing operational costs. This method is particularly effective for producing highly conductive, large-pore carbons for fast ion transport in electrochemical devices and high-throughput adsorption processes. The integration of these advanced methods into carbon gel fabrication provides several practical advantages: reduced processing time, lower energy requirements, tunable pore structures, and potential compatibility with low-cost or biomass-derived precursors. Moreover, these methods can be adapted to continuous or semi-continuous production lines, facilitating scalability without compromising structural quality. By incorporating such emerging, energy-efficient techniques into fabrication strategies, the pathway toward sustainable, large-scale production of high-performance porous carbons for energy storage, catalysis, and environmental remediation becomes more feasible and economically viable.

4. Applications

Carbon gels are utilized in energy storage and conversion technologies such as supercapacitors, lithium batteries, and fuel cells due to their high surface area and conductivity. They also serve as



gas diffusion electrodes and catalyst supports in electrochemical devices. In environmental and industrial applications, carbon gels are employed as filters, molecular sieves, and activated carbon for adsorption and separation processes. Their mechanical strength and thermal stability enable usage in insulation, structural materials, and metal casting. These broad application areas underline the significance of carbon gels as versatile materials in both energy-related and structural functionalities. This schematic diagram (Figure 12) highlights the diverse applications of carbon gels, emphasizing their multifunctional role in advanced materials and energy systems.

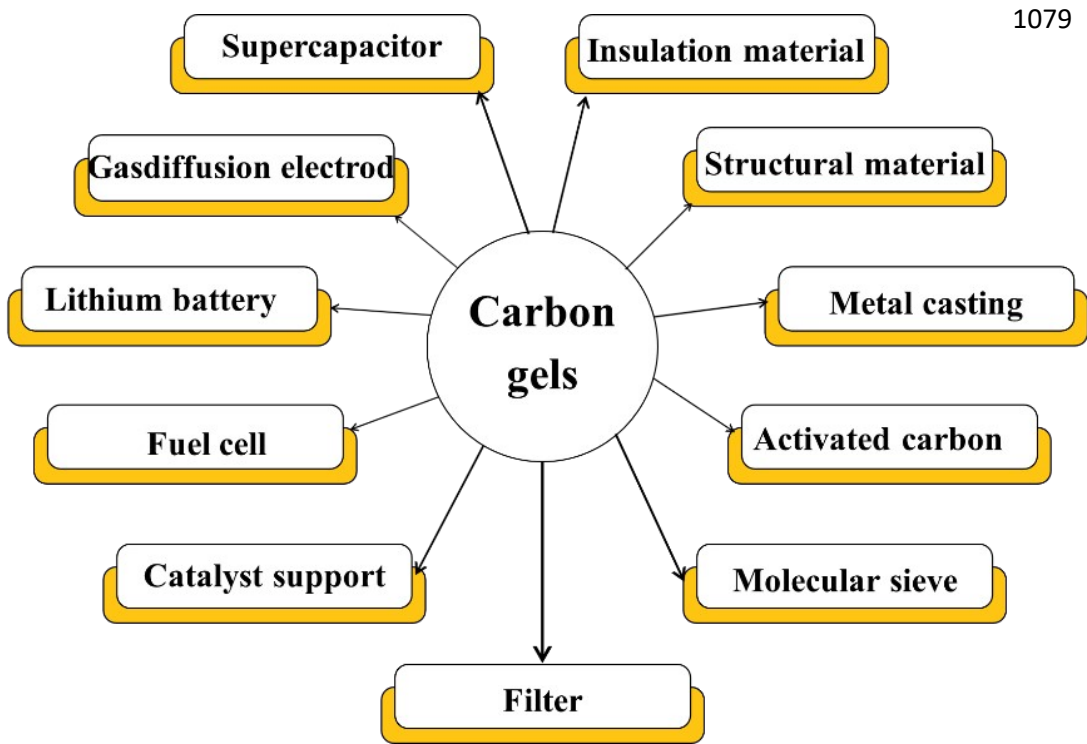


Figure 12. Prospective technological applications of carbon gels across diverse fields.

4.1 Supercapacitors

Supercapacitors, also known as ultracapacitors, represent a promising category of energy storage devices characterized by their exceptionally high power density, rapid charge-discharge capabilities, straightforward energy storage mechanisms, and extended operational lifespans [160, 161]. Supercapacitors are primarily classified into two types based on their charge storage mechanisms: EDLCs, which store energy through electrostatic separation of charge at the electrode-electrolyte interface, and pseudocapacitors, which rely on rapid, reversible redox reactions at or near the electrode surface to store charge (Figure 13a) [116, 162]. Carbon-based



1089 materials are widely used as electrodes in EDLCs due to their high surface area and excellent
1090 conductivity. In contrast, pseudocapacitors typically employ transition metal oxides- such as
1091 manganese, nickel, cobalt, vanadium, and iron oxides or conductive polymers like polyaniline and
1092 polypyrrole, which serve as effective electron donors or acceptors and facilitate rapid redox
1093 reactions for charge storage [163].



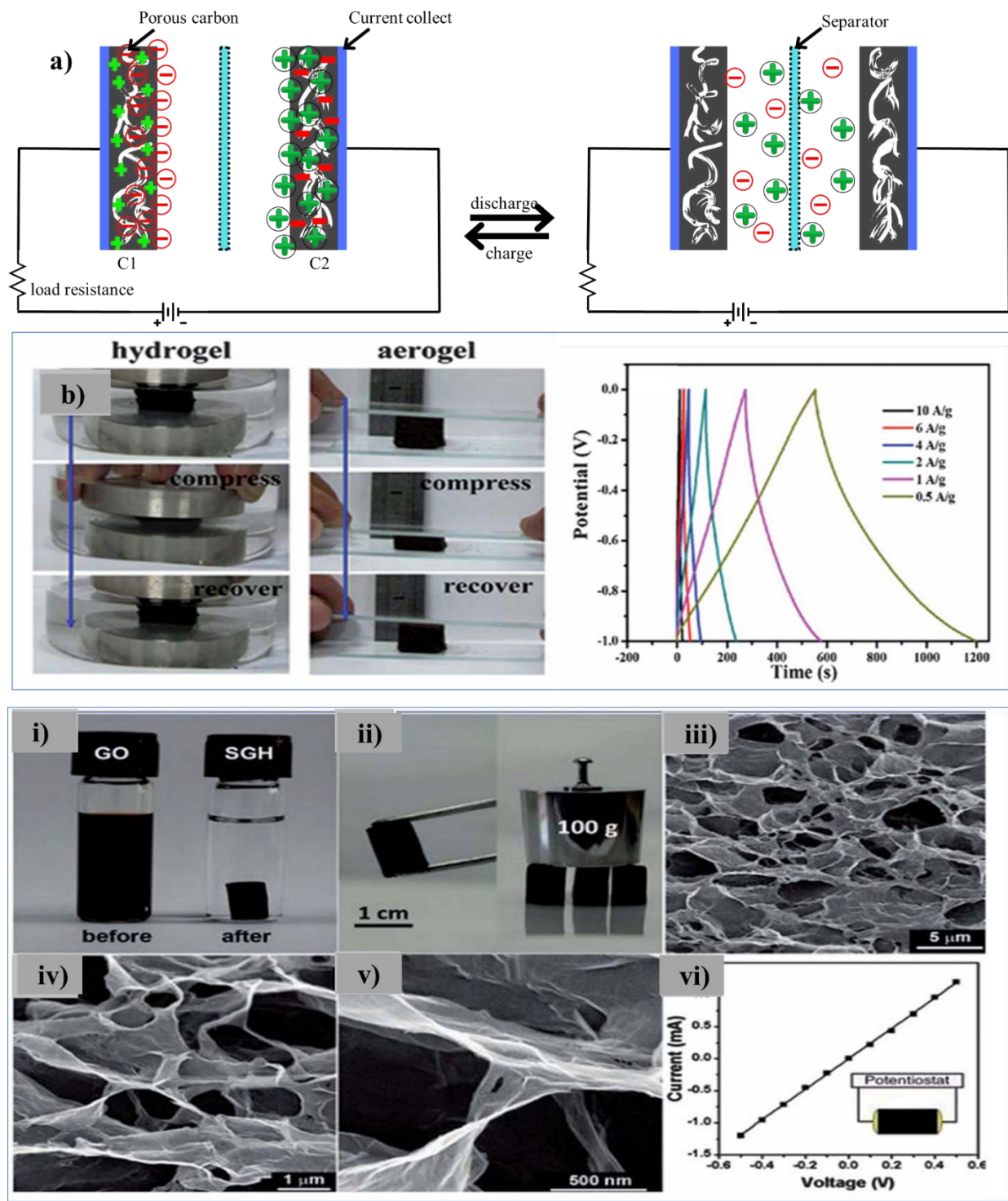


Figure 13. (a) Schematic illustration of charge accumulation and release mechanisms in an electric double-layer capacitor (EDLC). (b) Digital images demonstrating the compressive behavior of carbonaceous hydrogels and aerogels, along with charge-discharge curves of a magnetic carbon aerogel-based electrode at varying current densities. (i) Visual comparison of graphene oxide (GO)

suspension before and after hydrothermal treatment. (ii) Photographs highlighting the mechanical robustness and load-bearing capacity of the synthesized graphene hydrogel. (iii-v) SEM images revealing the porous network structure of the graphene hydrogel. (vi) Current-voltage (I-V) curve illustrating the electrical conductivity of the hydrogel. Reproduced from reference [164] with permission from Royal society of chemistry, copyright 2014.

4.1.1 Carbonaceous Gels for Supercapacitors

Significant research has been conducted in the last few decades to develop carbon-based hydrogels and aerogels for usage in supercapacitors. Based on where they come from, these materials can be broadly divided into four types: such as, aerogels made from synthetic polymers, aerogels made from carbon nanotubes, hydrogels and aerogels that contain graphene, and those made from precursors generated from biomass. Recent developments have concentrated on making these materials lightweight, flexible, and extremely effective in storing energy. Scientists are developing composite materials with even greater energy storage capacities by adding redox-active substances like conducting polymers and metal oxides to their structure to improve their performance even further.

4.1.1.1 Biomass-derived hydrogels and aerogels for supercapacitors

Carbon products made from biomass are becoming more and more popular because of their low cost, accessibility, and environmentally benign provenance. Because of their interconnected three-dimensional porous structures, which provide a large surface area and adaptable physical and chemical properties, hydrogels and aerogels stand out within this group. Biomass-derived gels are ideal for electrochemical applications, especially in supercapacitors, because of these structural benefits. Hydrogels made from biomass are mostly used as gel electrolytes because they allow for effective ion transport while preserving mechanical stability. Additionally, they act as binders in composite electrodes, improving the electrode materials' structural integrity and stickiness. Aerogels made from biomass, on the other hand, are mostly used as electrode materials because of their exceptional electrochemical performance, high conductivity, and lightweight composition. The synthesis of biomass-derived carbonaceous hydrogels is typically achieved through hydrothermal treatment, a process that converts raw biomass into a well-structured gel network while preserving essential functional groups. By fine-tuning synthesis conditions and integrating



functional additives, scientists are actively improving the electrochemical performance of biomass-derived carbon materials. With the growing global need for eco-friendly energy storage technologies, these sustainable carbon materials are proving to be strong contenders for the development of next-generation supercapacitors [165]. Due to their synergistic attributes-namely excellent biocompatibility, distinctive porous architecture, and robust mechanical integrity-biomass-derived hydrogels exhibit significant promise for use in supercapacitors, particularly as power sources for implantable biomedical devices. Furthermore, these carbon-rich hydrogels are frequently employed as solid electrolytes, thanks to their three-dimensional polymeric networks that can effectively absorb and retain water. For instance, Choudhury et al. demonstrated the feasibility of using gelatin-based hydrogel, a natural material, as a solid-state electrolyte in supercapacitor applications [166]. The supercapacitor exhibited a maximum specific capacitance of 81 F g^{-1} . In a related study, Yamazaki and colleagues developed innovative composite hydrogels composed of two natural biopolymers-cellulose and chitin- along with a dual ionic liquid system, aiming to enhance both ionic conductivity and environmental compatibility [167]. Biomass-derived carbonaceous hydrogels and aerogels have garnered significant attention as electrode materials for supercapacitors, thanks to the synergistic advantages of combining low-cost, sustainable biomass with the unique structural, large surface area, and strong mechanical properties of the hydrogels and aerogels. In a recent study, we fabricated carbonaceous gels using watermelon as a crude biomass source. The resulting carbonaceous hydrogels and aerogels exhibited an interconnected microscopic structure with an average pore diameter of approximately 45.8 nm. We then functionalized the 3D network of the aerogels by incorporating Fe_3O_4 nanoparticles, transforming them into magnetic carbon aerogels through pyrolysis. These magnetic carbon aerogels demonstrated a lightweight structure, an impressive capacitance of 333.1 F g^{-1} , and exceptional cycling stability, making them highly promising for use in supercapacitors [93]. Collectively, literature findings confirm that biomass-derived hydrogels and aerogels combine structural tunability, sustainable sourcing, and strong electrochemical performance, making them ideal for next-generation supercapacitors. Their versatility as both electrolytes and electrode materials-alongside recent advances in functionalization-positions them as competitive alternatives to conventional carbon-based systems in both energy storage efficiency and environmental compatibility.

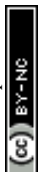


4.1.1.2 Graphene based hydrogels and aerogels for supercapacitors

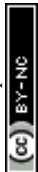
The remarkable properties of graphene, a two-dimensional carbon material made up of a single atomic layer, such as its high charge carrier mobility, remarkable flexibility, strong mechanical structure, and better thermal conductivity, have attracted a lot of interest. According to Zhu et al., graphene's inherent capacitance is 21 mF cm^{-2} . Graphene is a very appropriate material for energy storage applications due to its large theoretical specific surface area ($2630 \text{ m}^2 \text{ g}^{-1}$), good conductivity, and chemical stability. For example, Zhu et al. created activated GO and achieved improved electrical conductivity combined with an outstanding surface area of up to $3100 \text{ m}^2 \text{ g}^{-1}$. Particularly in ionic liquid electrolytes, this activated GO demonstrated a remarkable energy density of roughly 70 Wh kg^{-1} and a specific capacitance of 166 F g^{-1} when utilized as an electrode material in supercapacitors [168]. The unique properties of graphene, a one-atom-thick 2D carbon material, such as its remarkable mechanical strength and flexibility, high charge carrier mobility, and superior thermal conductivity, have led to extensive research in a number of sectors. Zhu et al. state that the intrinsic capacitance of graphene is 21 mFcm^{-2} . More importantly, graphene offers a great deal of potential for capacitance-related applications due to its high conductivity, distinct chemical stability, and enormous theoretical specific surface area ($2630 \text{ m}^2 \text{ g}^{-1}$). Zhu et al., for example, synthesized activated GO with a remarkable high surface area of up to $3100 \text{ m}^2 \text{ g}^{-1}$ and strong electrical conductivity. The activated GO showed a high specific capacitance of 166 Fg^{-1} when tested as an electrode material for supercapacitors.

4.1.1.2.1 Graphene based hydrogels for supercapacitors

Hydrogels based on graphene has garnered a lot of attention lately because of their possible uses in supercapacitors. GO is frequently used as the main component in the production of these hydrogels. For GO, a number of gelation methods have been investigated, such as chemical cross-linking by covalent bonding [169], ion or polymer-induced gelation [170], and self-assembly via hydrothermal processes [169]. For use in supercapacitors, graphene hydrogels produced by hydrothermally treating GO suspensions have been thoroughly investigated. By using this technique, graphene hydrogels were generated, as reported by Xu et al. (Figure 13 b(i-vi)) [171]. These hydrogels showed good electrical conductivity, excellent mechanical characteristics, and a specific capacitance of roughly 175 Fg^{-1} . In similar lines, further research has reported self-assembled graphene hydrogels made by hydrothermal processes that display particular capacitance



1189 values between 186 and 308 Fg⁻¹. Graphene hydrogels can be produced under mild conditions
1190 using small molecules as reducing agents. One effective approach involves the chemical reduction
1191 of graphene oxide (GO) with L-glutathione, resulting in the successful synthesis of self-assembled
1192 graphene hydrogels [172] and sodium ascorbate [173]. The resulting graphene-based materials
1193 show promising electrochemical performance. For example, an asymmetric supercapacitor
1194 utilizing L-glutathione-reduced graphene hydrogels combined with nanostructured MnO₂
1195 achieved a specific capacitance of 157.7 Fg⁻¹ at a current density of 1 Ag⁻¹. In comparison, a
1196 sodium ascorbate-reduced graphene hydrogel electrode demonstrated an even higher specific
1197 capacitance of 240 Fg⁻¹ at a current density of 1.2 Ag⁻¹. Yang et al. [174] introduced an innovative
1198 approach for developing a densely packed graphene hydrogel film by utilizing a capillary
1199 compression method. This breakthrough demonstrated that the flexible graphene hydrogel films
1200 exhibit remarkable properties, including low ion transport resistance and a highly accessible
1201 surface area for ions. These structural characteristics notably improve the electrochemical
1202 performance of the material in supercapacitor applications, yielding high specific capacitances of
1203 261.3 F cm⁻³ in organic electrolytes and 255.5 F cm⁻³ in aqueous electrolytes when tested at a
1204 current density of 0.1 A g⁻¹. Its compatibility with traditional paper-making processes, making
1205 large-scale production feasible makes this method particularly exciting. With its scalable nature
1206 and outstanding electrochemical performance, this advancement paves the way for real-world
1207 applications of graphene hydrogel films in energy storage systems. The porous structure of
1208 graphene hydrogels enables the incorporation of additional nanomaterials into their three-
1209 dimensional networks, forming graphene hydrogel-based composite materials. These composites,
1210 consisting of graphene hydrogels combined with conducting polymers [175], metal oxides [176],
1211 and CNTs, have demonstrated exceptional performance in supercapacitors due to their synergetic
1212 effects. For instance, Zhou et al. [176] fabricated a hybrid hydrogel composed of graphene and
1213 poly(3,4-ethylenedioxythiophene) (PEDOT). The hybrid hydrogel demonstrated remarkable
1214 mechanical robustness, a notable specific capacitance of 174.4 F g⁻¹, and an electrical conductivity
1215 of 0.73 S cm⁻¹. These enhanced properties are primarily due to the synergistic interplay between
1216 the high electrical conductivity and mechanical integrity of graphene and the pseudocapacitive
1217 behavior of PEDOT.



Further advancements in graphene hydrogel functionalization have led to remarkable improvements in capacitance. Xu et al. [177] engineered a functionalized graphene hydrogel by introducing hydroquinone, resulting in a notable specific capacitance of 441 F g^{-1} at a current density of 1 A g^{-1} . In recent developments, composite hydrogels combining graphene with Ni(OH)_2 have been effectively fabricated and utilized as three-dimensional electrode materials for supercapacitor applications [178]. These hybrid hydrogels exhibited an exceptional specific capacitance of 1247 F g^{-1} at a scan rate of 5 mV s^{-1} , along with outstanding cycling stability. Additionally, graphene hydrogels have been successfully integrated with three-dimensional nickel foam frameworks to form composite electrodes for supercapacitor applications [179]. These composite electrode materials demonstrate excellent capacitive performance, primarily due to the synergistic interaction between the high electrical conductivity and electrochemical stability of graphene hydrogels, and the efficient charge transfer enabled by the minimal distance between the hydrogel matrix and the current collector.

Table 1. Key performance characteristics of graphene hydrogel-based supercapacitors.

Method	Testing Conditions	Modification	Electrolyte	Surface Area (m^2/g)	Pore Size (nm)	Capacitance	Ref.
Hydrothermal	Two-electrode	Hydroquinones	1 M H_2SO_4	297	2–70	441 F g^{-1} (1 A g^{-1})	[180]
Hydrothermal	Three-electrode	Ni(OH)_2	6 M KOH	92	—	1247 F g^{-1} (5 mV s^{-1})	[178]
Hydrothermal	Two-electrode	CNTs	30% KOH	237	—	318 F g^{-1} (0.1 A g^{-1})	[181]
Hydrothermal	Three-electrode	Co_3O_4	6 M KOH	—	—	757.5 F g^{-1} (0.5 A g^{-1})	[182]
Chemical reduction	Two-electrode	Ethylene diamine	2 M KOH	745	47	232 F g^{-1} (1 A g^{-1})	[169]
Hydrothermal	Three-electrode	Urea	6 M KOH	>1300	1.7–4.3	308 F g^{-1} (3 A g^{-1})	[183]
Hydrothermal	Two-electrode	Hydroxyl amine	25% KOH	—	—	205 F g^{-1} (1 mV s^{-1})	[184]
Hydrothermal	Two-electrode	—	5 M KOH	—	—	175 F g^{-1} (1 A g^{-1})	[171]
Hydrothermal	Two-electrode	Organic amine	5 M KOH	—	—	190.1 F g^{-1} (10 A g^{-1})	[185]
Chemical reduction	Two-electrode	L-Glutathione	0.5 M Na_2SO_4	315.2	2–10	157.7 F g^{-1} (1 A g^{-1})	[172]



Filtration	Two-electrode	—	1 M H ₂ SO ₄	—	—	255.5 F cm ⁻³ (0.1 A g ⁻¹)	[174]
Deposition	Two-electrode	Nickel foam	5 M KOH	1260–1725	—	45.6 mF cm ⁻² (0.67 mA cm ⁻²)	[179]
Hydrothermal	Two-electrode	—	5 M KOH	951	—	220 F g ⁻¹ (1 A g ⁻¹)	[186]
Chemical reduction	Three-electrode	Sodium ascorbate	1 M H ₂ SO ₄	—	—	240 F g ⁻¹ (1.2 A g ⁻¹)	[187]
Hydrothermal	Three-electrode	PPy	3 M NaClO ₄	463	—	330 F g ⁻¹ (1.5 A g ⁻¹)	[188]
Chemical reduction	Three-electrode	PANI	6 M KOH	—	—	334 F g ⁻¹ (2 A g ⁻¹)	[189]
Polymer cross-linking	Two-electrode	PEDOT	1 M Na ₂ SO ₄	—	—	104 F g ⁻¹ (0.5 A g ⁻¹)	[190]
Hydrothermal	Two-electrode	—	H ₂ SO ₄ –PVA gel	414	2–70	186 F g ⁻¹ (1 A g ⁻¹)	[191]

4.1.1.2.2 Graphene based aerogels for supercapacitors

Substituting the aqueous phase within graphene hydrogels with air, while maintaining the integrity of the three-dimensional porous framework, results in the formation of graphene aerogels. These structures are generally produced through supercritical drying or freeze-drying methods applied to graphene-based wet gels. For instance, Chen et al. synthesized rGO aerogels by initiating gelation of rGO sheets in an aqueous medium, followed by freeze-drying to preserve the porous architecture [192]. The resulting rGO aerogels possess a robust three-dimensional porous architecture with notable mechanical strength. In recent years, there has been a surge of interest in the application of graphene aerogels for supercapacitors, largely due to their extensive 3D interconnected networks, continuous porosity, and high specific surface area. These structural features facilitate efficient ion transport and electrolyte access, enhancing charge storage capabilities. Consequently, rGO aerogels have been actively investigated and successfully employed as promising electrode materials in supercapacitor devices. Reduced graphene oxide (rGO) aerogels can be synthesized through various reduction methods, such as thermal reduction [193] or hydrogen (H₂) reduction [194] of graphene oxide (GO) aerogels. Alternatively, GO can be pre-reduced in its wet gel state, followed by freeze-drying or supercritical drying processes. Reducing agents like mercaptoacetic acid [195], L-ascorbic acid [173] and hypophosphorous acid [194] are commonly used to promote the gelation and reduction of GO. Liu et al. used thermally reduced graphene oxide (GO) aerogels

to create a flexible, folded structured graphene paper [196]. They showed that the electrodes made of graphene exhibited superior capacitive performance compared to the carbon materials that are currently accessible.

Additionally, these electrodes are more flexible, freestanding, binder-free, and mass-producible. Extensive efforts have been focused on developing graphene aerogel-based composites for supercapacitor applications. For example, Wu et al. prepared nitrogen and boron co-doped graphene aerogels by adding ammonia boron trifluoride to wet gels, followed by freeze-drying. These doped graphene aerogels were then used as electrode materials in an all-solid-state supercapacitor with a PVA-H₂SO₄ gel electrolyte. The supercapacitors demonstrated a specific capacitance of approximately 62 Fg⁻¹, an energy density of about 1600 W kg⁻¹, and excellent cycling stability [197]. Beyond elemental doping, organic molecules and polymers have been widely explored for modifying graphene aerogels. The synthesis of hybrid graphene-based aerogels using carbohydrates such as glucose, β -cyclodextrin, and chitosan has improved electrochemical performance with robust and stable capacitance retention [198]. In order to further enhance the electrochemical characteristics of graphene aerogel networks, the addition of metal oxides has also been studied. By adding metal oxides like CoO₄ and RuO₂ to the network structure, Wu et al. created graphene-based composite aerogels. These composite aerogels demonstrated remarkable cycle stability, high-rate capabilities, and an excellent specific capacitance of 226 Fg⁻¹. The synergistic impacts of the pseudocapacitive metal oxides and the intrinsic qualities of the graphene aerogels, such as their high surface area, superior electrical conductivity, and electrochemical stability, were responsible for the improved electrochemical performance [199]. Furthermore, Meng and colleagues developed graphene/carbon composite aerogels by embedding graphene into a carbon aerogel precursor (resorcinol-formaldehyde). These composite aerogels demonstrated a commendable specific capacitance of 122 Fg⁻¹ at a current density of 50 mA g⁻¹, along with impressive rate performance [200].



1279 **Table 2.** Overview of recent progress in graphene aerogel-based supercapacitors, detailing
1280 synthesis techniques and capacitance performance

Methods	Modification	Electrolyte	Testing conditions	Surface area and pore size	Capacitance	Ref.
Pyrolization	Carbon	6 M KOH	0.05 Ag ⁻¹ , two-electrode	361 – 763 m ² g ⁻¹ , 10 – 50 nm	122 F g ⁻¹	[200]
Freeze-drying	Carbohydrates	Na ₂ SO ₄	0.5 Ag ⁻¹ , three-electrode	12.5 – 364.6 m ² g ⁻¹ , —	161.6 F g ⁻¹	[198]
Supercritical-drying	Hypophosphorous acid	1 M H ₂ SO ₄	0.2 Ag ⁻¹ , three-electrode	830 m ² g ⁻¹ , 4 nm	278.6 F g ⁻¹	[194]
Supercritical-drying	-	Ionic liquid	0.1 Ag ⁻¹ , three-electrode	870 m ² g ⁻¹ , 2 – 50 nm	153 F g ⁻¹	[201]
Freeze-drying	Metal oxides	1 M H ₂ SO ₄	1 mV s ⁻¹ , three-electrode	350 m ² g ⁻¹ , 2 – 3.5 nm	226 F g ⁻¹	[199]
Freeze-drying	Nitrogen and boron co-doping	H ₂ SO ₄ -PVA	5 mV s ⁻¹ , three-electrode	249 m ² g ⁻¹	62 F g ⁻¹	[197]
Freeze-drying	L-Ascorbic acid	6 M KOH	0.05 Ag ⁻¹ , two-electrode	512 m ² g ⁻¹ , 1.5–55 nm	128F g ⁻¹	[201]
Freeze-drying	-	1 M H ₂ SO ₄	1 Ag ⁻¹ , two-electrode	-	172 F g ⁻¹	[196]

1281
1282 **Table 3.** Overview of Advanced Carbon Aerogel Materials Utilized in Energy Storage
1283 Applications.

Materials	Key Features	Energy Density	Power Density	Specific Capacitance	Ref.
Thionine-functionalized 3D graphene aerogel (ThGA)	Flexible, metal-free supercapacitor - Synergistic capacitance enhancement - Sponge-like structure for electrolyte ion access	32.6 Wh/kg	12.8 kW/kg	384 F/g (1 A/g)	[202]
N-doped graphene aerogel-	Direct growth of V ₂ O ₅ nanowires on N-GA backbone - Well-aligned nanowires observed in	98.6 Wh/kg	250 W/kg	711 F/g (0.5 A/g)	[203]

vanadium pentoxide (N-GA@V ₂ O ₅)	SEM - Enhanced electrochemical properties				
N-self-doped carbon nanofiber aerogel (NCNF)	In-situ synthesis of ZIF-8 on bacterial cellulose - 3D conductive network for efficient electron transport - Silk cocoon-like nodes for large electrochemical surface area	31.0 Wh/kg	250 W/kg	224 F/g (0.5 A/g) 612 mF/cm ² (1.37 mA/cm ²)	[204]

Shabangoli et al. and Sun et al. have demonstrated innovative approaches for enhancing supercapacitor performance using advanced graphene-based aerogels. Shabangoli et al. introduced a thionine-functionalized 3D graphene aerogel (Th-GA), which exhibited improved capacitance due to enhanced redox kinetics and increased active site accessibility, supported by its porous, sponge-like structure shown in figure (14a-c). Their device achieved a specific capacitance of 384 F/g, with energy and power densities of 32.6 Wh/kg and 12.8 kW/kg, respectively. In a related study, Sun et al. synthesized a nitrogen-doped graphene aerogel-vanadium pentoxide (NGA@V₂O₅) nanocomposite through the direct growth of V₂O₅ nanowires on the N-GA framework. The resulting structure showed excellent alignment and electrochemical performance, delivering a high specific capacitance of 711 F/g, along with an energy density of 98.6 Wh/kg and a power density of 250 W/kg shown in figure (14d(i-iii)). These findings highlight the potential of functionalized graphene aerogels as high-performance materials for next-generation energy storage devices [202, 203]. Overall, literature evidence shows that graphene-based aerogels, whether in pure, doped, or composite form, deliver exceptional capacitive performance due to their hierarchical porosity, high conductivity, and structural robustness. Functionalization strategies, particularly heteroatom doping and incorporation of pseudocapacitive components, further enhance their energy and power densities, confirming their strong potential for next-generation supercapacitors.



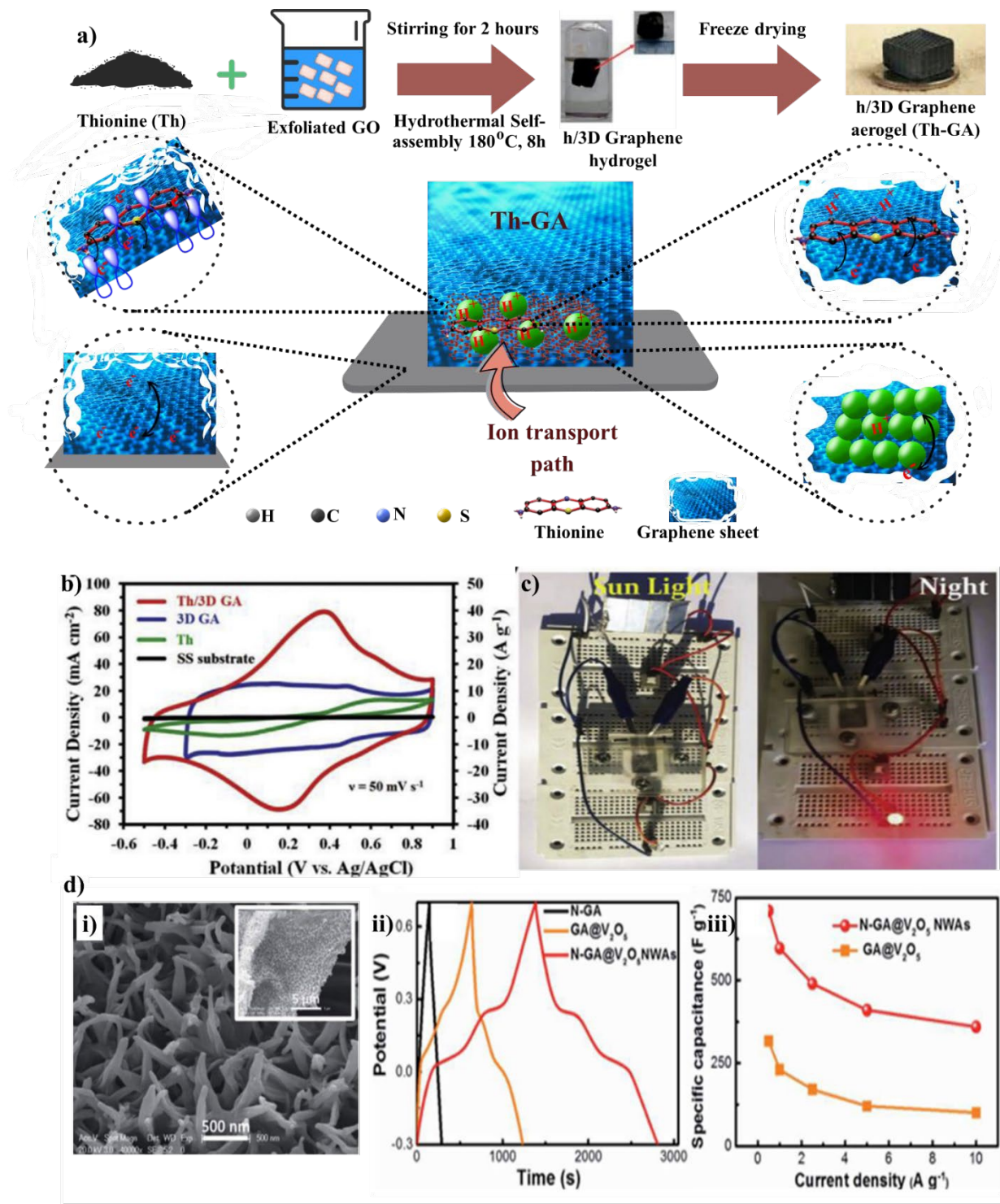


Figure 14. (a) Schematic illustration of the functionalization process of a 3D graphene aerogel with thionine. (b) Electrochemical performance comparison among stainless steel (SS) substrate, pure thionine (Th), graphene aerogel (GA), and thionine-functionalized graphene aerogel (Th–

GA) at a scan rate of 50 mV/s in 1 M H₂SO₄ electrolyte. (c) Experimental setup of an asymmetric Th-GA solar-powered device, demonstrating its ability to power a red LED for over 5 minutes. (d) (i) SEM images displaying the oriented growth of V₂O₅ nanowire arrays on a 3D nitrogen-doped graphene aerogel (N-GA@V₂O₅). (ii) Galvanostatic charge-discharge profiles for various samples. (f) Specific capacitance values of GA@V₂O₅ and N-GA@V₂O₅ mesoporous wide arrays (MWAs) at multiple current densities. Reproduced from reference [202, 203] with permission from Wiley & Royal society of chemistry, copyright 2018.

4.1.1.3 Carbon nanotube-based aerogels for supercapacitors

CNT aerogels are three-dimensional porous structures composed of CNTs as the primary building blocks. A variety of fabrication methods have been developed to produce CNT-based aerogels, including freeze-drying [205], critical-point drying [206, 207], and chemical vapor deposition (CVD) [205]. For instance, Zou et al. [208] synthesized a MWCNT aerogel using a freeze-drying method. In their approach, pristine MWCNTs were first dispersed in chloroform via sonication, with poly-(3-hexylthiophene)-b-poly(3-(trimethoxysilyl)propyl methacrylate) (P3HT-b-PTMSPMA) acting as both a surfactant and a cross-linking agent to facilitate the gelation process. This method enabled the formation of a well-structured MWCNT aerogel with enhanced properties suitable for various applications. Following polymer cross-linking, a wet gel was formed, which was subsequently converted into an aerogel via freeze-drying. The resulting MWCNT aerogel demonstrated a low mass density of 4 mg/cm³, an impressive electrical conductivity of 3.2×10^{-2} S/cm, and a significant surface area of 580 m²/g (Figure 15). Furthermore, it demonstrated excellent mechanical resilience, showing minimal thickness reduction even after 1000 compression-recovery cycles.



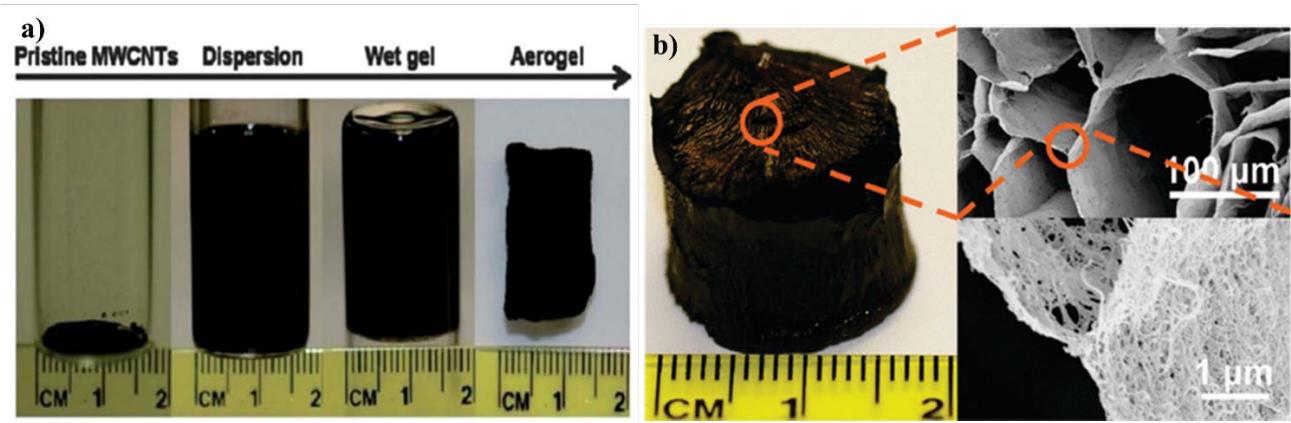
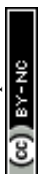


Figure 15. (a) Photographs showing the step-by-step fabrication process of MWCNT aerogels. (b) Image of an ultralight multiwalled carbon nanotube aerogel. Reprinted from reference [208] with permission from ACS, copyright 2010.

Recent studies have increasingly focused on hybrid and composite CNT aerogels for diverse applications. Qi et al. [209] developed cellulose-CNT hybrid aerogels through freeze-drying wet-gel precursors. These aerogels exhibited excellent mechanical properties, thermal stability, and high sensitivity to ambient pressure, making them promising candidates for applications in gas and volatile organic compound sensing. Similarly, Sun et al. [47] fabricated ultralight CNT-graphene composite aerogels by freeze-drying a CNT-graphene aqueous suspension. The aerogels' unique three-dimensional structure, featuring graphene walls and CNT ribs, endowed them with remarkable elasticity, low density (around 0.16 mg/cm³), excellent thermal stability, good electrical conductivity, and high adsorption capacities for organic compounds. A novel self-crosslinking approach has been introduced for the hydrothermal synthesis of PVA aerogels, facilitated by MWCNTs by Chong-Bo Ma [210]. PVA, a widely available and cost-effective polymer, simplifies the fabrication process while preserving its environmentally friendly nature by eliminating the need for additional organic crosslinkers. The tunability of crosslink density and other material properties is achieved by varying the concentration of PVA precursors. During hydrothermal treatment, dehydration between hydroxyl groups induces a transition in wettability from hydrophilic to hydrophobic, enabling the aerogel to efficiently absorb organic solvents such as bean oil and crude oil, with uptake values ranging from 10 to 52 times its initial weight. Moreover, cytotoxicity tests verify low toxicity, which qualifies these aerogels for use in environmental bioengineering. Furthermore, by undergoing in situ hybridization with polypyrrole,

these aerogels can be converted into conductive materials with a conductivity of 0.16 S/m. The aerogels' many hydroxyl groups also make it possible for additional chemical alterations, increasing their functional adaptability for a variety of cutting-edge uses.

Wanqing Wang has created a new ambient-dried technique that uses CNTs and cellulose nanofibrils (CNFs) to create functional aerogels without the need for chemical crosslinking [211]. This method creates aerogels with mechanically strong pore walls by crosslinking CNFs and CNTs using a freeze-thaw cycling procedure. Hybrid networks of hydrophilic and hydrophobic nanofibers are effectively created by utilizing a special dual-network interpenetrating structure made possible by the tubular dispersion of CNFs and CNTs. The resultant aerogels had a high specific surface area (157.24 m²/g), outstanding electrical conductivity (30.95 S/cm), and tunable densities (as low as 0.0519 g/cm³). Furthermore, these aerogels are more recyclable due to the lack of chemical crosslinkers. With diameters up to 8.68 cm, its structure and shape can be altered using mold-based or 3D printing methods, enabling scalable production. These aerogels show remarkable electromagnetic shielding performance (440.9 dB•cm³/g) in figure 16a. They also function as effective freestanding electrodes for active material loading, like MnO₂, resulting in remarkable energy storage capacities (551 F/g). In addition, the technique can be applied to various nanofiber systems, including polyimide (PI) and aramid nanofibers (ANF), opening the door to a wide variety of structural and functional uses. Large graphene walls and CNT ribs combine to form the 3D networks of CNT-graphene composite aerogels, which provide an amazing array of characteristics. Excellent elasticity, great thermal stability, outstanding electrical conductivity, ultralow density ($\rho < 0.16 \text{ mg cm}^{-3}$), and a notable capacity for organic chemical adsorption are all displayed by these aerogels. The CNT-based aerogels combine the special qualities of aerogels, such as their 3D porous structure, low mass density, continuous porosity, and high surface area, with the advantages of CNTs, such as their high electrical conductivity, mechanical resilience, and thermal conductivity. Because of these characteristics, CNT aerogels are excellent choices for polarizable electrodes in supercapacitors. Moreover, the interconnected 3D networks with multiple pores in the aerogels provide a perfect platform for incorporating various electrode materials, such as activated carbon, metal oxides, and conducting polymers, thereby increasing their capacitive performance.



Research on CNT-based supercapacitors has greatly increased during the last few decades. The initial use of CNTs as electrode materials in supercapacitors was reported by Niu et al. [212] in 1997. Their study demonstrated that nitric acid-treated CNT electrodes achieved a high surface area of 430 m²/g and a specific capacitance of 102 F/g. More recently, CNT aerogels have been explored as advanced electrode materials due to their unique structural and functional attributes. Li et al. [213] developed a CNT sponge (or aerogel) using the CVD technique, resulting in a three-dimensional conductive network with excellent compressibility and shape recovery. Electrochemical analysis revealed that the specific capacitance of CNT sponge-based electrodes remained above 90% even under 50% compressive strain and retained over 70% of capacitance under 80% strain. Such results indicate that these compressible and deformation-resistant electrodes hold promise for flexible supercapacitor applications. Additionally, CNT aerogels have been modified with conducting polymers to improve their electrochemical performance. For instance, Lee et al. [213] developed a transparent and flexible hybrid nanomembrane by coating CNT aerogel sheets with poly(3,4-ethylenedioxythiophene), which enhanced mechanical strength and flexibility. Supercapacitors utilizing these hybrid electrodes demonstrated a volumetric capacitance of about 40 F/cm³ at 100 V/s, an energy density of approximately 70 Wh/cm³, and a power density of around 7910 W/cm³. Similarly, Zhong et al. [214] synthesized polyaniline-coated CNT sponge composites, which exhibited excellent areal capacitance (1.62 – 1.85 F/cm²) alongside good cycling stability and high-rate capability. Furthermore, researchers have explored the creation of CNT composite aerogels by integrating CNTs with other carbon-based materials, such as cellulose nanofibers and mesoporous carbon, to further enhance their performance for supercapacitor applications.

Pore formation and heteroatom doping are key factors for improving the power and energy densities of nanostructured carbon electrodes. Chao Yang et al. [215] introduced an innovative method for fabricating bamboo-like nitrogen and sulfur co-doped carbon nanotube aerogels (NS-CNAs) using a straightforward process that includes MnO₂-templated polymerization, freeze-drying, and subsequent calcination. The cryptomelane-type MnO₂ nanowires act as self-sacrificing templates and oxidative initiators for pyrrole polymerization in an acidic medium. X-ray photoelectron spectroscopy (XPS) analysis reveals nitrogen and sulfur contents of 4.09% and 0.66%, respectively, with nitrogen primarily sourced from the pyrrole polymer backbone and sulfur from poly(styrenesulfonate) (PSS) with sulfonic acid groups. Due to their distinctive porous



structure and N/S co-doping, NS-CNA-based supercapacitors (SCs) deliver exceptional electrochemical performance (figure 16b,c) achieving a specific capacitance of 328 F g^{-1} at 1 A g^{-1} , a rate capability of 66.5% (from 1 A g^{-1} to 10 A g^{-1}), an energy density of 45.6 Wh kg^{-1} at 0.5 kW kg^{-1} , and impressive capacity retention of 97.4% after 10,000 cycles. Literature studies confirm that CNT-based aerogels combine the inherent conductivity and mechanical robustness of nanotubes with the high surface area and tunable porosity of aerogels, resulting in excellent performance as supercapacitor electrodes. Functionalization, composite formation, and heteroatom doping consistently improve their capacitance, rate capability, and cycling stability, underscoring their potential for flexible and high-energy-density energy storage devices.

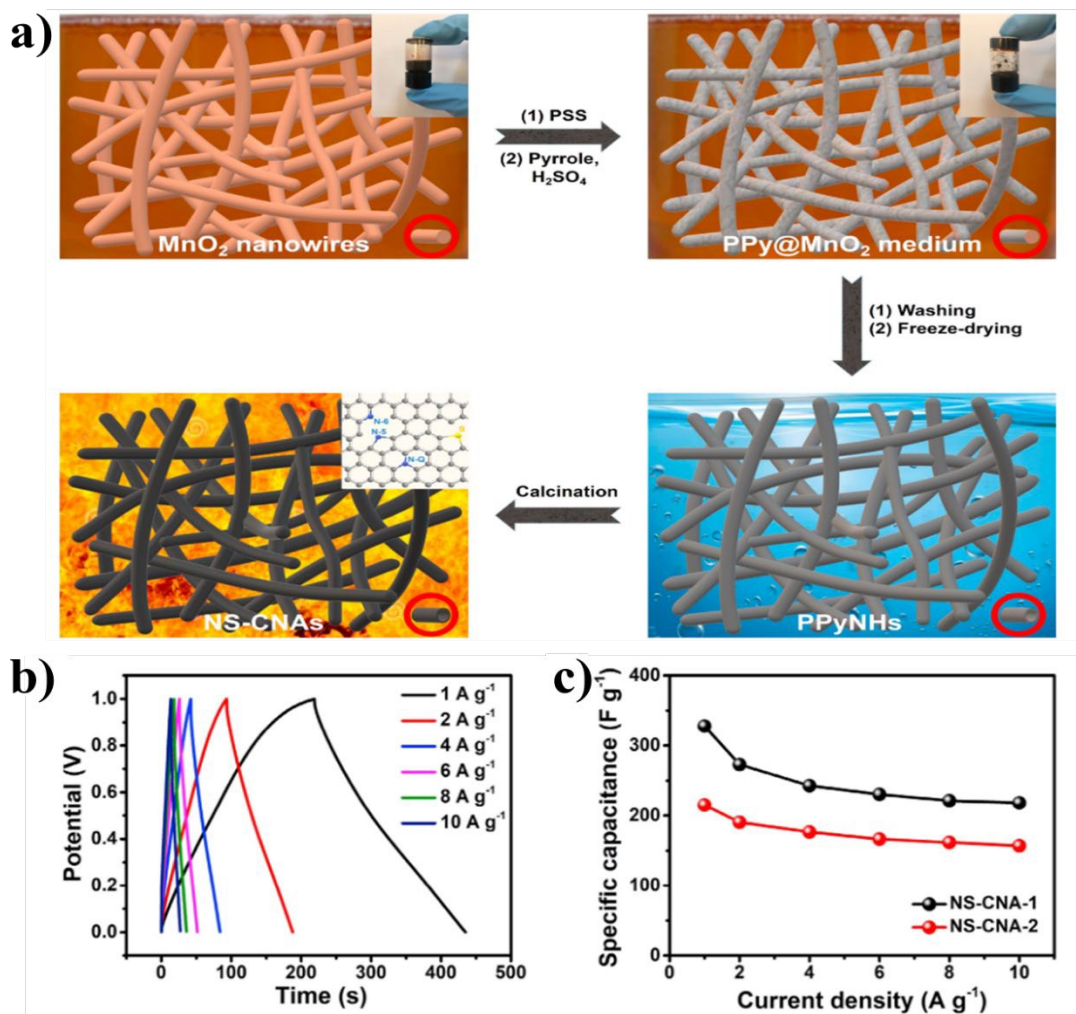


Figure 16. (a) Schematic illustration of the synthesis process for nitrogen and sulfur co-doped carbon nanotube aerogels (NS-CNAs) involving MnO₂-templated polymerization, freeze-drying, and calcination. Insets show photographs of MnO₂ nanowires and PPyNHs, along with a structural model of graphitized N/S-co-doped carbon. (b) Electrochemical performance of NS-CNA supercapacitors at different current densities. (c) Gravimetric specific capacitance measurements. Reprinted from reference [215] with permission from Elsevier, copyright 2021.

Table.4. Characteristics of various CNT aerogel-based supercapacitors

Method	Modification	Electrolyte	Testing conditions	Surface area and pore size	Capacitance	Ref.
CVD	Carbon aerogel	5 M KOH	1 mA, three-electrode	670–710 m ² g ⁻¹ , —	524 Fg ⁻¹	[216]
Freeze-drying	Mesoporous carbon	1 M KOH	10 mVs ⁻¹ , three-electrode	871 m ² g ⁻¹ , 1.3–50 nm	214 Fg ⁻¹	[217]
Supercritical drying	Cellulose nanofibers	H ₂ SO ₄ –PVA gel	5 mV s ⁻¹ , two-electrode	871 m ² g ⁻¹ , 1.3–50 nm	178 Fg ⁻¹	[218]
CVD	Microfibrinous carbon	5 M KOH	-, -	1059 m ² g ⁻¹ , 1.41 nm	524 Fg ⁻¹	[219]

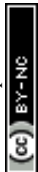
4.1.1.4 Other porous materials for supercapacitors

In addition to carbon gels, several other porous materials have been widely investigated for supercapacitor electrodes due to their high surface areas, tunable pore structures, and electrochemical stability. Activated carbons are the most commercially established, offering surface areas often exceeding 2000 m²/g, cost-effective large-scale production, and chemical stability in various electrolytes. However, their predominantly microporous structures can restrict ion transport at high charge-discharge rates, limiting power density. MOFs and their derivatives, particularly MOF-derived carbons, have attracted attention for their controllable pore sizes, high porosity, and ability to incorporate heteroatoms, thereby improving conductivity and pseudocapacitive behavior. Nevertheless, MOFs face challenges in cost, stability, and scalability for industrial applications. Functionalized nanomaterials, such as heteroatom-doped graphene, CNTs, and hybrid composites, combine high electrical conductivity with tunable surface chemistry

to enhance charge storage mechanisms. Nitrogen, sulfur, or phosphorus doping can increase wettability, active site density, and faradaic activity, while composite architectures-such as CNT/graphene hybrids-improve mechanical integrity and ion transport pathways. Additionally, porous transition metal compounds (oxides, hydroxides, sulfides) and conducting polymers can contribute pseudocapacitance, significantly boosting energy density, though they often suffer from cycling stability issues. Hybridizing these materials with porous carbons can mitigate such drawbacks by enhancing structural support and electrical connectivity. Compared to these alternatives, carbon gels offer a unique balance of hierarchical porosity, tunable surface chemistry, and precursor flexibility, enabling fast ion transport and high capacitance while allowing sustainable synthesis routes from biomass. This positions carbon gels alongside activated carbons, MOF-derived carbons, and functionalized nanocarbons as leading candidates for next-generation supercapacitor electrodes, with material choice dictated by the target balance between energy density, power density, cycle life, and production cost [220].

4.1.2 Advances in materials and design strategies for next-generation supercapacitors

Supercapacitors (SCs) have gained considerable attention for their ability to deliver high power density, long cycle life, and rapid charge–discharge capability, making them ideal for applications ranging from portable electronics to grid-level energy storage. The performance of SCs is largely determined by the properties of the electrode materials, which govern energy storage mechanisms, ion transport, and cycling stability. Conventional carbon-based electrodes, including carbon gels, offer high surface areas and tunable pore structures, supporting rapid EDLC. However, to achieve higher energy densities while maintaining power performance, recent research has explored integrating advanced nanostructured materials and surface engineering techniques. MXenes, particularly M_5X_4 phases (where M is an early transition metal and X is C or N), have emerged as promising candidates due to their metallic conductivity, hydrophilic nature, and interlayer tunability [221–224]. Surface engineering of MXenes-through heteroatom doping, defect modulation, or functional group grafting-can expand interlayer spacing, increase accessible active sites, and improve electrolyte wettability, thereby enhancing capacitance and rate capability [224]. Transition metal dichalcogenides (TMDs), such as MoS_2 and WS_2 , are also gaining attention as pseudocapacitive materials due to their layered structures and redox-active sites. Recent advances focus on hybridizing TMDs with conductive carbons (graphene, CNTs, carbon gels) to mitigate



1471 their poor intrinsic conductivity and structural degradation during cycling. These composites can
1472 synergistically combine the fast ion transport of porous carbons with the high capacitance of TMD
1473 layers, yielding devices with improved areal and volumetric energy densities [225].

1474 Black phosphorus (BP) has emerged as another multifunctional electrode material, offering a
1475 tunable bandgap, high carrier mobility, and abundant redox-active sites. In supercapacitor
1476 applications, BP can contribute both EDLC and pseudocapacitance, while also enabling flexible
1477 and wearable device architectures. However, BP's environmental instability remains a challenge;
1478 encapsulation, surface passivation, and hybridization with porous carbon matrices have proven
1479 effective in improving its durability and electrochemical stability [226]. Integrating these advanced
1480 materials with carbon gels offers a pathway to high-performance, next-generation supercapacitors
1481 that combine the hierarchical porosity, conductivity, and structural stability of carbon gels with the
1482 high-capacitance properties of pseudocapacitive nanomaterials. Such hybrid systems hold
1483 significant promise for bridging the gap between batteries and traditional SCs, enabling devices
1484 with both high energy and power densities. Carbon-based materials continue to serve as the
1485 foundational framework for high-performance supercapacitor electrodes due to their high
1486 electrical conductivity, chemical stability, and controllable porous architectures. They function not
1487 only as active charge storage media through electric double-layer capacitance but also as robust
1488 conductive skeletons for supporting pseudocapacitive materials, improving both mechanical
1489 integrity and electron transport. Recent reviews have highlighted the strategic design of carbon
1490 architectures-ranging from activated carbons to advanced carbons such as graphene, carbon
1491 nanotubes, and carbon gels-as a critical factor in achieving a balance between high energy and
1492 power densities [227, 228]. The integration of hierarchical porosity (micro-, meso-, and
1493 macropores) ensures rapid ion transport, maximized accessible surface area, and enhanced
1494 electrolyte penetration, while surface functionalization offers additional routes for improving
1495 wettability and interfacial charge transfer. Furthermore, combining carbon-based scaffolds with
1496 emerging high-capacitance materials-such as MXenes, transition metal dichalcogenides, and black
1497 phosphorus-creates hybrid systems that leverage the conductivity and structural stability of
1498 carbons with the redox activity of pseudocapacitive components. Such composite strategies are
1499 proving to be vital in bridging the performance gap between supercapacitors and batteries,
1500 enabling next-generation devices with enhanced energy density, rate capability, and long-term
1501 cycling stability.



4.2 Fuel cells

Fuel cells have drawn interest from the scientific community globally as viable power sources for portable devices and environmentally friendly electric cars. Fuel cells come in various types, each depending on factors such as the fuel used, the type of membrane, and the operating conditions. Among these, the most extensively researched are hydrogen-based fuel cells, direct methanol fuel cells (DMFCs), direct ethanol fuel cells (DEFCs), and microbial fuel cells (MFCs) [229]. Below is a schematic diagram illustrating the general working principle of a fuel cell (figure 17 a). In all fuel cell types, oxidation takes place at the anode: in hydrogen-based fuel cells, hydrogen undergoes oxidation, while in DEFCs and DMFCs, ethanol or methanol is oxidized to carbon dioxide. At the cathode, oxygen or air is reduced, resulting in the production of water, electricity, and heat as by-products [157, 230]. In MFCs, the electrochemical activity of bacteria facilitates electron exchange, converting chemical energy into electrical energy. This section explores recent advancements in the use of hydrogels in various fuel cell applications.

Du et al. [231] employed carbon aerogels as a catalyst support for loading Pt-Ru bimetallic nanoparticles, aiming to optimize both the Pt-Ru composition and the operating temperature for DMFC anodes configured with membrane electrode assemblies. The carbon aerogels, characterized by a high BET surface area of 576 m²/g, facilitated efficient mass transport of methanol fuel and CO₂ exhaust, thereby improving catalytic performance while minimizing the required amounts of Pt-Ru and reducing system costs. This porous aerogel structure proved especially advantageous for low-temperature DMFCs by supporting effective two-phase flow. Additionally, reduced Ru content was shown to be more beneficial under low-temperature conditions. Additionally, a Pt NPs/graphene hydrogel was deposited in the micropores of Ni foam for DMFC anodes, significantly improving electrocatalytic activity compared to Pt/reduced G.O catalysts. The three-dimensional Ni foam structure ensures the availability of small Pt NPs (4 – 6 nm), enhancing activity by 2.6 times and methanol oxidation rate by 27 times relative to Pt/reduced G.O. The graphene component reduces Pt usage while improving catalytic performance, allowing binder-free electrode application. The high conductivity and porous network enable efficient transport of methanol molecules, ions, and electrons. Optimal Pt precursor concentration is essential to prevent agglomeration and ensure homogeneous Pt distribution, while oxygen functionalities at graphene edges aid in Pt NPs anchoring [232].



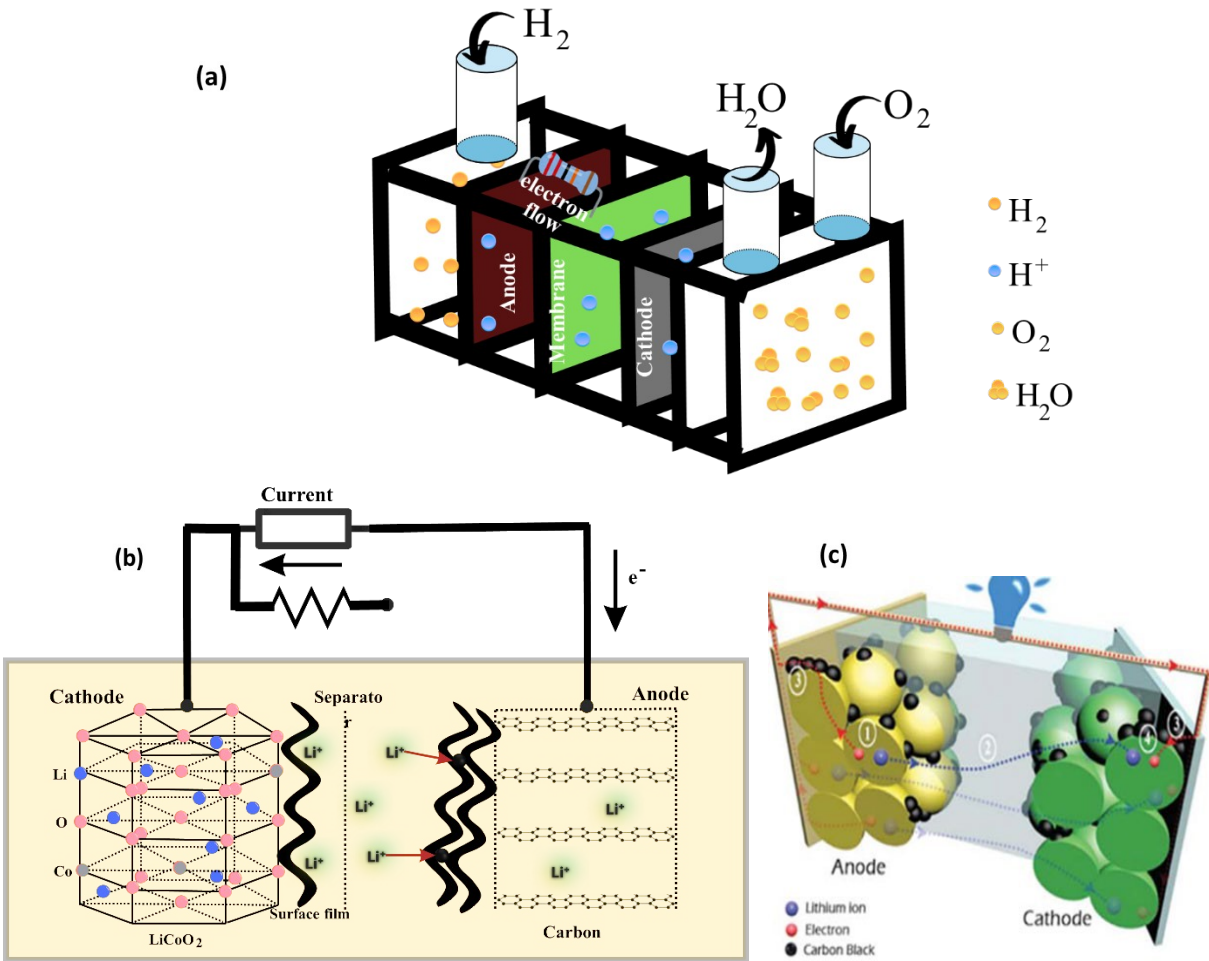


Figure 17. (a) Diagram of a basic fuel cell. (b) Schematic of a typical lithium-ion battery featuring a graphite anode and a LiCoO₂ cathode. (c) Illustration of lithium-ion and electron transport routes during the battery discharge process. Reproduced from reference [100] with permission from Royal society of chemistry, copyright 2019.

Kakaei et al. [233] synthesized Pd nanoparticles with an average size of approximately 3 nm, uniformly embedded within a nitrogen-doped graphene hydrogel matrix using a polyol reduction method. The resulting composite exhibited enhanced electrocatalytic activity, attributed to the strong synergistic effect between the conductive graphene network and the Pd nanoparticles. Similarly, hydrogels have been investigated as electrode platforms for DEFCs. For example, developing cyclodextrin-functionalized Pd nanoparticle hydrogels, this demonstrated significantly

improved ethanol oxidation performance. This enhancement is primarily due to host-guest interactions between cyclodextrin and ethanol molecules, promoting more efficient catalytic activity compared to conventional Pd-based systems. Zhu et al. [96] implemented an *in-situ* reduction strategy using sodium borohydride (NaBH_4) to simultaneously initiate gelation and reduce metal precursors, with reaction kinetics modulated by temperature. Notably, they pioneered the development of bimetallic hydrogel/aerogel composites incorporating non-noble metals, achieving rapid synthesis without the need for capping agents. By varying the ratios of binary metallic systems- such as PdCu, PtCu, and AgCu- they effectively optimized electrocatalytic activity. This approach represents a cost-efficient pathway for fabricating high-performance catalysts. In a subsequent study [234], a self-supporting trimetallic hydrogel composed of $\text{Ni:Pd}_x\text{Pt}_y$ (where x and y vary from 0 to 1) was synthesized. This architecture exhibited significantly enhanced electrocatalytic efficiency for ethanol oxidation, benefiting from the corrosion resistance of the freestanding structure, improved electron transfer through the metallic backbone, and efficient mass transport within the 3D carbon framework. The combined shape and compositional control of the Ni:PdPt nanoclusters contributed to their superior catalytic performance.

To overcome the inherent brittleness of carbon aerogels, which often compromises structural integrity during traditional electrode fabrication, introduced a versatile *in situ* silicone-confined gelation technique. This method enables the direct integration of metal aerogels- such as PtPd, PtAg, PdAg, and AuAg- onto robust macroporous substrates like carbon cloth, carbon fiber foam, and nickel foam. The resulting composite structures exhibit superior mechanical flexibility and retain the native 3D architecture of metal aerogels. This innovative strategy promotes enhanced electron conductivity and rapid mass diffusion, while also mitigating issues like Ostwald ripening and nanoparticle aggregation. In contrast to conventional ink-drop coating, which often compresses and damages aerogel structures, the silicone-confined gelation technique significantly improves both the electrocatalytic performance and operational stability of the resulting electrodes [234]. Because hydrogel-based electrodes can overcome important constraints in bioelectrochemical systems, especially those related to electron transfer efficiency and biocompatibility, they have demonstrated significant promise in MFC applications. For example, a carbon paper anode coated with a CNT-chitosan hydrogel showed increased electrocatalytic



Open Access Article. Published on 21 August 2025. Downloaded on 9/5/2025 7:05:43 PM.
This article is licensed under a Creative Commons Attribution-NonCommercial 3.0 Unported Licence.



activity, which was explained by the combined effects of chitosan's oxygen-containing functional groups and high electrical conductivity of CNTs [96]. Effective microbial electron transfer, a frequently limiting step in MFC efficiency, was further encouraged by the support of hydrogel matrix for the development of a strong, multi-layered biofilm. Furthermore, quinone-rich surface of CNTs enhanced charge transport between microorganisms and the electrode by acting as an inherent redox mediator. In a different method, a high-performance bioanode was a bacterial cellulose (BC) hydrogel coated with polypyrrole (PPy). The conductivity and electrocatalytic capabilities of PPy were combined with the biocompatibility and high-water retention of BC in this composite structure. A stable design that withstood microbial degradation, improved power and current densities, and a well-adhered microbial layer were the outcomes. Additionally, the BC surface's conductive polymer-coated fibers facilitated quick charge transfer, surpassing both untreated BC and traditional graphite anodes. This hydrogel-based material is a promising method for creating sustainable energy solutions because of its biocompatibility and capacity to promote biofilm development by effectively delivering water-soluble nutrients to bacteria. The performance of hydrogel-based electrodes in fuel cells is determined by a number of important factors. One important metric, the ratio of forward to backward anodic peak current density (I_x/I_b), indicates effective alcohol oxidation while reducing the buildup of carbonaceous species. These results demonstrate how hydrogel-based materials can be used to develop energy conversion systems. Overall, the literature indicates that integrating hydrogels and aerogels into fuel cell electrodes significantly enhances catalytic activity, durability, and mass transport properties. Tailoring composition, structure, and support materials has been shown to optimize efficiency across DMFCs, DEFCs, and MFCs, highlighting these materials' strong potential in advancing sustainable and high-performance fuel cell technologies.

Table 5. Hydrogels based on carbon for use in fuel cells

Type of hydrogel	Main material constituents	Main electrocatalytic features	Ref.
Metal particle-carbon based hydrogel	Bimetallic Pt-Ru loaded on carbon aerogels (Pt:Ru ratio	50 at% Ru content is the appropriate catalyst composition for high temperature direct methanol fuel cells (DMFCs), but at a temperature lower than 40 C, a lower Ru content is better and with only two-thirds of	[96]

	varied as 1:1, 2:1 and 3:1)	noble metal being used, the membrane electrode assembly (MEAs) prepared by PtRu/CA can reach the same power density of a commercial catalyst in a single DMFC test	
Metal NP-graphene based hydrogel	Pt/PdCu nanoboxes in a 3D-graphene matrix	Peak current density is 183 mAcm^{-2} , a single-cell for (direct ethanol fuel cell) DEFC gives a maximum power density of 40 mW cm^{-2} , for Pt/PdCu/3DGF almost two times that of Pt/C (21 mWcm^{-2})	[235]
Ternary Pt ₃₆ Pd ₄₁ Cu ₂₃ nanowire-based hydrogel	Pt, Pd, Cu nanowires synthesized via a surfactant-free, acid-etched method, integrated into a hydrogel matrix	Exhibit an ultrathin ($\sim 5 \text{ nm}$) nanowire structure with an optimal Pt:Pd:Cu ratio of 36:41:23. These nanowires demonstrate significantly enhanced electrocatalytic performance, achieving 4.38 mA/cm^2 for EOR ($19.8\times$ higher than Pt/C) and 1.16 mA/cm^2 for ORR ($5.7\times$ higher than Pt/C). When used in a DEFC, they deliver a power density of 21.7 mW/cm^2 at 80°C with a Pt loading of 1.2 mgPt/cm^2 , representing a $3.9\times$ improvement over conventional Pt/C catalysts. The superior performance is attributed to the synergistic interaction of Pt, Pd, and Cu, which enhances CO tolerance, promotes C–C bond cleavage, and improves durability by preventing Ostwald ripening and aggregation.	[236]
Metal NP-graphene based hydrogel	Pd NPs in an N-doped reduced graphene matrix synthesised via polyol-assisted reduction	Methanol oxidation catalyst, the ECSA of the PdNPs/RDNG is $55.8 \text{ m}^2 \text{ g}^{-1}$, If $\frac{1}{4}$ 2.71 Amg^{-1} Pd, electrocatalytic activity of 2.71 Amg^{-1} Pd and good cycle life (66.5% forward peak current retention after 1000 cycles), $I_f/I_b \frac{1}{4} 5$	[237]
Noble metal NP-graphene based hydrogel	Pt NPs in a graphene hydrogel matrix,	Methanol oxidation catalyst, (I_f) increases with Pt loading (mPt), highest at 139.0 mA cm^{-2} . Onset potentials (E_{onset}) $\frac{1}{4}$ 0.42 to 0.45 V, electrocatalytic	[238]



	deposited on Ni foam	activity (I_f/mPt) $\frac{1}{4}$ 481.5 mA mg^{-1} , highest I_f/I_b $\frac{1}{4}$ 18.2, showing high CO poison tolerance	
--	-------------------------	---	--

4.3 Gels for Lithium-ion batteries

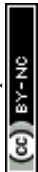
Though LIBs have been the dominant energy storage technology since the 1990s, continuing to evolve over the decades, LIBs face limitations such as low rate capabilities due to sluggish diffusion kinetics and reduced cycle life caused by electrode material expansion during the lithiation-de-lithiation process despite their widespread use [172, 239]. These issues hinder their application in fields such as electric vehicles which is very demanding. These figures illustrate the mechanism of LIBs. Given the extensive literature on electrochemical energy storage, this discussion focuses on fundamental mechanisms and recent advancements in hydrogel-based electrode materials.

Typical anode materials in LIBs encompass carbonaceous substances such as graphene and carbon nanotubes, along with transition metal oxides like TiO_2 (Fig.16 b,c). Recent studies highlight silicon (Si) anodes as a promising alternative due to their higher theoretical capacity [240, 241]. Although traditional carbon-based materials exhibit good conductivity and minimal structural changes during cycling, their low lithiation potential raises safety concerns. To address performance limitations, researchers have explored conversion materials ($MaOb$, where $M = Cu, Mn, Fe, Ni, Co$, etc.) and alloy-based materials ($LixM$, where $M = Sn, Si$, etc.) as high-performance anodes [242, 243]. Hybrid hydrogels have been introduced as an innovative class of electrode materials to overcome these challenges. Wu et al. developed a composite anode by integrating silicon (Si) nanoparticles into a polyaniline (PANI)-based conductive polymer hydrogel through an in situ polymerization approach [244]. This architecture delivered a specific capacity of 1100 mAh g^{-1} at a current density of 3 A g^{-1} and maintained 550 mAh g^{-1} even after 5000 cycles at 6 A g^{-1} . The superior electrochemical performance was largely due to the continuous conductive network provided by PANI and strong electrostatic interactions between the Si oxide surface layer and the positively charged polymer matrix. Phytic acid functioned both as a dopant and gelator, enhancing cross-linking via hydrogen bonding and facilitating a robust three-dimensional structure capable of buffering Si volume fluctuations during cycling. In another study, Bai et al. incorporated Si nanoparticles with an ultrathin silicon oxide (SiO_x) coating into a graphene hydrogel matrix.



The SiO_x layer, generated through ozone treatment, mitigated particle agglomeration and ensured uniform dispersion within the conductive network, achieving a capacity of 1020 mAh g⁻¹ at 4 A g⁻¹ [245]. Hydrogel frameworks have also been applied to TiO₂-based anodes, often in synergy with graphene or conductive polymers. Although TiO₂ typically offers lower capacity compared to Si and other transition metal oxide anodes such as MnO₂, CoO, and Fe₃O₄, it provides superior mechanical stability during cycling [246]. For instance, a TiO₂-conducting polymer-carbon nanotube (PEDOT:PSS/CNT) composite delivered 76 mAhg⁻¹ at 50 mV s⁻¹, while an N-doped MnO₂/graphene hydrogel exhibited a capacity of 1003 mAhg⁻¹ at 100 mA g⁻¹ [247]. A composite material comprising carbon-coated manganese monoxide quantum dots (C@MnO QDs) anchored on a graphene aerogel (GA) was synthesized through an in-situ gelation of manganese oxide on GA, followed by supercritical drying and subsequent carbonization. This strategy led to a uniform dispersion of nanoscale MnO QDs within a three-dimensional porous and conductive GA network. The nanosized MnO QDs facilitate efficient accommodation of volume changes and minimize ion diffusion distances, thereby enhancing electrochemical kinetics. Concurrently, the interconnected GA framework provides efficient pathways for electron transport and Li⁺ diffusion. As an anode material for lithium-ion batteries, the C@MnO QDs/GA composite demonstrated exceptional electrochemical characteristics, including a high discharge capacity, robust cycling performance, and impressive rate capability. Notably, a specific capacity of 1698 mAh g⁻¹ was achieved after 100 cycles at 200 mA g⁻¹, and a capacity of 702 mAh g⁻¹ was retained even under a high current density of 2000 mA g⁻¹. These findings highlight the promise of C@MnO QDs/GA as a high-performance anode and underscore its relevance for advancing oxide-based electrodes in next-generation alkali metal-ion batteries.

A new category of metal dichalcogenide-graphene hybrid hydrogels has gained attention for energy storage applications. Lingappan et al. synthesized a MoS₂-graphene composite hydrogel by integrating MoS₂ nanosheets into a graphene framework through a two-step hydrothermal process, achieving an impressive energy density of 890 Wh kg⁻¹ at a power density of 130 W kg⁻¹ [248]. The incorporation of nitrogen dopants further enhanced the material's electrochemical properties. In addition to graphene and conducting polymer-based hydrogels, Shi et al. introduced a carbon framework derived from a chitosan-glutaraldehyde hydrogel, which was used to host a tin-iron (Sn-Fe) alloy [247]. While Sn-based alloys offer significantly higher specific capacities compared



to conventional graphite anodes, they are often limited by severe volume expansion during cycling, which can result in mechanical failure and capacity fading. The developed hydrogel featured a double-network structure, reducing particle agglomeration and ensuring uniform volume variations. This framework resulted in a capacity of 491 mAhg⁻¹ at 1 Ag⁻¹. Hydrogels have also been employed in solid polymer electrolyte systems. Bae et al. used a 3D Li_{0.35}La_{0.55}TiO₃ (LLTO) hydrogel framework as a nanofiller in composite polymer electrolytes, achieving a high Li-ion conductivity of ~10⁻⁴ S cm⁻¹[249]. The LLTO framework facilitated percolation behavior, preventing agglomeration and improving ion transport. V₂O₅-based hydrogels were among the earliest reported examples. Coustier et al. (1998) synthesized a V₂O₅ hydrogel via protonation of sodium metavanadate solution, yielding an aerogel electrode with a capacity of 310 mAhg⁻¹ at 2.9 mAcm⁻² [250]. While most hydrogel-based LIB studies focus on anode materials, some extend to cathodes and hydrogel-derived electrolytes, demonstrating their broad applicability. In summary, hydrogel-based LIBs consistently demonstrates that tailored gel architectures can effectively address key limitations of conventional electrodes by enhancing structural stability, mitigating volume expansion, and improving ion/electron transport. These advances highlight the versatility of hydrogels in both electrode and electrolyte design, underscoring their potential to enable next-generation LIB systems with superior performance and durability.

Table 6. Hydrogels for lithium-ion battery applications

Type of Hydrogel	Main Material Constituents	Electrode Type	Initial Capacity	Capacity After Cycling	Other Features	Ref.
Metal Oxide-Based Hydrogel	V ₂ O ₅	Cathode	310 mAh/g at 2.9 mA/cm ²	0.5% capacity loss after 100 cycles at 2.9 mA/cm ²	Organic solvent-exchange method prevents gel-structure collapse	[250]
Conducting Polymer-Based Hydrogel	Si NPs coated with PANI, doped with phytic acid	Anode	1100 mAh/g at 3 A/g	~550 mAh/g at 6 A/g after 5000 cycles	Free spaces for Si expansion in a conductive PANI matrix	[244]

Graphene-Based Hydrogel	N-doped graphene/Fe ₃ O ₄	Anode	1014 mAh/g at 100 mA/g	1130 mAh/g after 200 cycles (NA rate)	Spacious matrix accommodates volume changes	[251]
Conducting Polymer Hydrogel	(a) TiO ₂ -CNT-PEDOT:PSS, (b) Si NPs-CNT-PEDOT:PSS	Anode	(a) 76 mAh/g at 50 mV/s, (b) 2.2 mAh/cm ² (max)	NA	Highly flexible battery electrodes	[252]
Graphene-Based Hydrogel	TiO ₂ nanocrystals in graphene matrix	Anode	~250 mAh/g at 0.1 A/g	200 mAh/g at 0.1 A/g after 50 cycles	Multifunctional material for photocatalysis and battery	[253]
Graphene-Based Hydrogel	CoO NPs in graphene matrix	Anode	890.2 mAh/g at 200 mA/g	1025.8 mAh/g at 100 mA/g after 82 cycles	Uniformly dispersed NPs in hydrogel matrix	[254]
Graphene-Based Hydrogel	MnO ₂ in N-doped graphene matrix	Anode	1003 mAh/g at 100 mA/g	909 mAh/g at 400 mA/g after 200 cycles	Facile synthesis using KMnO ₄ and graphene redox reaction	[255]
Graphene-Based Hydrogel	Si@SiOx-graphene matrix	Anode	1020 mAh/g at 4 A/g	1640 mAh/g at 0.1 A/g after 140 cycles	SiOx coating reduces Si NP agglomeration	[245]
Graphene-Based Hydrogel	MoS ₂ nanosheets in N-doped graphene matrix	Anode	1140 mAh/g at 100 mA/g	94% retention at 100 mA/g after 130 cycles	Optimum nitrogen doping, transition metal dichalcogenide use	[248]
Non-Conducting Polymer-	Sn-Fe alloy in carbon network from	Anode	491 mAh/g at 1 A/g	516 mAh/g at 0.1 A/g after 500 cycles	3D structure mitigates Sn-Fe	[247]



Based Hydrogel	chitosan-glutaraldehyde				volume changes during cycling	
----------------	-------------------------	--	--	--	-------------------------------	--

4.4 Carbon based Gels as adsorbents for water purification

Huang et al. reported a straightforward approach for fabricating graphene-based hydrogels utilizing agarose (AG) as both a stabilizing and reducing agent. In this synthesis, AG molecules interact with GO surfaces via strong hydrogen bonding and hydrophobic interactions with functional groups such as carboxyl, hydroxyl, and epoxide. These interactions promote the crosslinking of AG chains, resulting in the formation of a three-dimensional interconnected network. Structural characterization using SEM and FT-IR confirmed this architecture. Moreover, the presence of cracks and pores within the hydrogel matrix suggested the development of a loosely organized, porous structure stemming from the synergistic interaction between AG and graphene nanosheets. The AG hydrogels were subsequently investigated for their dye adsorption capabilities, capitalizing on the high surface area of graphene and the porous architecture of the hydrogel matrix. A popular triphenylmethane color called malachite green (MG) was employed as a model contaminant to assess the effectiveness of the adsorption process. The potential of graphene-AG hydrogels in environmental remediation applications was illustrated in this study, specifically with regard to the elimination of organic pollutants from aqueous solutions. Over 50% of MG was eliminated in 12 hours, according to UV-vis spectroscopy, and after seven days, adsorption reached 90%. These results demonstrate that graphene-AG hydrogels have a better capacity for adsorbing dyes than pure AG hydrogels, which makes them potentially useful materials for water purification applications [256].

A durable GO-CS composite hydrogel was presented by Bai et al. as a novel material for water purification applications. GO sheets and CS chains self-assembled to create the GO-CS hydrogels, which are shown in figure 18(a) as a loosely connected 3D network structure. According to SEM examination, the composite hydrogel was made up of GO sheets that had been crosslinked by CS, creating an extremely porous structure. This porous structure was essential in increasing the hydrogel matrix's total adsorption capacity by promoting the diffusion of adsorbates within it. Excellent adsorption capabilities for a range of organic dyes and heavy metal ions were



demonstrated by the GO-CS hydrogels that were produced. To evaluate the adsorption effectiveness of the GO-CS composite hydrogel, MB and eosin Y were selected as model dyes. It was discovered that the composition of hydrogel affected the adsorption capacity. In particular, a larger CS concentration boosted the adsorption of eosin Y, whereas a higher GO level increased the ability of hydrogel to adsorb MB. The unique interactions between the dye molecules and the constituents of hydrogel were responsible for this selective adsorption activity. In addition to its ability to remove dye, the GO-CS composite hydrogel showed a strong adsorption capacity for certain heavy metal ions, such as Cu(II) and Pb(II). Effective metal ion binding was made possible by the coordination interactions between GO, CS, and the metal ions, which were responsible for the better adsorption performance. According to these results, GO-CS hydrogels have a lot of promise for use in water purification applications since they provide an effective and eco-friendly method of eliminating both organic and inorganic contaminants from aqueous systems. Further studies could explore optimizing the hydrogel composition, evaluating its reusability, and assessing its performance under real-world water treatment conditions [257].

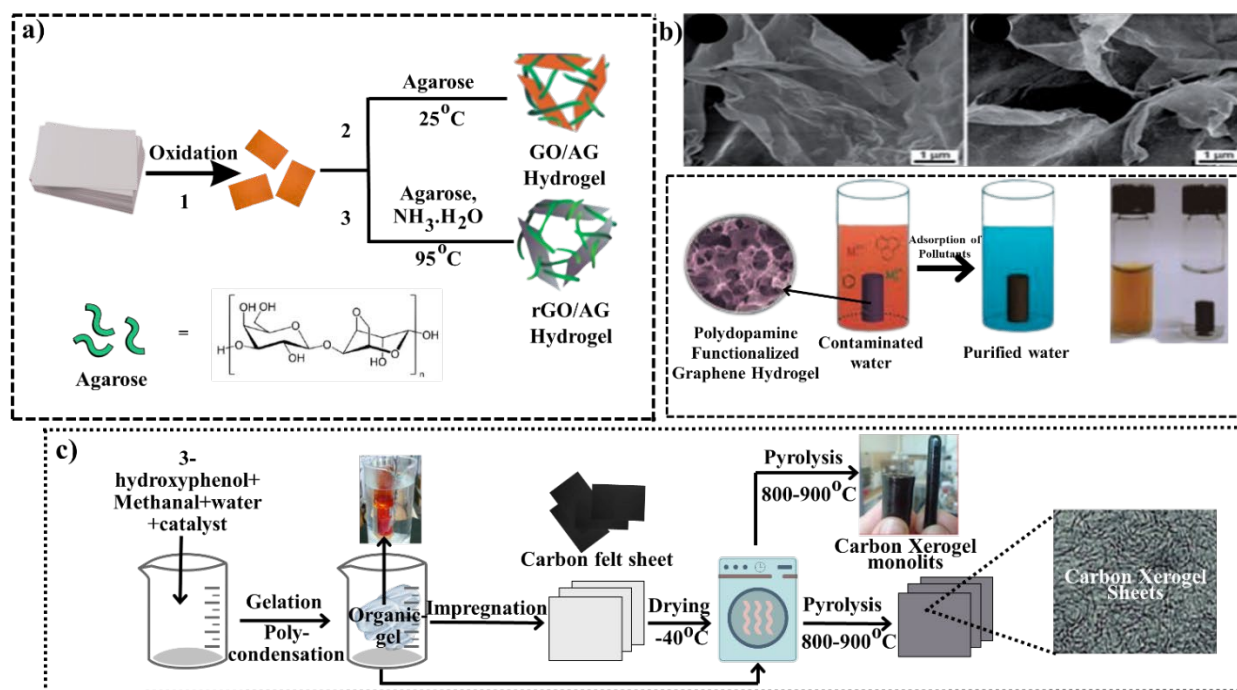
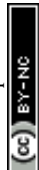


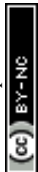
Figure 18. (a) Graphene-agarose (AG) hydrogel synthesis pathways diagram, displaying agarose structure and SEM images of GO-AG and RGO-AG microstructures. (b) Graphene hydrogel microstructure and adsorption illustration, featuring images of the GO-dopamine combination and the resultant PDA-GH. (c) Schematic of the desalination process using CX sheet electrodes made



from nanocarbon xerogels. Reproduced from reference [100, 258] with permission from Royal society of chemistry & MDPI, copyright 2019 & 2021

Polydopamine-modified graphene hydrogel (PDA-GH) was created by Duan et al. in a single process [259]. This method used graphene nanosheets' self-assembly and dopamine's spontaneous polymerization to create a porous hydrogel structure. Dopamine enhanced the stability and adsorption capacity of the hydrogel by acting as a reducing and surface functionalization agent. In order to create a homogenous mixture, dopamine was added to the GO aqueous dispersion after GO was prepared using a modified method of Hummers in figure 18b [260]. This was the first step in the synthesis of PDA-GH. PDA-GH was formed as a result of the reaction, which was carried out at 60°C under static circumstances. In contrast, a GO dispersion was hydrothermally treated at 180°C for 12 hours in an autoclave walled with Teflon to create hydrothermally synthesized HT-GH. Following treatment, the autoclave spontaneously cooled to ambient temperature, yielding the HT-GH product. Techniques like SEM, AFM, and XPS were used to describe the structural of hydrogels and compositional characteristics. PDA-GH and HT-GH's capacity to eliminate impurities such as Cd(II), Pb(II), rhodamine B, and p-nitrophenol from aqueous solutions was evaluated by adsorption assays. The findings showed that both PDA-GH and HT-GH outperformed traditional carbon nanomaterials commonly employed in water filtration, exhibiting noticeably enhanced adsorption capabilities for a variety of contaminants. These graphene-based hydrogels solved a number of issues with existing carbon-based polymers, including their difficult recovery procedures, low adsorption capability, and residue persistence. Interestingly, even after several cycles of adsorption and desorption, the hydrogels maintained their high adsorption efficiency, and their regeneration was made simple by readily available chemicals. These results highlight PDA-GH and potential of HT-GH as affordable, reusable adsorbents for use in water purification [259].

Using a freeze-drying technique, Liu et al. created Ni-doped graphene/carbon cryogels (NGCC) by adding formaldehyde and resorcinol to a graphene oxide (GO) suspension to create a hydrogel precursor [80]. Following a carbonization process, the Ni-doped graphene/resorcinol-formaldehyde cryogel (NGRC) was converted to NGCC. Using SEM, TEM, FT-IR, and XRD, structural and morphological characterisation was carried out. Even after being compressed over



4,000 times its own weight, the resulting cryogel showed exceptional mechanical qualities and retained its original shape. The removal of methyl blue (MB) dye, oil, and organic solvents was assessed using adsorption capabilities of NGCC. Because of its superwetting characteristics, which allowed for the quick absorption of oils and organic solvents, the results showed that the cryogel finished the adsorption process in less than a minute. Additionally, after seven adsorption-desorption cycles, the NGCC retained more than 90% of its adsorption capacity, demonstrating exceptional recyclability. According to the adsorption capacity-time profiles, equilibrium was reached quickly. The addition of graphene, which changed the shape of the cryogel to increase its surface area and porosity, was responsible for this quick adsorption process. The NGCC produced with a GO content of 6 mg/mL demonstrated the highest MB adsorption capability among the different samples evaluated. Adsorption is one of the simplest and most efficient methods for removing contaminants from water, and it continues to be a major area of scientific interest. Many graphene-based hydrogels have been investigated for their potential to adsorb common water pollutants, such as organic solvents, heavy metal ions, oils, and colors. The adsorption efficacy and capacity of graphene-based hydrogels are considerably enhanced by the addition of functional ingredients including agarose, chitosan, and Ni-doped cryogels, as demonstrated in earlier research. Furthermore, experimental results indicate that even after multiple reuse cycles, these materials maintain their high adsorption effectiveness [261].

The long-term adsorption effectiveness of these hydrogels across prolonged reuse cycles could be further improved in future studies, or their performance should be improved by adding more functional components. The advancement of water treatment technologies and the resolution of environmental pollution issues will depend heavily on the creation of graphene-based hydrogels that are more robust, economical, and highly effective. Although it is still difficult, the creation of sophisticated materials with adjustable wettability is essential for effective oil-water separation. Recent work has shown that controlled wettability and long-term hydrolytic stability are made possible by postcoordination modification of $\text{Mg}_2(\text{dobpdc})$ frameworks with monoamines of different alkyl chain lengths. The octylamine-functionalized framework (OctA) shown noteworthy efficacy in oil-water separation, and its incorporation into an aerogel form with decreased graphene oxide further improved organic solvent absorption and reusability. In parallel, sustainable adsorbents such as cotton-derived porous carbon (CDPC) and its oxidized variant (CDPCO) were synthesized via alkaline etching, showing excellent removal capabilities for both organic



1782 pollutants and heavy metals like Cd(II) and Co(II). These mechanisms were influenced by
1783 molecular size and electrostatic interactions. Furthermore, a low-cost carbon microbelt (CMB)
1784 aerogel fabricated from waste paper displayed exceptional absorption capacities up to 188 times
1785 its own weight for oils and could be regenerated effectively. Given the environmental burden of
1786 municipal solid waste, particularly waste paper, these materials offer promising, eco-friendly
1787 solutions for wastewater treatment and pollutant removal. Overall, literature reports confirm that
1788 functionalized carbon-based gels-particularly graphene-derived hydrogels and cryogels-offer high
1789 adsorption capacities, tunable selectivity, and excellent reusability, making them versatile
1790 candidates for removing diverse organic and inorganic pollutants from water. The incorporation
1791 of additional functional components further expands their applicability, providing a promising
1792 pathway toward next-generation, sustainable water purification technologies.



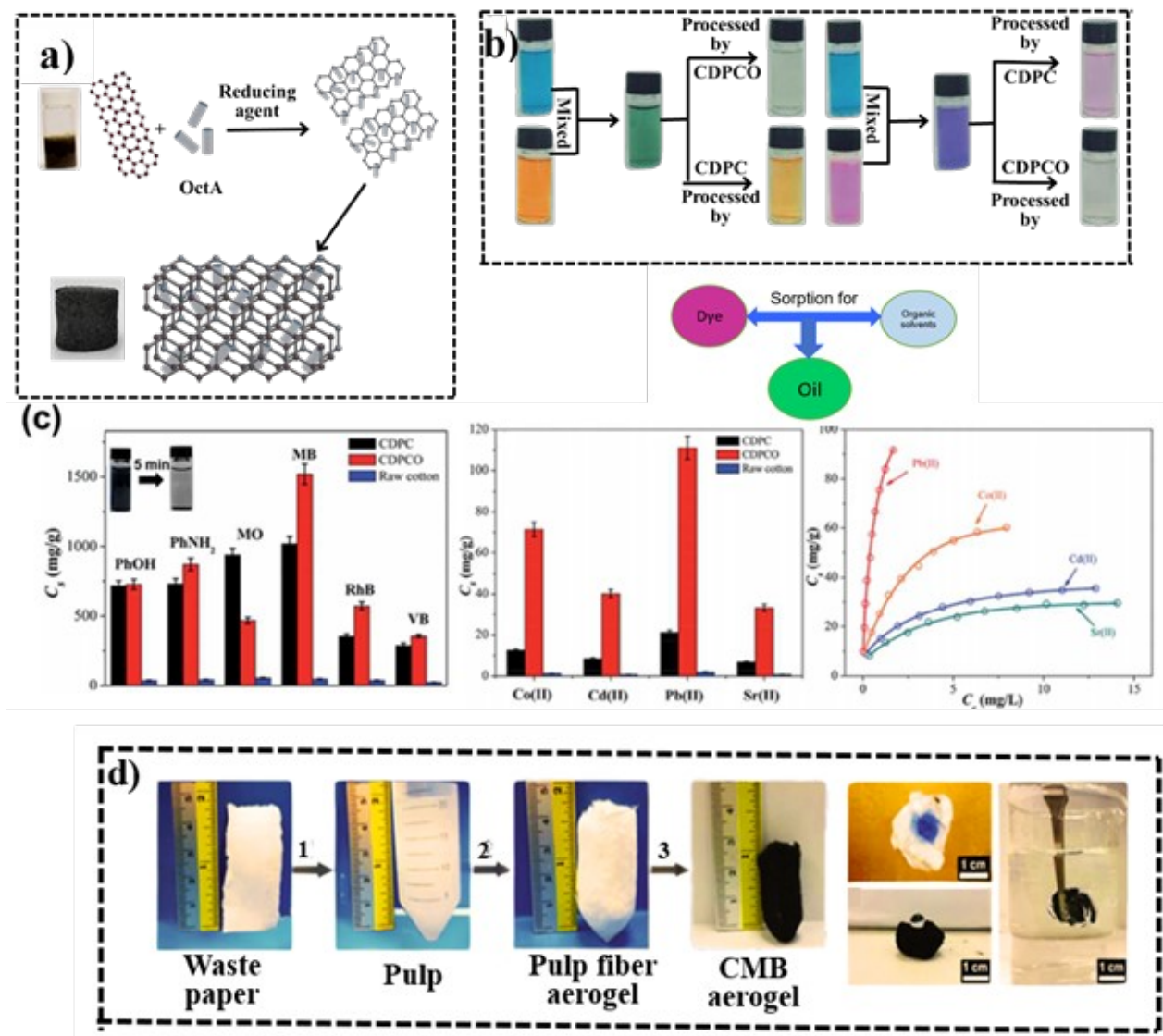


Figure 19. (a) Fabrication of OctA/rGA composites for oil–water separation. (b) Synthesis of cotton-derived porous carbon oxide for selective dye adsorption. (c) Sorption capacities for organic pollutants and metal ions. (d) Preparation of wastepaper-derived carbon microbelt aerogel with wettability demonstration.



Open Access Article. Published on 21 August 2025. Downloaded on 9/5/2025 7:05:43 PM.
This article is licensed under a Creative Commons Attribution-NonCommercial 3.0 Unported Licence.



Table.7. Overview of carbon aerogel materials utilized in water purification and treatment applications

Material	Key Features	Adsorption Capacity	Recyclability	Ref.
Octylamine-functionalized MOF (OctA) hybridized with rGO aerogel (OctA/rGA)	Hydrophobic modification for water stability - High porosity enhances oil and organic solvent separation - Effective for oil-water separation and dye removal	Enhanced compared to pristine OctA	Retained 85% adsorption capacity after 10 cycles	[204]
Cotton-derived porous carbon oxide (CDPCO) aerogel	Derived from biomass for low-cost, eco-friendly application - High specific surface area (1,160 m ² /g) - Efficient adsorption of organic solvents and heavy metals	Organic solvents: 354–1,519 mg/g - Heavy metals: Co(II) 71.4 mg/g, Cd(II) 40.2 mg/g, Pb(II) 111.1 mg/g, Sr(II) 33.3 mg/g	Not specified	[262]
Carbon microbelt aerogel (CMB) from wastepaper	Low density (5.8 mg/cm ³) - Hydrophobic with high sorption capacity for organic pollutants - Tested for oil and solvent absorption	56–188 mg/g	Evaluated using squeezing and distillation methods	[262]

4.5 Gas storage and separation Using Carbon gels

Carbon aerogels have demonstrated significant potential in gas storage and separation due to their uniform pore size distribution and high surface area, which enhance gas adsorption and selectivity [263]. The small size of gas molecules allows them to interact effectively with the well-controlled micropores in carbon aerogels, making these materials particularly suitable for applications in gas storage. The presence of uniform micropores in carbon aerogels enhances the physisorption of gas

molecules due to their small kinetic diameters and favorable interactions as described by the Lennard-Jones potential. Furthermore, the incorporation of metal atoms or heteroatoms into the carbon aerogel structure further increases gas adsorption capacities by facilitating stronger interactions between the adsorbent surface and the gas molecules, primarily through chemisorption [264]. Functionalization strategies, such as nitrogen doping, have been widely employed to enhance the affinity of carbon aerogels for CO₂ molecules, thereby increasing their gas capture efficiency [265, 266]. These characteristics make carbon aerogels highly promising for gas storage applications, as their porous structures and surface chemistry can be precisely engineered at the molecular level to optimize performance [180, 267, 268].

Li et al. synthesized a nitrogen-doped carbon aerogel (NCA) by using a porous organic polymer aerogel, which was prepared through a Schiff base reaction [269]. The nitrogen-doped carbon aerogel (NCA) displayed exceptional textural properties, including a high specific surface area of 2,356 m²/g, a large pore volume of 1.12 cm³/g, high bulk porosity (70%), and an ultra-low density of 5 mg/cm³. These structural attributes contributed to its impressive CO₂ adsorption capacities of 6.1 mmol/g at 273 K (1 bar) and 3.4 mmol/g at 298 K (1 bar). The study highlighted that the micropore volume fraction and nitrogen content played crucial roles in enhancing both CO₂ uptake and CO₂/N₂ selectivity. The optimized NCA sample exhibited a selectivity of 47.8 for CO₂ over N₂ at 298 K and 1 bar, as determined using the Ideal Adsorption Solution Theory (IAST) (Fig. 20a-d).



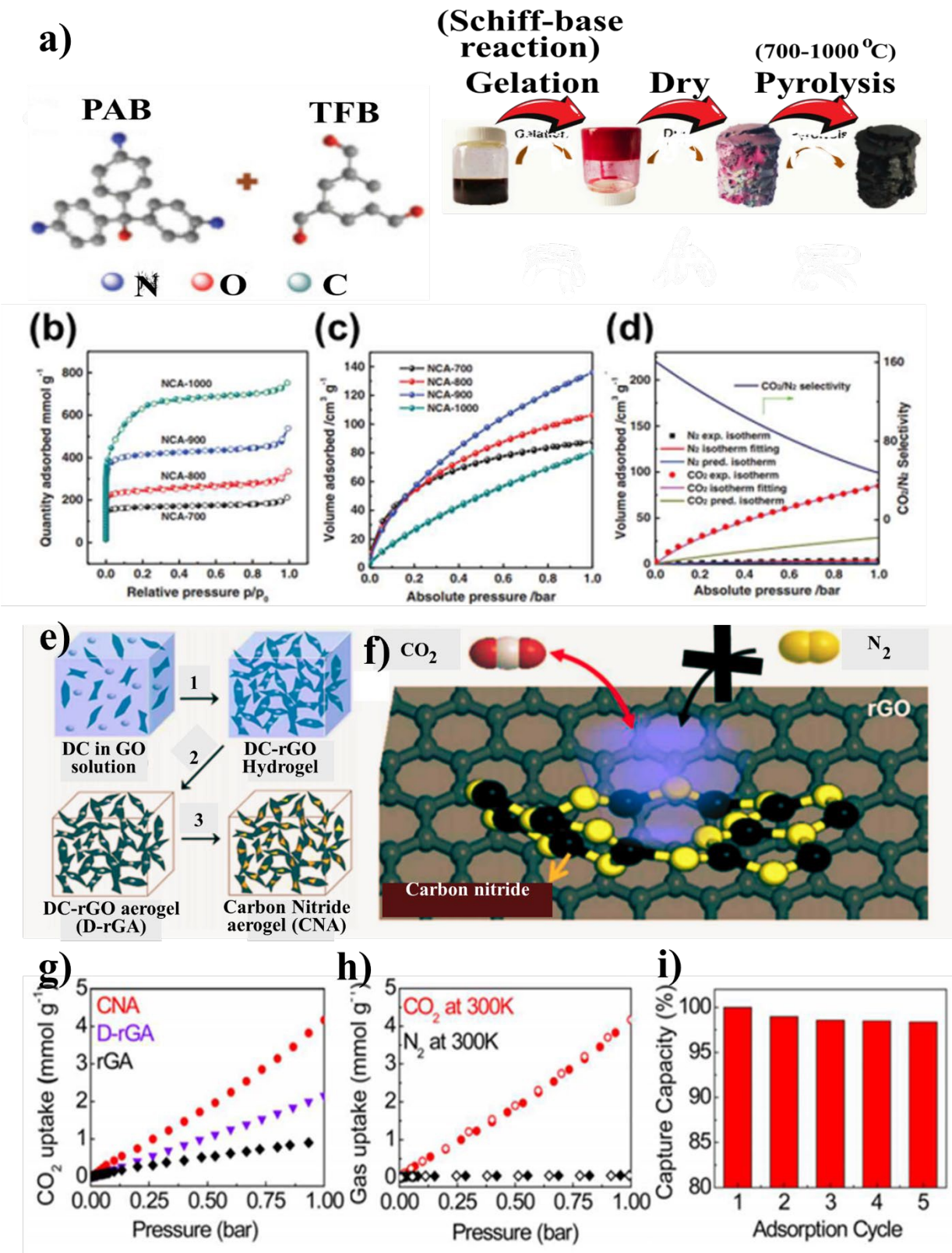


Figure 20. (a-b) Synthesis and N₂ sorption isotherms of nitrogen-doped carbon aerogels (NCAs). (c-d) CO₂ uptake and CO₂/N₂ selectivity of NCAs. (e-f) Synthesis of carbon nitride aerogel (CNA) and mechanism of selective CO₂ adsorption. (g-i) CO₂/N₂ adsorption behavior and recyclability of CNA. Reproduced from reference [205] with permission from Elsevier, copyright 2020.

Oh et al. synthesized a carbon nitride-functionalized porous reduced graphene oxide aerogel (CNA) to develop a highly selective and regenerable CO₂ adsorbent [269]. While strong interactions between gas molecules and adsorbent surfaces can lead to low reproducibility, the CNA material was engineered to achieve a balance between adsorption energy and regeneration efficiency [270, 271]. The synthesized CNA exhibited a specific surface area of 450 m²/g and a total pore volume of 1.5 cm³/g. Its CO₂ uptake reached 4.2 mmol/g at 300 K (1 bar), with an impressive retention of 97.6% of its initial adsorption capacity after five regeneration cycles. Additionally, the selectivity of the CNA for CO₂ over N₂ was recorded at 113 under a gas composition of 10% CO₂/90% N₂ (v/v) at 300 K and 1 bar shown in Figure 20(e-i). Liu et al. synthesized a three-dimensional glucose/graphene-based aerogel (G/GAs) for the adsorption of various target gases, including CO₂, CH₄, and H₂ [272]. The fabrication process utilized glucose as a binder to create a hierarchical graphene oxide matrix with enhanced gas adsorption properties. The resultant aerogel exhibited a large surface area (763 m²/g) and a high total pore volume (3.06 cm³/g). Its CO₂ and CH₄ adsorption capacities at 298 K and 1 bar were recorded at 1.7 mmol/g and 1.1 mmol/g (1.7 wt.%), respectively. Additionally, its H₂ uptake at 77 K and 1 bar was measured at 6.1 mmol/g (1.2 wt.%) (Figure 21 (a-e)). Jeon et al. investigated the effect of nitrogen doping on the CO₂ adsorption capacity of carbon aerogels by synthesizing nitrogen-doped carbon aerogels (CAs) with varying resorcinol/melamine (R/M) ratios [272]. The study found that, although the specific surface area was relatively low, increasing the nitrogen content significantly improved CO₂ adsorption. The highest CO₂ uptake of 2.7 mmol/g at 298 K and 1 bar was achieved with an optimized resorcinol/melamine (R/M) ratio of 1:0.3, highlighting the crucial role of nitrogen-doped sites in enhancing CO₂ affinity (Figure 21f-j). Overall, these studies consistently demonstrate that tailoring the pore structure, surface area, and heteroatom doping in carbon aerogels can substantially enhance gas uptake and selectivity. The reported works highlight



nitrogen doping, hierarchical porosity, and balanced adsorption–desorption energetics as key strategies for achieving high CO₂ capture efficiency and regeneration stability.

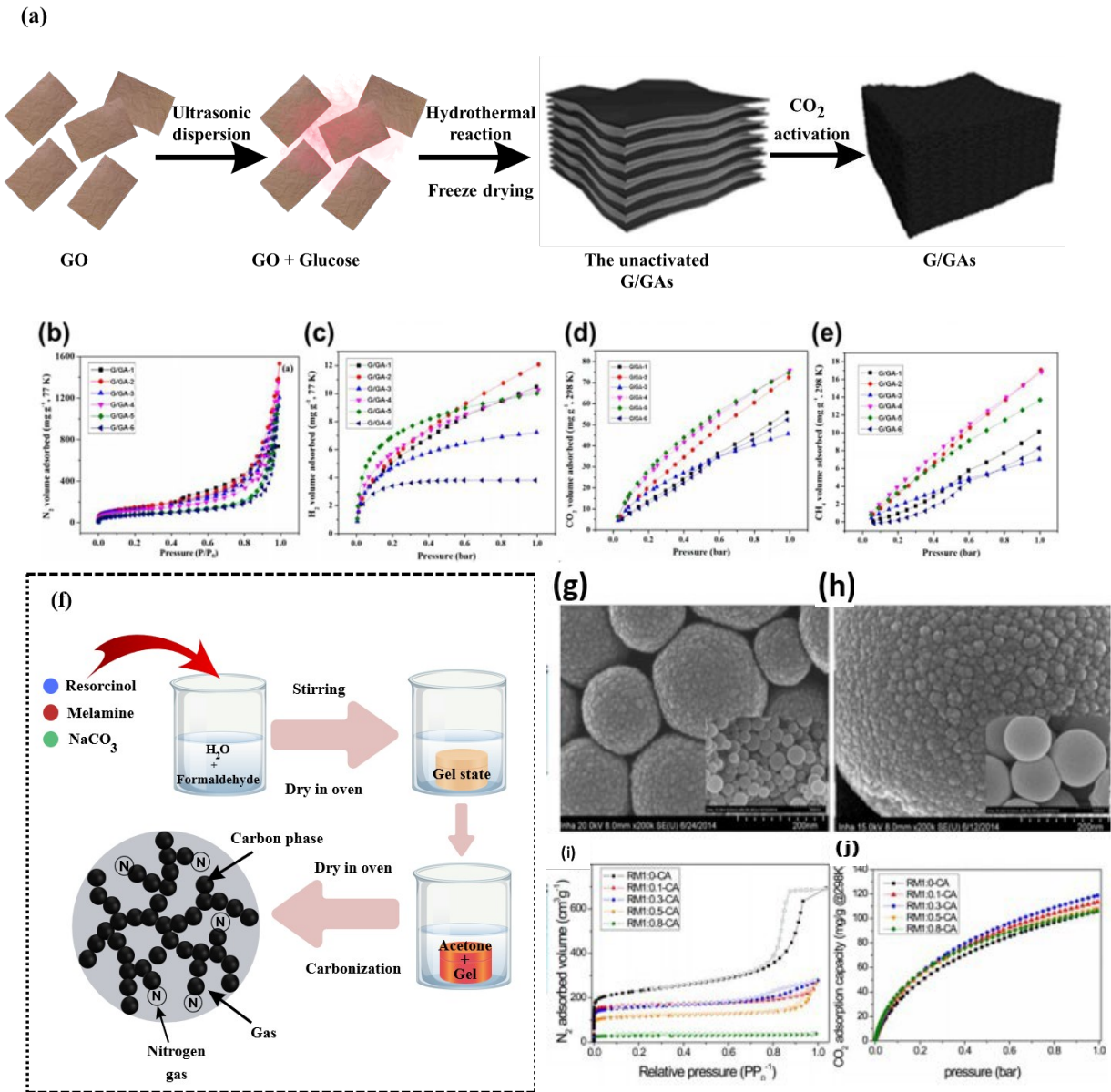
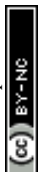


Figure 21. (a) Synthesis of 3D glucose/graphene aerogels (G/GAs). (b-e) Gas adsorption behavior of G/GAs for N₂, H₂, CO₂, and CH₄. (f-h) Fabrication and SEM analysis of nitrogen-doped carbon aerogels, with adsorption profiles influenced by precursor ratios. Reproduced from reference [205] with permission from Elsevier, copyright 2020.

4.6 Metal-doped carbon-based gels as catalysts

The textural characteristics of the synthesized samples are detailed in Table 7, and their pore size distributions are visually represented in Figure 22. These metal-doped carbon aerogels share similar features with the undoped carbon aerogel used for comparison, primarily exhibited macroporous structures. Mesopores were observed only in the tungsten-doped catalysts, and even then, their presence was minimal. The macropore volume followed the order $\text{ACr500} < \text{AMo500} < \text{AW500}$, but decreased as the carbonization temperature increased, as seen in the case of AW1000. In contrast, the PSD showed an inverse trend. The sample ACr500 exhibited the largest macropores, with diameters exceeding 2000 nm. AMo-500 showed a monomodal pore size distribution centered around 1500 nm, whereas AW-500 displayed a bimodal distribution with peaks near 180 nm and 1500 nm. The study found that as carbonization temperature increased, smaller macropores decreased in size, and larger macropores increased in volume. The undoped reference sample showed a uniform macropore size of around 130 nm, indicating a less porous structure and a higher density compared to the others. Following pretreatment in a helium flow, the supported A1000-5W catalyst showed a slight reduction in the specific surface area compared to the A1000 support. This decrease is attributed to partial pore blockage caused by the deposited metal phase; however, the overall macroporous structure appeared to remain unaffected.

Microporosity (W_0), and consequently the surface area, followed the same trend as macroporosity, but both increased with higher carbonization temperatures. Among the catalysts, AMo-500 exhibited the largest micropores (L_0). The overall porous structure of the carbon aerogels was a consequence of the conditions in four essential phases of their synthesis: gelation, drying, carbonization, and activation. Since the initial development of carbon gels, numerous studies have focused on how adjusting these conditions can effectively control aerogel porosity [273]. SEM images illustrating the sample surfaces are presented in Fig. 22. These images reveal structures made up of fused microbead particles, whose sizes were significantly influenced by the specific metal used. The textural characteristics of the aerogels appear to be linked to the size of these microparticles- smaller particles tend to produce a pore network with reduced interparticle voids, spanning macro- to mesopore ranges. The findings suggest that both morphology and pore structure were dependent on the type of metal salt used during synthesis [273-277]. Microporosity within individual particles is primarily developed during the carbonization stage. Accordingly, the



observed increase in W_0 and L_0 at higher carbonization temperatures is probably attributable to the significant amount of material lost during the carbonization process.

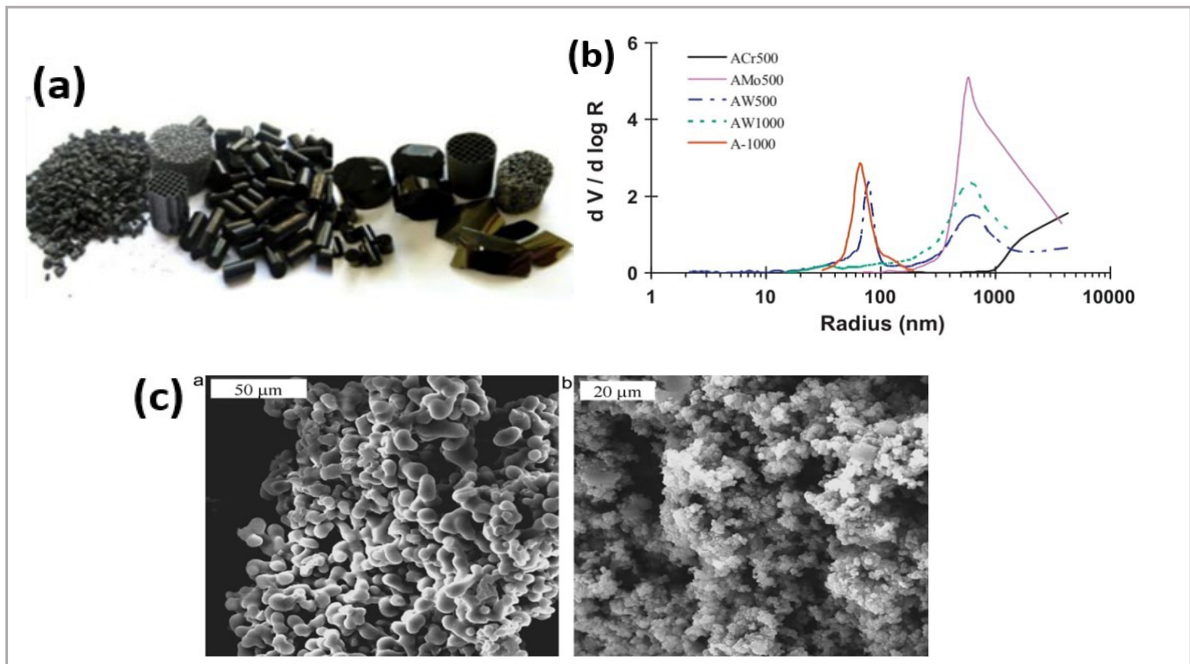


Figure 22. (a) Carbon gels formed in various shapes. (b) Pore size distribution of metal-doped carbon aerogels via mercury porosimetry. (c) SEM images revealing surface morphology of ACr500 and AW500 samples. Reproduced from reference [278, 279] with permission from Elsevier, copyright 2013 & 2011.

To determine the chemical identity and how the metals were distributed, XRD and TEM were employed. The XRD analysis did not reveal any distinct diffraction patterns associated with the metal components, suggesting excellent metal dispersion—findings consistent with previous studies [280]. Prior XPS data indicated partial reduction of Cr(VI) to Cr(III) and Mo(VI) to Mo(V), while tungsten retained its W(VI) state after carbonization at 500 °C. As illustrated in Fig. 3, all metal-doped catalysts demonstrated effective metal dispersion. The gelation process facilitated the incorporation of metal species into the organic gel network, followed by metal particle formation during carbonization. Consequently, strong interactions are established between the organic and inorganic components. The scanning electron microscopy (SEM) images provide evidence that metal nanoparticles, exhibiting a range of sizes and shapes, are evenly distributed throughout the carbon matrix. The specific characteristics of these nanoparticles are determined by the type of

metal used and the thermal treatment process [280, 281]. These observations also suggest that the doped-metal catalysts exhibit notable resistance to sintering, despite undergoing intense thermal processing. However, the particle sizes, although relatively large, still do not generate XRD diffraction peaks, implying that the metal phases possess an amorphous structure.

The conversion of feedstocks derived from biomass into chemicals and fuels presents considerable potential for enhancing carbon-supported catalysts. A prime illustration of this is the selective catalytic oxidation of glycerol, which is a byproduct generated from the production of biodiesel, to synthesize high-value fine chemicals like glyceric acid. Various carbon materials, including CNTs, activated carbons, and carbon xerogels, were employed as supports for gold nanoparticles. It was observed that surface oxygen negatively impacted catalytic activity, whereas the existence of narrow pores increased the selectivity for glyceric acid. The best selectivity (75%) was attained with gold supported on activated carbon [282]. These studies collectively indicate that the type of metal dopant, synthesis conditions, and resulting pore architecture play decisive roles in determining catalyst morphology, porosity, and metal dispersion. Reported findings emphasize that optimized macropore-micropore balance, strong metal–support interactions, and controlled nanoparticle formation are key to enhancing catalytic performance in biomass-derived feedstock conversions.

Table.7. Structural characteristics of carbon aerogels doped with metal components.

Sample	Metal (%)	$p(\text{g cm}^{-3})$	$SN_2(\text{m}^2 \text{g}^{-1})$	V_3	V_2	W_0	$L_0(\text{nm})$ ($\text{cm}^3 \text{g}^{-1}$)	Ref.
ACr500	3.6	0.56	397	0.99	0.00	0.17	1.03	[283]
AMo500	1.9	0.50	481	1.40	0.00	0.18	1.12	[284]
AW500	1.4	0.43	528	1.53	0.05	0.20	1.06	[276]
AW1000	2.1	0.54	610	1.32	0.01	0.26	1.06	[277]
A1000	—	0.72	470	0.63	0.00	0.27	1.08	[273]
A1000-5W (He/500 ⁰ C/2h)	5	0.72	410	0.61	0.00	—	—	[284]



4.7 Other porous materials for Energy and environmental technologies

Beyond carbon gels, a wide range of porous materials-including activated carbons, MOFs, COFs, porous polymers, and functionalized nanomaterials-have emerged as promising candidates for energy and environmental applications. Activated carbons remain the most industrially adopted option due to their low cost, scalability, and high surface areas ($>1000\text{ m}^2/\text{g}$), making them ideal for adsorption-based water purification, gas storage, and supercapacitor electrodes. However, their predominantly microporous structure can limit ion transport in high-power energy storage systems. In contrast, MOFs offer crystalline, highly ordered pore structures with tunable chemistry, enabling exceptional selectivity for CO_2 capture, gas separation, and catalytic conversions. Despite these advantages, the high synthesis cost, moderate stability, and often low conductivity of MOFs restrict large-scale deployment, particularly in electrochemical systems. Functionalized nanomaterials, such as doped graphene, CNTs, and hybrid composites, provide high electrical conductivity, structural integrity, and tunable surface chemistry for targeted applications. Heteroatom doping (N, S, P, or B) can enhance wettability, catalytic activity, and charge storage capacity, while hybrid structures improve mass transport pathways. In environmental remediation, these materials can be functionalized to selectively adsorb heavy metals, dyes, or emerging contaminants, although synthesis complexity and cost remain challenges.

Porous transition metal compounds (oxides, hydroxides, sulfides) and conducting polymers also contribute significantly to energy and environmental technologies. Transition metal oxides (e.g., MnO_2 , Fe_2O_3) and hydroxides offer high pseudocapacitance and catalytic activity for water splitting, while conducting polymers such as polyaniline and polypyrrole show promise for capacitive deionization and electrocatalysis. However, these materials often suffer from limited cycling stability or structural degradation, issues that can be mitigated through composite formation with porous carbons. Compared to these materials, carbon gels occupy a distinctive position due to their hierarchical porosity, adjustable surface chemistry, and flexibility in precursor selection-from synthetic monomers to renewable biomass. This allows optimization for both high-rate ion transport in supercapacitors and broad-spectrum adsorption in environmental applications. Although the fabrication cost of carbon gels may exceed that of conventional activated carbon,

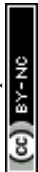
their superior rate performance, tunable structure, and potential for green synthesis make them competitive for specialized, high-value applications in both sectors. Ultimately, the choice among porous materials depends on balancing performance metrics (surface area, conductivity, selectivity, stability) with production cost and scalability, positioning carbon gels alongside activated carbons, MOFs, and functionalized nanomaterials as key players in the future of sustainable energy and environmental technologies.

4.8 Applications of carbon gels in catalysis

4.8.1 Carbon gels supporting catalysts.

The tunable porosity of carbon gels makes them superior catalyst supports for fuel cell applications compared to conventional carbon black, as this feature allows for the minimization of mass transfer limitations in the catalytic layer [285]. Additionally, the type and quantity of surface functional groups present in carbon gels significantly influence the metal phase's loading, dispersion, oxidation state, and stability-factors that directly impact catalyst performance [286].

In terms of textural characteristics, carbon gels provide notable advantages over activated carbon supports, particularly regarding pore size and shape. The mesoporous, tubular structure of carbon gels provides an advantage over the microporous, slit-shaped structure of activated carbons in achieving catalyst selectivity. In the hydrogenation of cinnamaldehyde to cinnamyl alcohol, for example, monometallic Pt catalysts struggle with selectivity due to preferential C=C bond adsorption. Bimetallic PtSn catalysts supported on mesoporous carbon gels, however, can enhance selectivity by favoring C=O bond adsorption ("head-on," Figure 23 a). This "head-on" adsorption is facilitated by the mesoporous structure of carbon gels, unlike the slit-shaped pores of activated carbons, which force a "sideways" adsorption that favors the hydrogenation of the C=C bond [287]. The trimetallic PtFeZn catalyst supported on carbon xerogel achieved exceptional selectivity even with high reactant conversion [288]. More recently, the exceptional selectivity observed for a bifunctional catalyst- consisting of gold supported on a carbon xerogel that had been modified with acidic sites- in the oxidation of cellobiose to gluconic acid was explained by a change in the shape of reactant within the large pores of the carbon gel. This conformational change made the glycosidic bond more accessible for hydrolysis [289]. These reported studies highlight that the



unique mesoporous architecture and adjustable surface chemistry of carbon gels enable superior control over reactant adsorption modes, leading to enhanced catalytic activity and selectivity. The literature demonstrates that tailoring pore geometry and introducing specific metal or acidic functionalities are key strategies for optimizing catalyst performance in diverse reactions.

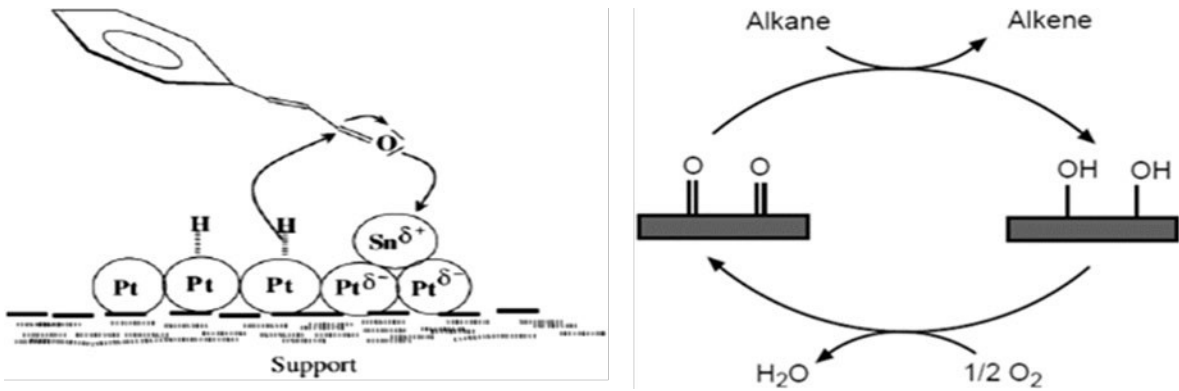


Figure 23. (a) Illustration of cinnamaldehyde molecules adsorbing in a 'head-on' orientation onto a PtSn bimetallic catalyst. (b) Proposed catalytic cycle for hydrocarbon oxidative dehydrogenation on carbon-based materials. Reproduced from reference [290] with permission from Elsevier, copyright 2005.

4.8.2 Carbon gel catalysts.

The catalytic capabilities of carbon-based materials have been demonstrated across a wide variety of reactions, including both acid-base and oxidation-reduction mechanisms [291]. The ability to synthesize carbon gels without metallic impurities and the ease with which their surface properties can be adjusted make them ideal model systems for metal-free catalysis. Active catalytic sites can then be engineered by incorporating specific surface functional groups and heteroatoms. For example, the esterification reaction between acetic acid and ethanol can be catalyzed by carbon xerogels that have been modified to include sulfonic acid groups [292]. Meanwhile, the basic surface properties of nitrogen-doped carbon xerogels make them effective catalysts for the oxidation of NO and The breakdown of organic contaminants using advanced oxidation techniques [293]. Additionally, Oxidized carbon xerogel materials have been identified as effective catalysts for the process of oxidative dehydrogenation, where isobutane is converted to isobutene. In this

process, carbonyl (quinone) groups act as active sites, whereas carboxylic groups negatively impact catalytic performance by reducing electron density at these sites, thereby lowering activity [294]. The reaction mechanism proposed for hydrocarbon oxidative dehydrogenation is illustrated in Fig. 22 (b). This quinone-hydroquinone cycle might represent a general pathway for various oxidation reactions catalyzed by carbon-containing materials.

4.9 Applications in Responsive drug delivery

Carbon-based hybrid nanogels have emerged as promising candidates for highly efficient stimuli-responsive drug delivery systems. Their suitability is attributed to the inherent porous structure, high surface area, and favorable drug-nanocarbon interactions, which collectively enable exceptionally high drug loading capacities. Additionally, these nanogels exhibit excellent colloidal stability in aqueous solutions. To date, both endogenous and exogenous stimuli have been extensively employed to regulate the controlled release of therapeutic agents in vivo, thereby enhancing the efficacy of disease treatment [295].

4.9.1 Endogenous activation-responsive drug delivery

Endogenous activation is typically achieved through variations in specific physicochemical characteristics of the pathological microenvironment, such as pH, temperature, and the presence of certain biomolecules [296]. Several carbon-based hybrid nanogels have been developed to facilitate responsive drug delivery. For instance, Majumdar et al. synthesized an alginate-carbon dot (CD) hybrid nanogel designed for pH-responsive drug release, wherein the drug release rate is modulated by the concentration of methicillin-resistant *Staphylococcus aureus* (MRSA) at the target site [297]. Notably, the incorporation of CDs into alginate nanogels significantly enhances the drug loading capacity, increasing it from 19% to 78% for a garlic extract model drug containing allicin. These alginate-CD hybrid nanogels exhibit pH-dependent controlled drug release, thereby improving therapeutic efficacy. Importantly, the system not only responds to stimuli but also enables controlled drug release based on pathogen concentration. Specifically, the presence of *Staphylococcus aureus* (MRSA) leads to cell division and the production of acidic secondary metabolites, resulting in a local decrease in pH. This pH drop subsequently triggers drug release from the nanogels, effectively inducing MRSA cell death. In a separate study, Bardajee et al.





developed a new class of thermo- and pH-dual-responsive biodegradable hybrid nanogels through the copolymerization and crosslinking of N-isopropylacrylamide (NIPAM) and acrylic acid (AA) monomers in the presence of salep-modified GO [298]. The resulting P(NIPAM-AA)-salep-GO hybrid nanogels demonstrated a high loading capacity for the anticancer drug doxorubicin (DOX), along with thermo- and pH-responsive drug release behavior. Specifically, the system exhibited minimal drug release at neutral pH and lower temperatures, while a significantly enhanced release was observed under acidic conditions and elevated temperatures- without any initial burst release. Moreover, the GO-based hybrid nanogels showed no cytotoxicity within the tested concentration range of up to 410 $\mu\text{g mL}^{-1}$. However, the dual-responsive and sustained release of DOX from the hybrid nanogels led to a marked increase in cytotoxicity against HeLa cells compared to the equivalent concentration of free DOX, indicating improved therapeutic efficacy. Kim et al. reported the rational design of therapeutic contact lenses by incorporating nanodiamonds (NDs) into enzyme-responsive nanogel matrices, demonstrating their potential as effective platforms for ocular drug delivery shown in Figure 24a [299].

The timolol maleate-loaded nanodiamond-polyethylenimine-chitosan (ND-PEI-chitosan) hybrid nanogel was successfully embedded within a hydrogel matrix and cast into contact lenses. This hybrid nanogel retains timolol through short-range chemical interactions, effectively preventing premature drug elution while preserving its bioactivity for subsequent release [300]. Drug release is triggered by the enzymatic degradation of the chitosan-based nanogel via lysozyme cleavage. Beyond enabling controlled drug delivery, the incorporation of a small amount of nanodiamonds into the lens matrix significantly improved the mechanical properties by enhancing tensile strength and increasing the elastic modulus through polymer matrix reinforcement. The resulting contact lenses exhibited excellent water and oxygen permeability, optical transparency, and mechanical robustness, along with sustained drug release in response to lysozyme activation. This innovative ND-based system represents a promising platform for the development of advanced enzyme-responsive drug delivery devices tailored for sustained ocular therapy. These studies demonstrate that integrating carbon-based nanomaterials into hybrid nanogels enables precise, stimuli-responsive drug release tailored to pathological conditions. Reported findings emphasize that pH, temperature, and enzyme triggers, combined with high drug-loading capacity and

biocompatibility, can significantly enhance therapeutic efficacy while minimizing premature release.

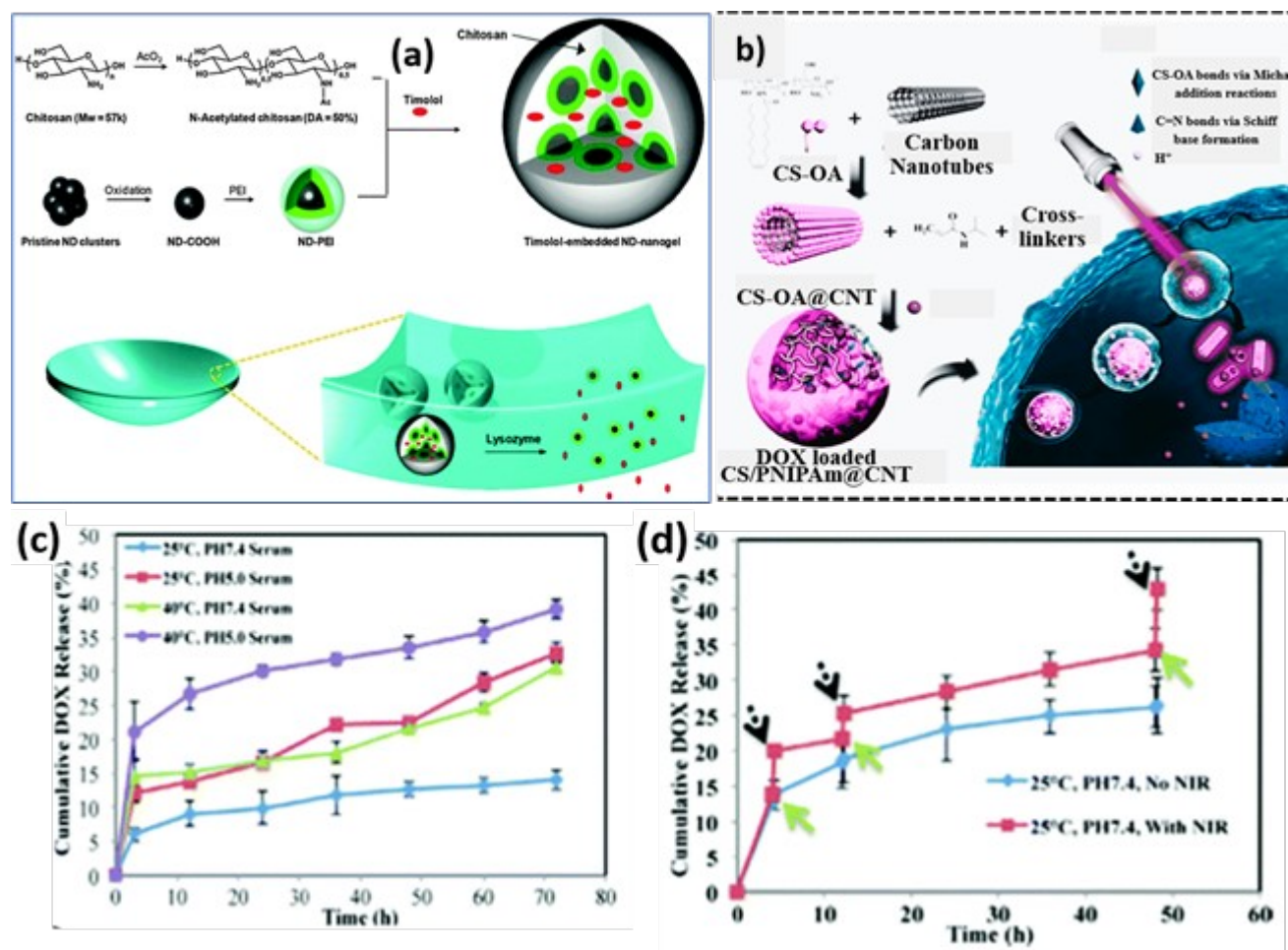


Figure 24. (a) Synthesis of drug-loaded ND-PEI-chitosan nanogels and their integration into lysozyme-responsive contact lenses. (b-d) DOX-loaded CS/PNIPAM@CNT nanogels: stimuli-responsive drug release triggered by pH, temperature, and NIR light. Reproduced from reference [301] with permission from Royal society of chemistry, copyright 2015.

4.9.2 Exogenous activation-responsive drug delivery

Exogenous activation of drug release has garnered significant attention, as it eliminates the need for modifying the physical or chemical properties of the biological environment- an advantage that helps avoid the potential adverse effects on healthy cells and tissues often associated with the harsh conditions required for endogenous activation in *in vivo* applications [302, 303]. A promising



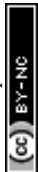
strategy for exogenous activation involves the application of external stimuli such as electric fields, magnetic fields, or near-infrared (NIR) light. These triggers can initiate drug release from hybrid nanogel carriers with precise spatial and temporal control, thereby enhancing site-specific drug accumulation. Such control is particularly advantageous in cancer therapy, where localized treatment can significantly improve therapeutic efficacy while minimizing systemic side effects. For example, Lu et al. integrated reduced rGO nanosheets into a thermosensitive poly(N-isopropylacrylamide) (PNIPAM) nanogel, resulting in a dual-responsive drug delivery system responsive to both light and temperature [304]. The rGO content within the hybrid nanogels plays a crucial role in modulating both thermal and photic sensitivity. At lower rGO concentrations (<47.5 wt%), the rGO-PNIPAM hybrid nanogels exhibit temperature-responsive drug release, with an increased release rate as the temperature rises. In contrast, when the rGO content exceeds 64.5 wt%, the nanogels lose their thermoresponsive behavior and instead display photo-responsive drug release. In a separate study, Spizzirri et al. developed a biocompatible gelatin-CNT hybrid nanogel, which demonstrated electric field-responsive drug release [305]. The application of an electric field (9V) to the hybrid nanogel system resulted in a 20% increase in drug release. Hybrid nanogels with higher concentrations of CNTs exhibited a greater release of drug molecules in response to the same electric field strength. These electro-responsive CNT-based hybrid nanogels could be integrated into a suitable topical drug delivery device, enabling controlled release of therapeutics upon the application of an external voltage.

4.9.3 Combined endogenous/exogenous activation-responsive drug delivery

The combination of both endogenous and exogenous activation-responsive drug delivery presents a promising approach to enhance the therapeutic efficacy of cancer treatment in a synergistic manner [306]. Such combined therapy is expected to reduce the required drug dosage while still achieving comparable cytotoxicity to the equivalent dose of the drug without exogenous activation, thereby minimizing the systemic side effects commonly associated with chemotherapeutic agents. For instance, Xu et al. developed a GO-hybridized biodegradable alginate nanogel that demonstrates combined anticancer effects through both endogenous and exogenous activation mechanisms [307]. The doxorubicin (DOX)-encapsulated AGD hybrid nanogels exhibited limited drug release under normal physiological conditions but demonstrated accelerated DOX release under acidic and reducible conditions, which simulate the extracellular tumor microenvironment



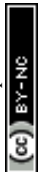
and intracellular compartments. The dual-stimuli responsive release properties of the GO-based hybrid nanogels facilitate effective anticancer drug delivery to tumor cells, leading to high intracellular drug accumulation over an extended period and resulting in significant antitumor cytotoxicity. This effect can be further enhanced when coupled with NIR laser photothermal treatment. These GO-based hybrid nanogels present promising potential for the development of novel combinatory anticancer therapies. In a separate study, pH and NIR light-responsive hyaluronic acid- (2-aminoethyl)-carbamate (HA-EDA-PHEA-DVS-GO) double-network hybrid nanogels were also designed to integrate both endogenous and exogenous activation for responsive drug delivery, specifically targeting the treatment of colorectal carcinoma cells [308]. The large aromatic surface area of GO enables the hybrid nanogels to load significant amounts of poorly water-soluble anticancer drugs, such as irinotecan (33.0 wt%). Both the pH of the external medium and near-infrared (NIR) irradiation can effectively control the release of this antitumor drug. The irinotecan-loaded GO-based hybrid nanogels are readily internalized by cancer cells and can synergistically enhance the hyperthermic and drug cytotoxic effects upon NIR irradiation, resulting in high therapeutic efficacy through the combined photothermal and chemotherapeutic approaches. In a separate study, Qin et al. developed a carbon-based CS/PNIPAM@CNT hybrid nanogel, wherein chitosan-coated CNTs were randomly embedded within poly(N-isopropylacrylamide) (PNIPAM)-PEG nanogels. This system also integrates both endogenous and exogenous activation-responsive drug release, thereby improving the anti-cancer therapeutic efficacy [309]. The pH/thermo dual-responsive CS/PNIPAm@CNT hybrid nanogels demonstrated a faster release of doxorubicin (DOX) at 40°C compared to 25°C, when maintained at the same pH values. Similarly, the release rate of DOX was higher at pH 5.0 than at pH 7.4, under identical temperature conditions (Figure 24b-d). Furthermore, the DOX-loaded CS/PNIPAm@CNT hybrid nanogels exhibited significantly greater cytotoxicity in HeLa cells upon near-infrared (NIR) irradiation, attributed to the NIR-triggered increase in temperature, which facilitated enhanced DOX release. These findings collectively show that integrating both endogenous and exogenous triggers within carbon-based hybrid nanogels enables synergistic control over drug release, improving therapeutic efficacy while reducing systemic toxicity. Literature reports highlight that combining pH, thermal, or redox sensitivity with photothermal or other external stimuli can significantly enhance cancer cell targeting and treatment outcomes.



5. Challenges and Future Perspectives

Despite the remarkable potential of carbon-based gel materials—including aerogels, xerogels, and hydrogels—in diverse applications such as energy storage, environmental remediation, and biomedical systems, several critical challenges hinder their broader commercialization. Foremost among these are the complexity and cost of synthesis, particularly for aerogels. Supercritical drying methods, though effective in preserving pore structure, are energy-intensive, time-consuming, and economically unsustainable for large-scale production. Alternatives like freeze-drying and ambient drying offer cost advantages but may compromise mechanical strength or porosity. Furthermore, scalability and environmental sustainability remain concerns, as most conventional carbon gels still rely on petrochemical-derived precursors such as resorcinol and formaldehyde. Biomass-derived precursors—lignin, cellulose, agricultural residues—present a sustainable alternative, yet require optimization to ensure batch-to-batch consistency, high yield, and reproducible performance.

Tunable structure–property relationships are another critical area for development. Precisely controlling porosity, surface chemistry, and electrical conductivity during scale-up is challenging, hindering reliable tailoring for specific functions such as supercapacitor electrodes or selective adsorption membranes. This challenge is not unique to carbon gels; similar issues are encountered in other advanced porous materials like MXenes, Prussian Blue frameworks, COFs, MOFs, and hydrogen-bonded organic frameworks (HOFs). For example, in-plane ordered MXenes have been shown to address limitations in biosensor applications through enhanced conductivity and surface tunability, while MXene–COF hybrids leverage complementary properties to improve mechanical robustness and chemical stability. Likewise, MOF–MXene composites have achieved outstanding electrochemical performance in supercapacitors by combining the high surface area and tunable porosity of MOFs with the conductive layers of MXenes. HOF-derived materials also offer promising structural stability and ion diffusion pathways for supercapacitors, and Prussian Blue frameworks have emerged as sustainable cathode materials in sodium- and potassium-ion batteries, offering scalability potential that parallels carbon gel development goals.



2169

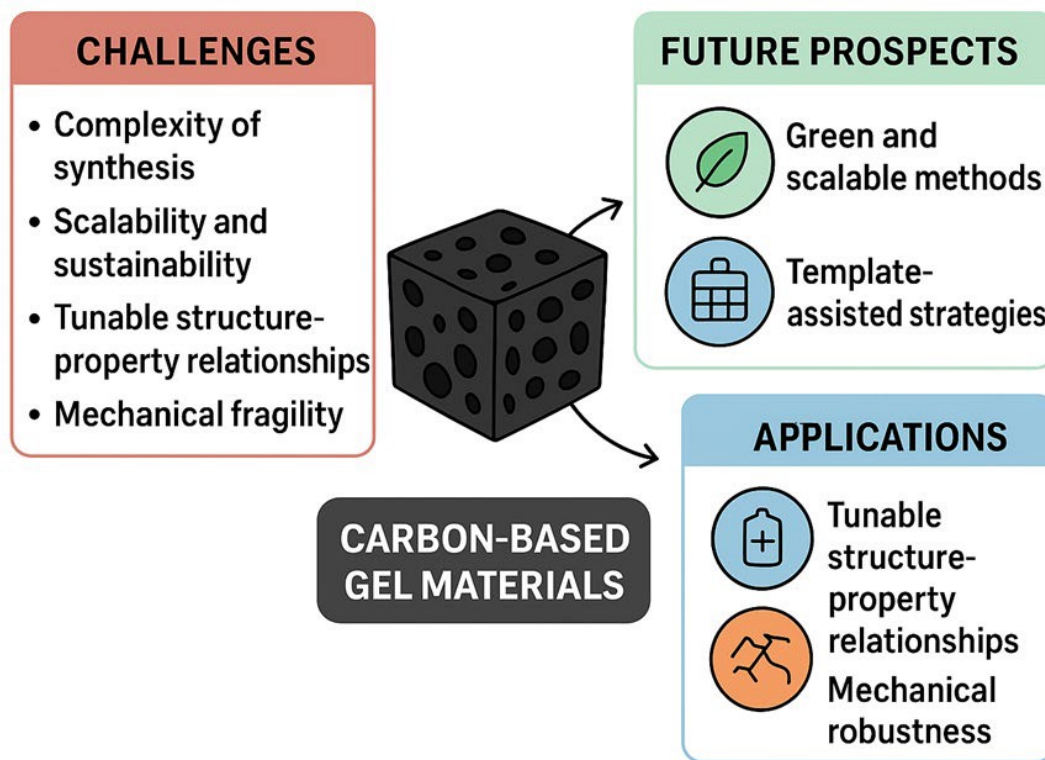


Figure 25. Schematic representation of the key challenges, future prospects of carbon-based gel

Mechanical fragility remains a limitation for high-porosity aerogels, necessitating hybridization or polymer reinforcement. Such approaches have parallels in MXene-polymer composites and COF-MOF hybrids, where synergistic reinforcement enhances structural integrity without sacrificing functionality. On the application side, integration into devices such as electrodes, filtration membranes, and wearable electronics demands multifunctionality-high surface area, mechanical durability, biocompatibility, and electrical conductivity-properties also being engineered in next-generation 2D and framework materials.

Future progress will rely on green and scalable synthesis strategies, including solvent-free processing, ambient drying, and waste-derived feedstocks. Template-assisted assembly and self-organization techniques, inspired by advances in MOF, COF, and MXene fabrication, could offer precise control over pore architecture and chemical functionality. Furthermore, coupling carbon gels with emerging high-performance frameworks-such as MXenes for conductivity enhancement,



Open Access Article. Published on 21 August 2025. Downloaded on 9/5/2025 7:05:43 PM.
This article is licensed under a Creative Commons Attribution-NonCommercial 3.0 Unported Licence.



MOFs/COFs for selective adsorption, and HOFs for lightweight energy storage-may yield multifunctional hybrid systems with unprecedented performance. Machine learning and AI-guided materials discovery can accelerate optimization by predicting structure–property relationships, while standardized performance metrics across material classes will improve comparability and facilitate commercialization. Ultimately, interdisciplinary collaboration among materials science, chemical engineering, and device manufacturing-paralleling strategies used to transition MXene and MOF technologies from lab to market-will be essential to fully exploit the potential of carbon-based gels in next-generation sustainable technologies.

6. Techno-Economic Outlook on Application Prospects

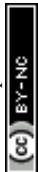
The successful commercialization of carbon-based gel materials hinges on their ability to deliver high performance while remaining cost-competitive and scalable. From a techno-economic perspective, current synthesis routes-particularly supercritical and freeze-drying methods-pose cost barriers due to high energy consumption, long processing times, and specialized equipment requirements. Emerging alternatives, such as ambient pressure drying, solvent-free synthesis, and biomass-derived precursors, present opportunities to significantly reduce production costs and environmental impact. For instance, utilizing low-cost feedstocks like agricultural waste or lignocellulosic biomass not only lowers material costs but also aligns with circular economy principles. On the application side, carbon gels are already proving viable in high-value markets such as supercapacitors, CO₂ capture, water purification, and biomedical devices, where performance advantages can justify higher initial costs. However, broader adoption in large-scale energy storage or industrial environmental remediation will require further reductions in production costs to achieve competitive \$/kg pricing relative to activated carbon and conventional electrode materials. Economic modeling suggests that integrating carbon gel production into biorefinery or waste valorization facilities could enhance profitability through resource sharing and co-product generation. Additionally, modular, continuous-flow synthesis systems could streamline manufacturing and reduce operational expenses. The techno-economic feasibility is further strengthened by the multifunctionality of carbon gels-offering high surface area, tunable porosity, and adaptability to various functionalizations-which enables their deployment across diverse sectors without extensive re-engineering. Future market competitiveness will depend on balancing performance optimization with cost minimization through process intensification,

Materials Advances Accepted Manuscript

automation, and green chemistry innovations. Strategic partnerships between academia, industry, and policymakers will be essential to accelerate technology transfer, standardize quality benchmarks, and create favorable regulatory environments that support the large-scale commercialization of carbon-based gels.

7. Conclusions

To sum up, carbon-based gels have developed into a flexible class of materials with enormous potential for improving sensor, energy storage, and environmental remediation technologies. From conventional sol-gel processes to innovative, environmentally friendly techniques using biomass-derived precursors, this study has clarified state-of-the-art synthesis pathways that provide fine control of pore design, chemical functionality, and mechanical resilience. These gels' inherent electrical conductivity and catalytic qualities have been further improved by the addition of nanostructured materials like graphene and carbon nanotubes, expanding their range of potential uses in high-performance supercapacitors, batteries, and fuel cells. Notwithstanding these noteworthy developments, a number of issues still exist, such as the requirement for cost-effective and scalable production methods, enhanced process repeatability, and long-term material stability under operational stress. In order to maximize material performance at the nanoscale, future research should focus on developing novel templating techniques and sustainable synthesis strategies that utilize green chemistry principles along with cutting-edge computational and in situ characterization capabilities. The commercialization of these innovations also depends on closing the gap between laboratory-scale success and practical industrial use. The discipline is positioned to produce ground-breaking discoveries that can solve important worldwide issues in energy and environmental sustainability by combining multidisciplinary insights from materials science, chemical engineering, and environmental technology. In the end, advancements in carbon-based gels not only demonstrate their present significance but also lay out a clear path for upcoming developments meant to bring about a more technologically sophisticated and sustainable future.



Author contributions: Md Shariful Islam, Shreyase Kundu, Mst Samsunnahar: Writing Original draft; Tasmina Khandaker, Ahmed B.M. Ibrahim: Writing and editing; Md Al-Amin Mia Anik, Md. Kamrul Hasan: Proof reading and editing; Muhammad Sarwar Hossain: Methodology, resources, validation, writing and editing, and supervision

Conflict of Interest: The authors declare that they have no known financial or personal conflicts of interest that could have influenced the work reported in this paper.

Ethical Approval: This article does not contain any studies with human participants or animals performed by any of the authors. As a review manuscript, it synthesizes existing research and does not involve new data collection requiring ethical approval.

Acknowledgements: The authors extend their sincere thanks to the Chemistry Discipline at Khulna University, Bangladesh, for providing a supportive research environment and essential facilities.

References

- Chini, C.M., L.E. Excell, and A.S. Stillwell, *A review of energy-for-water data in energy-water nexus publications*. Environmental Research Letters, 2021. **15**(12): p. 123011.
- Olsson, G., *Water and energy: threats and opportunities*. 2015: IWA publishing.
- Mukherjee, S. and T. Pradeep, *Nanomaterials-enabled technologies for clean water and their sustainability aspects*, in *Industrial applications of nanoparticles*. 2023, CRC Press. p. 16-31.
- Worku, A.K. and D.W. Ayele, *Recent advances of graphene-based materials for emerging technologies*. Results in Chemistry, 2023. **5**: p. 100971.
- Nardecchia, S., et al., *Three dimensional macroporous architectures and aerogels built of carbon nanotubes and/or graphene: synthesis and applications*. Chemical Society Reviews, 2013. **42**(2): p. 794-830.
- Afreen, S., et al., *Carbon-based nanostructured materials for energy and environmental remediation applications*. Approaches in bioremediation: The new era of environmental microbiology and nanobiotechnology, 2018: p. 369-392.
- Priya, A., M. Muruganandam, and S. Suresh, *Bio-derived carbon-based materials for sustainable environmental remediation and wastewater treatment*. Chemosphere, 2024: p. 142731.
- Reza, M.S., et al., *Advanced applications of carbonaceous materials in sustainable water treatment, energy storage, and CO₂ capture: a comprehensive review*. Sustainability, 2023. **15**(11): p. 8815.
- Ren, W., et al., *Advanced gel polymer electrolytes for safe and durable lithium metal batteries: Challenges, strategies, and perspectives*. Energy Storage Materials, 2021. **34**: p. 515-535.



- 2278 10. Mehdi-pour-Ataei, S. and E.J.C. Aram, *Mesoporous carbon-based materials: A review of*
2279 *synthesis, modification, and applications*. 2022. **13**(1): p. 2.
- 2280 11. Pekala, R.J.J.o.m.s., *Organic aerogels from the polycondensation of resorcinol with*
2281 *formaldehyde*. 1989. **24**: p. 3221-3227.
- 2282 12. Inagaki, M., K. Kaneko, and T. Nishizawa, *Nanocarbons—recent research in Japan*.
2283 Carbon, 2004. **42**(8-9): p. 1401-1417.
- 2284 13. Chen, Y., et al., *Carbons as low-platinum catalyst supports and non-noble catalysts for*
2285 *polymer electrolyte fuel cells*. 2023. **98**: p. 101101.
- 2286 14. Canal-Rodríguez, M., et al., *Carbon xerogels graphitized by microwave heating as anode*
2287 *materials in lithium-ion batteries*. 2018. **137**: p. 384-394.
- 2288 15. Kumar, Y.A., et al., *A review on in-plane ordered MXenes-based materials in addressing*
2289 *challenges faced by biosensor applications*. Journal of Energy Storage, 2025. **121**: p.
2290 116507.
- 2291 16. Ramachandran, T., et al., *Multifunctional covalent-organic frameworks (COFs)-2D*
2292 *MXenes composites for diverse applications*. Journal of Energy Storage, 2023. **73**: p.
2293 109299.
- 2294 17. Mouli, K.V.C., et al., *Cutting-edge advancements in HOFs-derived materials for energy*
2295 *storage supercapacitor application*. International Journal of Hydrogen Energy, 2024. **90**:
2296 p. 1-24.
- 2297 18. Kumar, Y.A., et al., *Supercharging the future: MOF-2D MXenes supercapacitors for*
2298 *sustainable energy storage*. Journal of Energy Storage, 2024. **80**: p. 110303.
- 2299 19. Kumar, Y.A., et al., *From lab to field: Prussian blue frameworks as sustainable cathode*
2300 *materials*. Dalton Transactions, 2024. **53**(26): p. 10770-10804.
- 2301 20. Alam, M.S., et al., *Advances of MAX phases: Synthesis, characterizations and challenges*.
2302 Engineering Reports, 2024. **6**(8): p. e12911.
- 2303 21. Torres, C.E.I., et al., *Carbon-based aerogels and xerogels: Synthesis, properties, oil*
2304 *sorption capacities, and DFT simulations*. Journal of Environmental Chemical
2305 Engineering, 2021. **9**(1): p. 104886.
- 2306 22. Girirajan, M., et al., *An insight into the nanoarchitecture of electrode materials on the*
2307 *performance of supercapacitors*. 2024. **518**: p. 216080.
- 2308 23. Jiang, Q., et al., *Nitrogen-doped carbon materials as supercapacitor electrodes: a mini*
2309 *review*. 2024. **38**(12): p. 10542-10559.
- 2310 24. Liu, H., et al., *Multifunctional aerogel: A unique and advanced biomaterial for tissue*
2311 *regeneration and repair*. 2024. **243**: p. 113091.
- 2312 25. Pierre, A.C. and G.M. Pajonk, *Chemistry of aerogels and their applications*. Chemical
2313 reviews, 2002. **102**(11): p. 4243-4266.
- 2314 26. Rashid, A.B., et al., *Silica aerogel: Synthesis, characterization, applications, and recent*
2315 *advancements*. Particle & Particle Systems Characterization, 2023. **40**(6): p. 2200186.
- 2316 27. Song, Z., et al., *Self-cleaning, energy-saving aerogel composites possessed sandwich*
2317 *structure: Improving indoor comfort with excellent thermal insulation and acoustic*
2318 *performance*. Energy and Buildings, 2024. **310**: p. 114098.
- 2319 28. Qi, L., et al., *Coupled electron delocalization and multi-dimensional porosity engineering*
2320 *in TiO₂ hollow spheres-embedded carbon nanofiber aerogels for efficient photocatalytic*
2321 *aniline degradation*. 2025: p. 163690.
- 2322 29. Wang, X., et al., *Synthesis of flashed graphene nanocellulose aerogel for microplastic*
2323 *adsorption in aquatic environment*. 2025: p. 117530.



- 2324 30. Madyan, O.A., et al., *Enhancing mechanical properties of clay aerogel composites: An*
2325 *overview*. Composites Part B: Engineering, 2016. **98**: p. 314-329.
- 2326 31. Abdusalamov, R., et al., *Modeling and simulation of the aggregation and the structural*
2327 *and mechanical properties of silica aerogels*. 2021. **125**(7): p. 1944-1950.
- 2328 32. Hu, B.C., et al., *Robust carbonaceous nanofiber aerogels from all biomass precursors*.
2329 *Advanced Functional Materials*, 2023. **33**(1): p. 2207532.
- 2330 33. Wu, Z.Y., et al., *Emerging carbon-nanofiber aerogels: chemosynthesis versus*
2331 *biosynthesis*. Angewandte Chemie International Edition, 2018. **57**(48): p. 15646-15662.
- 2332 34. dos Santos-Gómez, L., et al., *Ultralight-weight graphene aerogels with extremely high*
2333 *electrical conductivity*. 2021. **17**(41): p. 2103407.
- 2334 35. Chen, W., et al., *Self-assembly and embedding of nanoparticles by in situ reduced*
2335 *graphene for preparation of a 3D graphene/nanoparticle aerogel*. *Advanced materials*,
2336 2011. **23**(47): p. 5679-5683.
- 2337 36. Mu, J., et al., *Sheath-run artificial muscles*. *Science*, 2019. **365**(6449): p. 150-155.
- 2338 37. Wang, H., et al., *Porous two-dimensional materials for photocatalytic and electrocatalytic*
2339 *applications*. 2020. **2**(6): p. 1377-1413.
- 2340 38. Payanda Konuk, O., et al., *The effect of synthesis conditions and process parameters on*
2341 *aerogel properties*. *Frontiers in Chemistry*, 2023. **11**: p. 1294520.
- 2342 39. Ulker, Z. and C. Erkey, *An emerging platform for drug delivery: Aerogel based systems*.
2343 *Journal of Controlled Release*, 2014. **177**: p. 51-63.
- 2344 40. Jadhav, S. and P. Sarawade, *Recent advances and prospective of reinforced silica aerogel*
2345 *Nanocomposites and their applications*. *European Polymer Journal*, 2024. **206**: p. 112766.
- 2346 41. Luo, Y., et al., *Rapid synthesis and characterization of ambient pressure dried monolithic*
2347 *silica aerogels in ethanol/water co-solvent system*. *Journal of Non-Crystalline Solids*,
2348 2019. **503**: p. 214-223.
- 2349 42. Baker, J.M., J.P. Nederveen, and G. Parise, *Aerobic exercise in humans mobilizes HSCs in*
2350 *an intensity-dependent manner*. *Journal of Applied Physiology*, 2017. **122**(1): p. 182-190.
- 2351 43. Shalaby, M.N. and M.A. Fadl, *Relative Indicators and Predicative Ability of Some*
2352 *Biological Variables on Cardiac Neural Activity for Volleyball Players*. *Systematic*
2353 *Reviews in Pharmacy*, 2020. **11**(9).
- 2354 44. Cheng, X., et al., *Rapid synthesis of ambient pressure dried monolithic silica aerogels*
2355 *using water as the only solvent*. *Materials Letters*, 2017. **204**: p. 157-160.
- 2356 45. Cuce, E., et al., *Toward aerogel based thermal superinsulation in buildings: A*
2357 *comprehensive review*. *Renewable and Sustainable Energy Reviews*, 2014. **34**: p. 273-299.
- 2358 46. Lee, J.-H. and S.-J.J.C. Park, *Recent advances in preparations and applications of carbon*
2359 *aerogels: A review*. 2020. **163**: p. 1-18.
- 2360 47. Sun, H., Z. Xu, and C. Gao, *Multifunctional, ultra-flyweight, synergistically assembled*
2361 *carbon aerogels*. *Advanced materials*, 2013. **25**(18): p. 2554-2560.
- 2362 48. Chemere, E.B., et al., *A comprehensive review of types, synthesis strategies, advanced*
2363 *designing and applications of aerogels*. 2025. **12**(5): p. 241975.
- 2364 49. Ghaffari-Mosanenzadeh, S., et al., *Recent advances in tailoring and improving the*
2365 *properties of polyimide aerogels and their application*. *Advances in Colloid and Interface*
2366 *Science*, 2022. **304**: p. 102646.
- 2367 50. Veselov, G.B. and A.A.J.M. Vedyagin, *Resorcinol-Formaldehyde-Derived Carbon*
2368 *Xerogels: Preparation, Functionalization, and Application Aspects*. 2023. **16**(19): p. 6566.



- 2369 51. Job, N., et al., *Porous carbon xerogels with texture tailored by pH control during sol-gel*
2370 *process*. 2004. **42**(3): p. 619-628.
- 2371 52. González, N.G., et al., *Towards the valorisation of glycerol by designing the surface*
2372 *chemistry of carbon xerogels by doping and oxygen functionalization*. 2024. **256**: p.
2373 119190.
- 2374 53. Wang, Z., *Design, fabrication, and testing of nanostructured carbons and composites*.
2375 2008: University of Minnesota.
- 2376 54. Mohd Faizal, A.N. and M.A.J.T.R. Ahmad Zaini, *Dyes adsorption properties of KOH-*
2377 *activated resorcinol-formaldehyde carbon gels-kinetic, isotherm and dynamic studies*.
2378 2022. **41**(1): p. 186-197.
- 2379 55. Roy, N., et al., *Biomass-derived nanostructures and hydrothermal carbon spheres: A*
2380 *review of electrochemical applications in redox flow battery*. Journal of Industrial and
2381 Engineering Chemistry, 2025. **144**: p. 228-254.
- 2382 56. Khandaker, T., et al., *Biomass-derived carbon materials for sustainable energy*
2383 *applications: a comprehensive review*. Sustainable Energy & Fuels, 2025. **9**(3): p. 693-
2384 723.
- 2385 57. Ramachandran, T., et al., *Sustainable carbon electrode materials from biomass for redox*
2386 *flow batteries*. Biomass and Bioenergy, 2025. **198**: p. 107846.
- 2387 58. Zhao, Y., et al., *Unlocking the potential of vanadium redox flow batteries: Recent advances*
2388 *in biomass lignin-based carbon fibers and future outlook*. Biomass and Bioenergy, 2025.
2389 **200**: p. 108052.
- 2390 59. Wang, Y., et al., *Biomass derived carbon as binder-free electrode materials for*
2391 *supercapacitors*. 2019. **155**: p. 706-726.
- 2392 60. Jiang, M., et al., *An N, P, O-doped porous carbon electrode material derived from a lignin-*
2393 *modified chitosan xerogel for a supercapacitor*. 2023. **22**: p. 100372.
- 2394 61. Liang, J., et al., *Sulfur and nitrogen dual-doped mesoporous graphene electrocatalyst for*
2395 *oxygen reduction with synergistically enhanced performance*. 2012. **124**(46): p. 11664-
2396 11668.
- 2397 62. Abidin, A.F.Z., et al., *Nitrogen-doped carbon xerogels catalyst for oxygen reduction*
2398 *reaction: Improved structural and catalytic activity by enhancing nitrogen species and*
2399 *cobalt insertion*. 2019. **44**(54): p. 28789-28802.
- 2400 63. Shen, Y. and J.J.G.C. Yang, *Progress in the synthesis of carbon aerogels for advanced*
2401 *energy storage applications*. 2024. **26**(16): p. 8969-9004.
- 2402 64. Medina Erazo, O.E., *Development of Multifunctional Nanomaterials for the co-Production*
2403 *of Upgraded Heavy Crude Oil and Hydrogen at Different Pressures and Temperatures*.
2404 2023.
- 2405 65. Zhang, H., et al., *A graphene hybrid supramolecular hydrogel with high stretchability, self-*
2406 *healable and photothermally responsive properties for wound healing*. RSC advances,
2407 2021. **11**(11): p. 6367-6373.
- 2408 66. Slaughter, B.V., et al., *Hydrogels in regenerative medicine*. Advanced materials, 2009.
2409 **21**(32-33): p. 3307-3329.
- 2410 67. Zhang, H., et al., *A chemical blowing strategy to fabricate biomass-derived carbon-*
2411 *aerogels with graphene-like nanosheet structures for high-performance supercapacitors*.
2412 ChemSusChem, 2019. **12**(11): p. 2462-2470.
- 2413 68. Hauck, M., et al., *Overcoming water diffusion limitations in hydrogels via microtubular*
2414 *graphene networks for soft actuators*. Advanced Materials, 2023. **35**(41): p. 2302816.



- 2415 69. Zhu, Z., et al., *An aptamer cross-linked hydrogel as a colorimetric platform for visual*
2416 *detection*. *Angewandte Chemie-International Edition*, 2010. **49**(6): p. 1052-1056.
- 2417 70. Cheng, Q.-Y., et al., *Supramolecular self-assembly induced graphene oxide based*
2418 *hydrogels and organogels*. *Langmuir*, 2012. **28**(5): p. 3005-3010.
- 2419 71. Narayanaswamy, R. and V.P. Torchilin, *Hydrogels and their applications in targeted drug*
2420 *delivery*. *The road from nanomedicine to precision medicine*, 2020: p. 1117-1150.
- 2421 72. Hua, M., et al., *Strong tough hydrogels via the synergy of freeze-casting and salting out*.
2422 *Nature*, 2021. **590**(7847): p. 594-599.
- 2423 73. Fan, R., et al., *Thermosensitive hydrogels and advances in their application in disease*
2424 *therapy*. 2022. **14**(12): p. 2379.
- 2425 74. Oh, H.M., et al., *Preparation and characterization of an in situ crosslinkable glycol*
2426 *chitosan thermogel for biomedical applications*. *Journal of Industrial and Engineering*
2427 *Chemistry*, 2019. **80**: p. 820-828.
- 2428 75. Hussain, S. and S.S. Maktedar, *Structural, functional and mechanical performance of*
2429 *advanced Graphene-based composite hydrogels*. *Results in Chemistry*, 2023. **6**: p. 101029.
- 2430 76. Rolland, J.P., et al., *Direct fabrication and harvesting of monodisperse, shape-specific*
2431 *nanobiomaterials*. *Journal of the American Chemical Society*, 2005. **127**(28): p. 10096-
2432 10100.
- 2433 77. Tagliazucchi, M., K. Huang, and I. Szleifer, *Routes for nanoparticle translocation through*
2434 *polymer-brush-modified nanopores*. *Journal of Physics: Condensed Matter*, 2018. **30**(27):
2435 p. 274006.
- 2436 78. Zhang, H., et al., *New progress and prospects: The application of nanogel in drug delivery*.
2437 *Materials Science and Engineering: C*, 2016. **60**: p. 560-568.
- 2438 79. Firoozi, A.A., et al., *Enhanced perspectives on silica aerogels: Novel synthesis methods*
2439 *and emerging engineering applications*. 2025. **25**: p. 103615.
- 2440 80. Wei, G., et al., *Ni-doped graphene/carbon cryogels and their applications as versatile*
2441 *sorbents for water purification*. *ACS applied materials & interfaces*, 2013. **5**(15): p. 7584-
2442 7591.
- 2443 81. Ramachandran, T., et al., *From graphene aerogels to efficient energy storage: current*
2444 *developments and future prospects*. *Journal of Alloys and Compounds*, 2025. **1010**: p.
2445 177248.
- 2446 82. Chaitanya, B., et al. *Trends in solar powered water desalination using hydrogels: a short*
2447 *review*. in *2023 Advances in Science and Engineering Technology International*
2448 *Conferences (ASET)*. 2023. IEEE.
- 2449 83. Zafar, M., et al., *Graphene-based polymer nanocomposites for energy applications: Recent*
2450 *advancements and future prospects*. 2024: p. 107655.
- 2451 84. Arakawa, H., et al., *Self-assembly and hydrogel formation ability of Fmoc-dipeptides*
2452 *comprising α -methyl-L-phenylalanine*. 2020. **52**(8): p. 923-930.
- 2453 85. Santhiran, A., et al., *Graphene synthesis and its recent advances in applications—a review*.
2454 2021. **7**(4): p. 76.
- 2455 86. Agudosi, E.S., et al., *A review of the graphene synthesis routes and its applications in*
2456 *electrochemical energy storage*. 2020. **45**(5): p. 339-377.
- 2457 87. Qu, Y., et al., *Hierarchical-graphene-coupled polyaniline aerogels for electrochemical*
2458 *energy storage*. *Carbon*, 2018. **127**: p. 77-84.
- 2459 88. Hussain, S. and S.S.J.R.i.C. Maktedar, *Structural, functional and mechanical performance*
2460 *of advanced Graphene-based composite hydrogels*. 2023. **6**: p. 101029.



- 2461 89. Formanek, M., et al., *Gel formation in reversibly cross-linking polymers*. 2021. **54**(14): p. 6613-6627.
- 2462
- 2463 90. Zhang, H., et al., *Hybridized graphene for supercapacitors: Beyond the limitation of pure graphene*. 2021. **17**(12): p. 2007311.
- 2464
- 2465 91. Karchoubi, F., et al., *New insights into nanocomposite hydrogels; a review on recent advances in characteristics and applications*. 2024. **7**(1): p. 54-78.
- 2466
- 2467 92. Stealey, S.T., A.K. Gaharwar, and S.P.J.P. Zustiak, *Laponite-based nanocomposite hydrogels for drug delivery applications*. 2023. **16**(6): p. 821.
- 2468
- 2469 93. Wu, X.-L., et al., *Biomass-derived sponge-like carbonaceous hydrogels and aerogels for supercapacitors*. ACS nano, 2013. **7**(4): p. 3589-3597.
- 2470
- 2471 94. Du, R., et al., *Synthesis of conducting polymer hydrogels with 2D building blocks and their potential-dependent gel-sol transitions*. Chemical Communications, 2011. **47**(22): p. 6287-6289.
- 2472
- 2473
- 2474 95. Cheng, P., et al., *Biomass-derived carbon fiber aerogel as a binder-free electrode for high-rate supercapacitors*. The Journal of Physical Chemistry C, 2016. **120**(4): p. 2079-2086.
- 2475
- 2476 96. Mashkour, M., et al., *Application of wet nanostructured bacterial cellulose as a novel hydrogel bioanode for microbial fuel cells*. ChemElectroChem, 2017. **4**(3): p. 648-654.
- 2477
- 2478 97. Liang, H.-W., et al., *Bacterial cellulose derived nitrogen-doped carbon nanofiber aerogel: An efficient metal-free oxygen reduction electrocatalyst for zinc-air battery*. Nano Energy, 2015. **11**: p. 366-376.
- 2479
- 2480
- 2481 98. Zheng, X., A.M. Zuria, and M. Mohamedi, *Free-Standing Tunnel-Structured MnO₂ Nanorods-Doped with Nickel and Cobalt Cations as Bifunctional Electrocatalysts for Zn-Air Batteries*. Advanced Materials Technologies, 2023. **8**(24): p. 2301142.
- 2482
- 2483
- 2484 99. Mooste, M., et al., *Bifunctional oxygen electrocatalyst based on Fe, Co, and nitrogen co-doped graphene-coated alumina nanofibers for Zn-air battery air electrode*. Applied Surface Science, 2024. **660**: p. 160024.
- 2485
- 2486
- 2487 100. Anjali, J., V.K. Jose, and J.-M. Lee, *Carbon-based hydrogels: synthesis and their recent energy applications*. Journal of materials chemistry A, 2019. **7**(26): p. 15491-15518.
- 2488
- 2489 101. Firestone, M.A., S.C. Hayden, and D.L. Huber, *Greater than the sum: Synergy and emergent properties in nanoparticle-polymer composites*. MRS bulletin, 2015. **40**(9): p. 760-767.
- 2490
- 2491
- 2492 102. Kumar, Y.A., et al., *Advancements in novel electrolyte materials: Pioneering the future of supercapacitive energy storage*. Journal of Industrial and Engineering Chemistry, 2025. **145**: p. 191-215.
- 2493
- 2494
- 2495 103. Zaini, M.A.A., et al., *Preliminary evaluation of resorcinol-formaldehyde carbon gels for water pollutants removal*. Acta chimica slovac, 2017. **10**(1): p. 54.
- 2496
- 2497 104. Li, T., et al., *Mechanism of base-catalyzed resorcinol-formaldehyde and phenol-resorcinol-formaldehyde condensation reactions: A theoretical study*. Polymers, 2017. **9**(9): p. 426.
- 2498
- 2499
- 2500 105. Zhang, H., et al., *Controlling the microstructure of resorcinol-furfural aerogels and derived carbon aerogels via the salt templating approach*. RSC advances, 2019. **9**(11): p. 5967-5977.
- 2501
- 2502
- 2503 106. Salihovic, M., et al., *Carbon aerogels with improved flexibility by sphere templating*. 2018. **8**(48): p. 27326-27331.
- 2504
- 2505 107. Neema, P., S.K. Verma, and M.A.J.I.J.o.H.E. Shaz, *Physically activated resorcinol-formaldehyde derived carbon aerogels for enhanced hydrogen storage*. 2024.
- 2506



- 2507 108. Soni, R.U., et al., *Preparation of carbon aerogels from polymer-cross-linked xerogel*
2508 *powders without supercritical fluid drying and their application in highly selective CO2*
2509 *adsorption*. 2022. **34**(11): p. 4828-4847.
- 2510 109. Canal-Rodríguez, M., et al., *Graphene-doped carbon xerogel combining high electrical*
2511 *conductivity and surface area for optimized aqueous supercapacitors*. Carbon, 2017. **118**:
2512 p. 291-298.
- 2513 110. Zhang, Q., et al., *Mechanically robust honeycomb graphene aerogel multifunctional*
2514 *polymer composites*. Carbon, 2015. **93**: p. 659-670.
- 2515 111. Sen, S., et al., *Recent developments in biomass derived cellulose aerogel materials for*
2516 *thermal insulation application: a review*. 2022. **29**(9): p. 4805-4833.
- 2517 112. Wu, G., et al., *Three-dimensional directional cellulose-based carbon aerogels composite*
2518 *phase change materials with enhanced broadband absorption for light-thermal-electric*
2519 *conversion*. Energy Conversion and Management, 2022. **256**: p. 115361.
- 2520 113. Gad, Y.H. and S.M. Nasef, *Radiation synthesis of graphene oxide/composite hydrogels*
2521 *and their ability for potential dye adsorption from wastewater*. Journal of Applied Polymer
2522 Science, 2021. **138**(41): p. 51220.
- 2523 114. White, R.J., et al., *Always look on the "light" side of life: sustainable carbon aerogels*.
2524 ChemSusChem, 2014. **7**(3): p. 670-689.
- 2525 115. Crane, M.J., et al., *Rapid synthesis of transition metal dichalcogenide-carbon aerogel*
2526 *composites for supercapacitor electrodes*. Microsystems & nanoengineering, 2017. **3**(1):
2527 p. 1-9.
- 2528 116. Shen, Y. and J. Yang, *Progress in the synthesis of carbon aerogels for advanced energy*
2529 *storage applications*. Green Chemistry, 2024. **26**(16): p. 8969-9004.
- 2530 117. Barım, Ş.B., et al., *Control of average particle size of carbon aerogel supported platinum*
2531 *nanoparticles by supercritical deposition*. Microporous and Mesoporous Materials, 2017.
2532 **245**: p. 94-103.
- 2533 118. Zhang, S., et al., *Role of freeze-drying in cellulose-based aerogels: Freezing optimization*
2534 *strategies and diverse water treatment applications*. 2024. **42**(7): p. 1119-1137.
- 2535 119. Vazhayal, L., P. Wilson, and K. Prabhakaran, *Waste to wealth: Lightweight, mechanically*
2536 *strong and conductive carbon aerogels from waste tissue paper for electromagnetic*
2537 *shielding and CO2 adsorption*. Chemical Engineering Journal, 2020. **381**: p. 122628.
- 2538 120. Du, X., et al., *Heterogeneous photoelectro-Fenton catalyzed by FeCu@ PC for efficient*
2539 *degradation of sulfamethazine*. Electrochimica Acta, 2022. **412**: p. 140122.
- 2540 121. Anas, M., et al., *Thermodynamics of adsorption of carbon dioxide on various aerogels*.
2541 Journal of CO2 Utilization, 2017. **21**: p. 82-88.
- 2542 122. Feng, J., et al., *Carbon aerogel composites prepared by ambient drying and using oxidized*
2543 *polyacrylonitrile fibers as reinforcements*. ACS Applied Materials & Interfaces, 2011.
2544 **3**(12): p. 4796-4803.
- 2545 123. Zhou, Y., et al., *Controlled preparation of nitrogen-doped hierarchical carbon cryogels*
2546 *derived from Phenolic-Based resin and their CO2 adsorption properties*. 2022. **246**: p.
2547 123367.
- 2548 124. Zhang, F., et al., *The potassium hydroxide-urea synergy in improving the capacitive*
2549 *energy-storage performance of agar-derived carbon aerogels*. Carbon, 2019. **147**: p. 451-
2550 459.
- 2551 125. Hanzawa, Y., et al., *Structural changes in carbon aerogels with high temperature*
2552 *treatment*. Carbon, 2002. **40**(4): p. 575-581.



- 2553 126. Gutiérrez-Pardo, A., et al., *Effect of catalytic graphitization on the electrochemical*
2554 *behavior of wood derived carbons for use in supercapacitors*. Journal of Power Sources,
2555 2015. **278**: p. 18-26.
- 2556 127. Paliotta, L., et al., *Highly conductive multilayer-graphene paper as a flexible lightweight*
2557 *electromagnetic shield*. Carbon, 2015. **89**: p. 260-271.
- 2558 128. Canal-Rodríguez, M., et al., *Carbon xerogels graphitized by microwave heating as anode*
2559 *materials in lithium-ion batteries*. Carbon, 2018. **137**: p. 384-394.
- 2560 129. Hou, X., et al., *Activated carbon aerogel supported copper catalysts for the hydrogenation*
2561 *of methyl acetate to ethanol: effect of KOH activation*. 2019. **43**(24): p. 9430-9438.
- 2562 130. Bailón-García, E., et al., *Development of carbon xerogels as alternative Pt-supports for the*
2563 *selective hydrogenation of citral*. Catalysis Communications, 2015. **58**: p. 64-69.
- 2564 131. Enterría, M. and J. Figueiredo, *Nanostructured mesoporous carbons: Tuning texture and*
2565 *surface chemistry*. Carbon, 2016. **108**: p. 79-102.
- 2566 132. Lawtae, P. and C. Tangsathitkulchai, *A new approach for controlling mesoporosity in*
2567 *activated carbon by the consecutive process of air oxidation, thermal destruction of surface*
2568 *functional groups, and carbon activation (the OTA method)*. Molecules, 2021. **26**(9): p.
2569 2758.
- 2570 133. Lawtae, P., et al., *Improving porous properties of activated carbon from carbon gel by the*
2571 *OTA method*. RSC advances, 2023. **13**(21): p. 14065-14077.
- 2572 134. Tabata, Y., *Biomaterial technology for tissue engineering applications*. Journal of the
2573 Royal Society interface, 2009. **6**(suppl_3): p. S311-S324.
- 2574 135. Shantha, K. and D. Harding, *Synthesis and evaluation of sucrose-containing polymeric*
2575 *hydrogels for oral drug delivery*. Journal of applied polymer science, 2002. **84**(14): p.
2576 2597-2604.
- 2577 136. Sahu, N., D. Gupta, and U. Nautiyal, *Hydrogel: preparation, characterization and*
2578 *applications*. Asian Pacific Journal of Nursing and Health Sciences, 2020. **3**(1): p. 1-11.
- 2579 137. Mishra, S., et al., *Applications of biopolymeric gels in agricultural sector*. Polymer Gels:
2580 Perspectives and Applications, 2018: p. 185-228.
- 2581 138. Kabiri, K. and M.M. ZOHOURIAN, *Superabsorbent hydrogels from concentrated solution*
2582 *terpolymerization*. 2004.
- 2583 139. Chen, J. and Y. Zhao, *Relationship between water absorbency and reaction conditions in*
2584 *aqueous solution polymerization of polyacrylate superabsorbents*. Journal of Applied
2585 Polymer Science, 2000. **75**(6): p. 808-814.
- 2586 140. Madduma-Bandarage, U.S. and S.V. Madihally, *Synthetic hydrogels: Synthesis, novel*
2587 *trends, and applications*. Journal of Applied Polymer Science, 2021. **138**(19): p. 50376.
- 2588 141. Kiatkamjornwong, S., *Superabsorbent polymers and superabsorbent polymer composites*.
2589 ScienceAsia, 2007. **33**(1): p. 39-43.
- 2590 142. Mierke, C.T.J.F.i.C. and D. Biology, *Viscoelasticity, like forces, plays a role in*
2591 *mechanotransduction*. 2022. **10**: p. 789841.
- 2592 143. Gharat, J.S., Y.V.J.A.J.o.P. Dalvi, and Technology, *Compressive review on hydrogel*.
2593 2018. **8**(3): p. 172-181.
- 2594 144. Debie, S., et al., *A model-based protocol to quantify scission-crosslinking competition and*
2595 *gelation from molecular to material level for grafting-based reactive extrusion of poly*
2596 *(lactic acid)*. 2025. **507**: p. 160744.
- 2597 145. Demeter, M., A. Scărișoreanu, and I. Călina, *State of the art of hydrogel wound dressings*
2598 *developed by ionizing radiation*. Gels, 2023. **9**(1): p. 55.



- 2599 146. Sinha, S., *Biodegradable superabsorbents: methods of preparation and application—a*
2600 *review*. *Fundamental biomaterials: polymers*, 2018: p. 307-322.
- 2601 147. Liu, H., et al., *Carbon-based nanomaterials for bone and cartilage regeneration: a review*.
2602 2021. **7**(10): p. 4718-4735.
- 2603 148. Bratovcic, A., *Nanocomposite hydrogels reinforced by carbon nanotubes*. *Int. J. Eng. Res.*
2604 *Appl*, 2020. **10**(5): p. 30-41.
- 2605 149. Ye, D., C. Chang, and L. Zhang, *High-strength and tough cellulose hydrogels chemically*
2606 *dual cross-linked by using low-and high-molecular-weight cross-linkers*.
2607 *Biomacromolecules*, 2019. **20**(5): p. 1989-1995.
- 2608 150. Gubaidullin, A.T., et al., *Modulation of molecular structure and mechanical properties of*
2609 *κ -carrageenan-gelatin hydrogel with multi-walled carbon nanotubes*. *Polymers*, 2022.
2610 **14**(12): p. 2346.
- 2611 151. Nanda, J., et al., *Formation of hybrid hydrogels consisting of tripeptide and different silver*
2612 *nanoparticle-capped ligands: modulation of the mechanical strength of gel phase*
2613 *materials*. *The Journal of Physical Chemistry B*, 2012. **116**(40): p. 12235-12244.
- 2614 152. Lin, F., et al., *A bioinspired hydrogen bond crosslink strategy toward toughening*
2615 *ultrastrong and multifunctional nanocomposite hydrogels*. *Journal of Materials Chemistry*
2616 *B*, 2020. **8**(18): p. 4002-4015.
- 2617 153. Lin, X., et al., *Stimuli-responsive toughening of hydrogels*. *Chemistry of Materials*, 2021.
2618 **33**(19): p. 7633-7656.
- 2619 154. Gebeyehu, E.K., et al., *Cellulosic-based conductive hydrogels for electro-active tissues: A*
2620 *review summary*. *Gels*, 2022. **8**(3): p. 140.
- 2621 155. Guillet, J.-F., et al., *Electrical properties of double-wall carbon nanotubes nanocomposite*
2622 *hydrogels*. *Carbon*, 2019. **146**: p. 542-548.
- 2623 156. Pournemati, B., et al., *Injectable conductive nanocomposite hydrogels for cardiac tissue*
2624 *engineering: Focusing on carbon and metal-based nanostructures*. *European Polymer*
2625 *Journal*, 2022. **174**: p. 111336.
- 2626 157. Khandaker, T., et al., *Recent progress in gel catalysts: boosting efficiency for sustainable*
2627 *energy applications*. *Catalysis Science & Technology*, 2025.
- 2628 158. Tonu, N.T., et al., *Fabrication of waste biomass-derived KOH activated carbon for*
2629 *enhanced CO₂ capture*. *New Journal of Chemistry*, 2024. **48**(48): p. 20212-20224.
- 2630 159. Ruan, S., et al., *Innovative approaches of porous carbon materials derived from energy*
2631 *waste and their electrochemical properties*. *Energy Materials*, 2025. **5**(7): p. N/A-N/A.
- 2632 160. Wang, J., et al., *Electrochemical energy storage performance of 2D nanoarchitected*
2633 *hybrid materials*. *Nature communications*, 2021. **12**(1): p. 3563.
- 2634 161. Zhou, Q. and H. Yao, *Recent development of carbon electrode materials for*
2635 *electrochemical supercapacitors*. *Energy Reports*, 2022. **8**: p. 656-661.
- 2636 162. Kumar, N., et al., *Recent advancements in zero-to three-dimensional carbon networks with*
2637 *a two-dimensional electrode material for high-performance supercapacitors*. 2023. **5**(12):
2638 p. 3146-3176.
- 2639 163. Dong, W., et al., *Materials design and preparation for high energy density and high power*
2640 *density electrochemical supercapacitors*. 2023. **152**: p. 100713.
- 2641 164. Wu, X.-L. and A.-W. Xu, *Carbonaceous hydrogels and aerogels for supercapacitors*.
2642 *Journal of Materials Chemistry A*, 2014. **2**(14): p. 4852-4864.
- 2643 165. Muzaffar, A., et al., *Green supercapacitors: Latest developments and perspectives in the*
2644 *pursuit of sustainability*. 2024. **195**: p. 114324.



- 2645 166. Choudhury, N.A., S. Sampath, and A. Shukla, *Gelatin hydrogel electrolytes and their*
2646 *application to electrochemical supercapacitors*. Journal of The Electrochemical Society,
2647 2007. **155**(1): p. A74.
- 2648 167. Yamazaki, S., et al., *An acidic cellulose–chitin hybrid gel as novel electrolyte for an*
2649 *electric double layer capacitor*. Electrochemistry Communications, 2009. **11**(1): p. 68-70.
- 2650 168. Zhu, Y., et al., *Carbon-based supercapacitors produced by activation of graphene*. science,
2651 2011. **332**(6037): p. 1537-1541.
- 2652 169. Tien, H.N., et al., *Synthesis of a highly conductive and large surface area graphene oxide*
2653 *hydrogel and its use in a supercapacitor*. Journal of Materials Chemistry A, 2013. **1**(2): p.
2654 208-211.
- 2655 170. Liao, G., et al., *Preparation, properties, and applications of graphene-based hydrogels*.
2656 Frontiers in chemistry, 2018. **6**: p. 450.
- 2657 171. Xu, Y., et al., *Self-assembled graphene hydrogel via a one-step hydrothermal process*.
2658 ACS nano, 2010. **4**(7): p. 4324-4330.
- 2659 172. Gao, H., et al., *High-performance asymmetric supercapacitor based on graphene hydrogel*
2660 *and nanostructured MnO₂*. ACS applied materials & interfaces, 2012. **4**(5): p. 2801-2810.
- 2661 173. Tang, X.-N., et al., *Graphene aerogel derived by purification-free graphite oxide for high*
2662 *performance supercapacitor electrodes*. Carbon, 2019. **146**: p. 147-154.
- 2663 174. Yang, X., et al., *Liquid-mediated dense integration of graphene materials for compact*
2664 *capacitive energy storage*. science, 2013. **341**(6145): p. 534-537.
- 2665 175. Bigdeloo, M., et al., *Recent advances in utilizing graphene-based materials for flexible*
2666 *supercapacitor electrodes*. 2024. **80**: p. 110242.
- 2667 176. Zhang, Y., et al., *High-performance supercapacitors based on compact graphene*
2668 *composite hydrogels*. Electrochimica Acta, 2024. **476**: p. 143699.
- 2669 177. Xu, Y., et al., *Functionalized graphene hydrogel-based high-performance*
2670 *supercapacitors*. Advanced Materials (Deerfield Beach, Fla.), 2013. **25**(40): p. 5779-5784.
- 2671 178. Xu, Y., et al., *One-step strategy to graphene/Ni (OH)₂ composite hydrogels as advanced*
2672 *three-dimensional supercapacitor electrode materials*. Nano research, 2013. **6**: p. 65-76.
- 2673 179. Chen, J., et al., *Graphene hydrogels deposited in nickel foams for high-rate*
2674 *electrochemical capacitors*. Advanced Materials (Deerfield Beach, Fla.), 2012. **24**(33): p.
2675 4569-4573.
- 2676 180. Alhwaige, A.A., et al., *Biobased chitosan hybrid aerogels with superior adsorption: Role*
2677 *of graphene oxide in CO₂ capture*. Rsc Advances, 2013. **3**(36): p. 16011-16020.
- 2678 181. Wang, Y., et al., *Preventing graphene sheets from restacking for high-capacitance*
2679 *performance*. The Journal of Physical Chemistry C, 2011. **115**(46): p. 23192-23197.
- 2680 182. Yuan, J., et al., *Graphene-based 3D composite hydrogel by anchoring Co₃O₄*
2681 *nanoparticles with enhanced electrochemical properties*. Physical Chemistry Chemical
2682 Physics, 2013. **15**(31): p. 12940-12945.
- 2683 183. Guo, H.-L., et al., *Synthesis and characterization of nitrogen-doped graphene hydrogels*
2684 *by hydrothermal route with urea as reducing-doping agents*. Journal of Materials
2685 Chemistry A, 2013. **1**(6): p. 2248-2255.
- 2686 184. Chang, Y., et al., *Larger-scale fabrication of N-doped graphene-fiber mats used in high-*
2687 *performance energy storage*. Journal of Power Sources, 2014. **252**: p. 113-121.
- 2688 185. Chen, P., et al., *Hydrothermal synthesis of macroscopic nitrogen-doped graphene*
2689 *hydrogels for ultrafast supercapacitor*. Nano Energy, 2013. **2**(2): p. 249-256.



- 2690 186. Zhang, L. and G. Shi, *Preparation of highly conductive graphene hydrogels for fabricating*
2691 *supercapacitors with high rate capability*. The Journal of Physical Chemistry C, 2011.
2692 **115**(34): p. 17206-17212.
- 2693 187. Sheng, K.-x., et al., *High-performance self-assembled graphene hydrogels prepared by*
2694 *chemical reduction of graphene oxide*. New Carbon Materials, 2011. **26**(1): p. 9-15.
- 2695 188. Zhao, Y., et al., *Highly compression-tolerant supercapacitor based on polypyrrole-*
2696 *mediated graphene foam electrodes*. Advanced Materials (Deerfield Beach, Fla.), 2012.
2697 **25**(4): p. 591-595.
- 2698 189. Tai, Z., X. Yan, and Q. Xue, *Three-dimensional graphene/polyaniline composite hydrogel*
2699 *as supercapacitor electrode*. Journal of the Electrochemical Society, 2012. **159**(10): p.
2700 A1702.
- 2701 190. Zhou, H., et al., *Graphene/poly (3, 4-ethylenedioxythiophene) hydrogel with excellent*
2702 *mechanical performance and high conductivity*. Carbon, 2013. **59**: p. 495-502.
- 2703 191. Xu, Y., et al., *Flexible solid-state supercapacitors based on three-dimensional graphene*
2704 *hydrogel films*. ACS nano, 2013. **7**(5): p. 4042-4049.
- 2705 192. Chen, M., et al., *A one-step method for reduction and self-assembling of graphene oxide*
2706 *into reduced graphene oxide aerogels*. Journal of Materials Chemistry A, 2013. **1**(8): p.
2707 2869-2877.
- 2708 193. Karthick, R. and F. Chen, *Free-standing graphene paper for energy application: Progress*
2709 *and future scenarios*. Carbon, 2019. **150**: p. 292-310.
- 2710 194. Si, W., et al., *Reduced graphene oxide aerogel with high-rate supercapacitive performance*
2711 *in aqueous electrolytes*. Nanoscale Research Letters, 2013. **8**: p. 1-8.
- 2712 195. Zhang, P., et al., *Reduced graphene oxide composite aerogel prepared by europium-*
2713 *assisting radiation reduction as a broad-spectrum adsorbent for organic pollutants*.
2714 Journal of Materials Chemistry A, 2023. **11**(6): p. 2804-2813.
- 2715 196. Liu, F., et al., *Folded structured graphene paper for high performance electrode materials*.
2716 Advanced Materials (Deerfield Beach, Fla.), 2012. **24**(8): p. 1089-1094.
- 2717 197. Wu, Z.-S., et al., *Three-dimensional nitrogen and boron co-doped graphene for high-*
2718 *performance all-solid-state supercapacitors*. Advanced materials, 2012. **24**(37).
- 2719 198. Ji, C.-C., et al., *Self-assembly of three-dimensional interconnected graphene-based*
2720 *aerogels and its application in supercapacitors*. Journal of colloid and interface science,
2721 2013. **407**: p. 416-424.
- 2722 199. Wu, Z.-S., et al., *Three-dimensional graphene-based macro-and mesoporous frameworks*
2723 *for high-performance electrochemical capacitive energy storage*. Journal of the American
2724 Chemical Society, 2012. **134**(48): p. 19532-19535.
- 2725 200. Meng, F., et al., *Alkali-treated graphene oxide as a solid base catalyst: synthesis and*
2726 *electrochemical capacitance of graphene/carbon composite aerogels*. Journal of Materials
2727 Chemistry, 2011. **21**(46): p. 18537-18539.
- 2728 201. Zhang, X., et al., *Mechanically strong and highly conductive graphene aerogel and its use*
2729 *as electrodes for electrochemical power sources*. journal of materials chemistry, 2011.
2730 **21**(18): p. 6494-6497.
- 2731 202. Shabangoli, Y., et al., *Thionine functionalized 3D graphene aerogel: combining simplicity*
2732 *and efficiency in fabrication of a metal-free redox supercapacitor*. Advanced Energy
2733 Materials, 2018. **8**(34): p. 1802869.



- 2734 203. Sun, W., et al., *A facile strategy for fabricating hierarchical nanocomposites of V₂O₅*
2735 *nanowire arrays on a three-dimensional N-doped graphene aerogel with a synergistic*
2736 *effect for supercapacitors*. Journal of Materials Chemistry A, 2018. **6**(21): p. 9938-9947.
- 2737 204. Chen, H., et al., *Free-standing N-self-doped carbon nanofiber aerogels for high-*
2738 *performance all-solid-state supercapacitors*. Nano Energy, 2019. **63**: p. 103836.
- 2739 205. Lee, J.-H. and S.-J. Park, *Recent advances in preparations and applications of carbon*
2740 *aerogels: A review*. Carbon, 2020. **163**: p. 1-18.
- 2741 206. Liu, B.-W., et al., *Multifunctional protective aerogel with superelasticity over– 196 to 500°*
2742 *C*. Nano Research, 2022. **15**(9): p. 7797-7805.
- 2743 207. Chhetri, K., et al., *A review on nanofiber reinforced aerogels for energy storage and*
2744 *conversion applications*. Journal of Energy Storage, 2022. **46**: p. 103927.
- 2745 208. Zou, J., et al., *Ultralight multiwalled carbon nanotube aerogel*. ACS nano, 2010. **4**(12): p.
2746 7293-7302.
- 2747 209. Qi, H., E. Mäder, and J. Liu, *Electrically conductive aerogels composed of cellulose and*
2748 *carbon nanotubes*. Journal of Materials Chemistry A, 2013. **1**(34): p. 9714-9720.
- 2749 210. Ma, C.B., B. Du, and E. Wang, *Self-crosslink method for a straightforward synthesis of*
2750 *poly (vinyl alcohol)-based aerogel assisted by carbon nanotube*. Advanced Functional
2751 Materials, 2017. **27**(10): p. 1604423.
- 2752 211. Huang, Z., et al., *Large-scale preparation of electrically conducting cellulose*
2753 *nanofiber/carbon nanotube aerogels: Ambient-dried, recyclable, and 3D-Printable*.
2754 Carbon, 2022. **194**: p. 23-33.
- 2755 212. Niu, C., et al., *High power electrochemical capacitors based on carbon nanotube*
2756 *electrodes*. Applied physics letters, 1997. **70**(11): p. 1480-1482.
- 2757 213. Li, P., et al., *Highly deformation-tolerant carbon nanotube sponges as supercapacitor*
2758 *electrodes*. Nanoscale, 2013. **5**(18): p. 8472-8479.
- 2759 214. Zhong, J., et al., *Carbon nanotube sponges as conductive networks for supercapacitor*
2760 *devices*. Nano Energy, 2013. **2**(5): p. 1025-1030.
- 2761 215. Yang, C., et al., *Bamboo-like N/S-codoped carbon nanotube aerogels for high-power and*
2762 *high-energy supercapacitors*. Journal of Alloys and Compounds, 2021. **861**: p. 157946.
- 2763 216. Bordjiba, T. and M. Mohamedi, *Molding versus dispersion: effect of the preparation*
2764 *procedure on the capacitive and cycle life of carbon nanotubes aerogel composites*. Journal
2765 of Solid State Electrochemistry, 2011. **15**: p. 765-771.
- 2766 217. Tao, T., et al., *Functional mesoporous carbon-coated CNT network for high-performance*
2767 *supercapacitors*. New Journal of Chemistry, 2013. **37**(5): p. 1294-1297.
- 2768 218. Gao, K., et al., *Cellulose nanofibers/multi-walled carbon nanotube nanohybrid aerogel for*
2769 *all-solid-state flexible supercapacitors*. RSC advances, 2013. **3**(35): p. 15058-15064.
- 2770 219. Bordjiba, T., M. Mohamedi, and L.H. Dao, *New class of carbon-nanotube aerogel*
2771 *electrodes for electrochemical power sources*. Advanced materials, 2008. **20**(4): p. 815-
2772 819.
- 2773 220. Zhou, K., et al., *Fluorination effect for stabilizing cationic and anionic redox activities in*
2774 *cation-disordered cathode materials*. Energy Storage Materials, 2020. **32**: p. 234-243.
- 2775 221. Alam, M.S., et al., *Advancements in MAX phase materials: structure, properties, and novel*
2776 *applications*. RSC advances, 2024. **14**(37): p. 26995-27041.
- 2777 222. Alam, M.S., et al., *Self-generated B-MAX phase composites: The effect of sintering*
2778 *temperature on surface morphology and phase composition*. Materials Letters, 2025. **378**:
2779 p. 137568.



- 2780 223. Alam, M.S., et al., *Tailoring the thermal and thermomechanical characteristics of novel*
2781 *MAX phase boron composites in high-temperature applications*. *Nanoscale Advances*,
2782 2025. **7**(10): p. 3077-3087.
- 2783 224. Mangiri, R., et al., *Surface engineering of M5X4 MXenes for next-gen energy solutions*.
2784 *Materials Today Chemistry*, 2025. **48**: p. 102864.
- 2785 225. Khan, R., et al., *Transition metal dichalcogenides for next-generation supercapacitors:*
2786 *recent advances, challenges, and future perspectives*. *Journal of Alloys and Compounds*,
2787 2025: p. 182874.
- 2788 226. Ramachandran, T., et al., *Black Phosphorus as a Multifunctional Electrode Material for*
2789 *all Energy Storage Devices*. *Journal of Alloys and Compounds*, 2025: p. 182500.
- 2790 227. Kumar, Y.A., et al., *The landscape of energy storage: Insights into carbon electrode*
2791 *materials and future directions*. *Journal of Energy Storage*, 2024. **86**: p. 111119.
- 2792 228. Anil Kumar, Y., et al., *Carbon materials as a conductive skeleton for supercapacitor*
2793 *electrode applications: a review*. *Nanomaterials*, 2023. **13**(6): p. 1049.
- 2794 229. Souza, L., et al., *Lignin-incorporated bacterial nanocellulose for proton exchange*
2795 *membranes in microbial fuel cells*. *Materials Chemistry and Physics*, 2023. **293**: p. 126963.
- 2796 230. Narimani-Qurtlar, A., et al., *Investigating the environmental impacts of lithium-oxygen*
2797 *battery cathode production: A comprehensive assessment of the effects associated with*
2798 *oxygen cathode manufacturing*. 2024. **482**: p. 144199.
- 2799 231. Du, H., et al., *Carbon aerogel supported Pt–Ru catalysts for using as the anode of direct*
2800 *methanol fuel cells*. 2007. **45**(2): p. 429-435.
- 2801 232. Zhan, F., et al., *Recent advances on support materials for enhanced Pt-based catalysts:*
2802 *applications in oxygen reduction reactions for electrochemical energy storage*. 2025: p. 1-
2803 25.
- 2804 233. Kakaei, K. and M.J.R.E. Rahnavardi, *Synthesis of nitrogen-doped reduced graphene oxide*
2805 *and its decoration with high efficiency palladium nanoparticles for direct ethanol fuel cell*.
2806 2021. **163**: p. 1277-1286.
- 2807 234. Cai, B., et al., *Multimetallic hierarchical aerogels: shape engineering of the building*
2808 *blocks for efficient electrocatalysis*. *Advanced Materials*, 2017. **29**(11): p. 1605254.
- 2809 235. Liu, W., et al., *High-performance electrocatalysis on palladium aerogels*. *Angewandte*
2810 *Chemie International Edition*, 2012. **51**(23): p. 5743-5747.
- 2811 236. Wang, K., et al., *Surface-tailored PtPdCu ultrathin nanowires as advanced*
2812 *electrocatalysts for ethanol oxidation and oxygen reduction reaction in direct ethanol fuel*
2813 *cell*. *Journal of Energy Chemistry*, 2021. **52**: p. 251-261.
- 2814 237. Chao, L., et al., *Robust three dimensional N-doped graphene supported Pd nanocomposite*
2815 *as efficient electrocatalyst for methanol oxidation in alkaline medium*. *international journal*
2816 *of hydrogen energy*, 2017. **42**(22): p. 15107-15114.
- 2817 238. Wang, X., C. Li, and G. Shi, *A high-performance platinum electrocatalyst loaded on a*
2818 *graphene hydrogel for high-rate methanol oxidation*. *Physical Chemistry Chemical*
2819 *Physics*, 2014. **16**(21): p. 10142-10148.
- 2820 239. Tan, Y., et al., *Porous nanocomposites by cotton-derived carbon/NiO with high*
2821 *performance for lithium-ion storage*. *Journal of Alloys and Compounds*, 2021. **874**: p.
2822 159788.
- 2823 240. Feidenhans'l, A.A., et al., *Precious metal free hydrogen evolution catalyst design and*
2824 *application*. *Chemical Reviews*, 2024. **124**(9): p. 5617-5667.



241. Kumari, R., et al., *Emerging 3D nanomaterials as electrocatalysts for water splitting reactions*. International Journal of Hydrogen Energy, 2024. **74**: p. 214-231.
242. Zhao, L., et al., *1 T-rich MoS₂/nitrogen-doped graphene composites: Advanced anode materials to improve the performance of lithium-ion batteries*. 2024. **102**: p. 113970.
243. Wang, R., et al., *"Fast-charging" anode materials for lithium-ion batteries from perspective of ion diffusion in crystal structure*. 2024. **18**(4): p. 2611-2648.
244. Wu, H., et al., *Stable Li-ion battery anodes by in-situ polymerization of conducting hydrogel to conformally coat silicon nanoparticles*. Nature communications, 2013. **4**(1): p. 1943.
245. Bai, X., et al., *Si@ SiO_x/graphene hydrogel composite anode for lithium-ion battery*. Journal of Power Sources, 2016. **306**: p. 42-48.
246. Fang, S., D. Bresser, and S.J.T.M.O.f.E.E.S. Passerini, *Transition metal oxide anodes for electrochemical energy storage in lithium-and sodium-ion batteries*. 2022: p. 55-99.
247. Shi, H., et al., *Double-network nanostructured hydrogel-derived ultrafine Sn-Fe alloy in three-dimensional carbon framework for enhanced lithium storage*. Nano letters, 2018. **18**(5): p. 3193-3198.
248. Lingappan, N. and D.J. Kang, *Molybdenum disulfide nanosheets interconnected nitrogen-doped reduced graphene oxide hydrogel: a high-performance heterostructure for lithium-ion batteries*. Electrochimica Acta, 2016. **193**: p. 128-136.
249. Bae, J., et al., *Cover Picture: A 3D Nanostructured Hydrogel-Framework-Derived High-Performance Composite Polymer Lithium-Ion Electrolyte (Angew. Chem. Int. Ed. 8/2018)*. Angewandte Chemie International Edition, 2018. **57**(8): p. 2007-2007.
250. Coustier, F., S. Passerini, and W. Smyrl, *A 400 mAh/g Aerogel-like V₂O₅ Cathode for Rechargeable Lithium Batteries*. Journal of the Electrochemical Society, 1998. **145**(5): p. L73.
251. Chang, Y., et al., *Synthesis of 3D nitrogen-doped graphene/Fe₃O₄ by a metal ion induced self-assembly process for high-performance Li-ion batteries*. Journal of Materials Chemistry A, 2013. **1**(46): p. 14658-14665.
252. Chen, Z., et al., *A three-dimensionally interconnected carbon nanotube-conducting polymer hydrogel network for high-performance flexible battery electrodes*. Advanced energy materials, 2014. **4**(12): p. 1400207.
253. Qiu, B., M. Xing, and J. Zhang, *Mesoporous TiO₂ nanocrystals grown in situ on graphene aerogels for high photocatalysis and lithium-ion batteries*. Journal of the American Chemical Society, 2014. **136**(16): p. 5852-5855.
254. Zhang, M., Y. Wang, and M. Jia, *Three-dimensional reduced graphene oxides hydrogel anchored with ultrafine CoO nanoparticles as anode for lithium ion batteries*. Electrochimica acta, 2014. **129**: p. 425-432.
255. Sui, Z.-Y., et al., *Manganese dioxide-anchored three-dimensional nitrogen-doped graphene hybrid aerogels as excellent anode materials for lithium ion batteries*. Journal of Materials Chemistry A, 2015. **3**(19): p. 10403-10412.
256. Wang, Y., et al., *A facile and green method to fabricate graphene-based multifunctional hydrogels for miniature-scale water purification*. RSC advances, 2013. **3**(24): p. 9240-9246.
257. Chen, Y., et al., *Graphene oxide-chitosan composite hydrogels as broad-spectrum adsorbents for water purification*. Journal of Materials Chemistry A, 2013. **1**(6): p. 1992-2001.



- 2871 258. Hristea, G., M. Iordoc, and A. Culcea, *Nanocarbon Type Xerogel Materials Designed for*
2872 *Water Desalination*. Materials, 2021. **14**(17): p. 4932.
- 2873 259. Gao, H., et al., *Mussel-inspired synthesis of polydopamine-functionalized graphene*
2874 *hydrogel as reusable adsorbents for water purification*. ACS applied materials &
2875 interfaces, 2013. **5**(2): p. 425-432.
- 2876 260. Cong, H.-P., et al., *Macroscopic multifunctional graphene-based hydrogels and aerogels*
2877 *by a metal ion induced self-assembly process*. ACS nano, 2012. **6**(3): p. 2693-2703.
- 2878 261. Yilmaz, E. and M. Sezgin, *Enhancement of the activity and enantioselectivity of lipase by*
2879 *sol-gel encapsulation immobilization onto β -cyclodextrin-based polymer*. Applied
2880 biochemistry and biotechnology, 2012. **166**: p. 1927-1940.
- 2881 262. Chen, H., et al., *Cotton derived carbonaceous aerogels for the efficient removal of organic*
2882 *pollutants and heavy metal ions*. Journal of Materials Chemistry A, 2015. **3**(11): p. 6073-
2883 6081.
- 2884 263. Zhang, L., et al., *Carbon material-based aerogels for gas adsorption: fabrication,*
2885 *structure design, functional tailoring, and applications*. 2022. **12**(18): p. 3172.
- 2886 264. Wu, P., Y. Wang, and Y.J.C.E.J. Liu, *Recent advances in heteroatom-doped porous carbon*
2887 *for adsorption of gaseous pollutants*. 2024: p. 152142.
- 2888 265. Wang, W., et al., *2D/3D assemblies of amine-functionalized graphene silica (templated)*
2889 *aerogel for enhanced CO₂ sorption*. ACS Applied Materials & Interfaces, 2019. **11**(33):
2890 p. 30391-30400.
- 2891 266. Kong, Y., et al., *Development of monolithic adsorbent via polymeric sol-gel process for*
2892 *low-concentration CO₂ capture*. Applied Energy, 2015. **147**: p. 308-317.
- 2893 267. Alhwaige, A.A., H. Ishida, and S. Qutubuddin, *Carbon aerogels with excellent CO₂*
2894 *adsorption capacity synthesized from clay-reinforced biobased chitosan-polybenzoxazine*
2895 *nanocomposites*. ACS Sustainable Chemistry & Engineering, 2016. **4**(3): p. 1286-1295.
- 2896 268. Moon, C.-W., et al., *Effect of Activation temperature on CO₂ capture behaviors of*
2897 *resorcinol-based carbon aerogels*. Bulletin of the Korean Chemical Society, 2014. **35**(1):
2898 p. 57-61.
- 2899 269. Li, H., et al., *Ultra-high surface area nitrogen-doped carbon aerogels derived from a*
2900 *schiff-base porous organic polymer aerogel for CO₂ storage and supercapacitors*.
2901 Advanced Functional Materials, 2019. **29**(40): p. 1904785.
- 2902 270. Kong, Y., et al., *Amine hybrid aerogel for high-efficiency CO₂ capture: Effect of amine*
2903 *loading and CO₂ concentration*. Chemical Engineering Journal, 2016. **306**: p. 362-368.
- 2904 271. Kong, Y., et al., *A new aerogel based CO₂ adsorbent developed using a simple sol-gel*
2905 *method along with supercritical drying*. Chemical communications, 2014. **50**(81): p.
2906 12158-12161.
- 2907 272. Liu, K.-K., B. Jin, and L.-Y. Meng, *Glucose/graphene-based aerogels for gas adsorption*
2908 *and electric double layer capacitors*. Polymers, 2018. **11**(1): p. 40.
- 2909 273. Morales-Torres, S., et al., *Design of low-temperature Pt-carbon combustion catalysts for*
2910 *VOC's treatments*. Journal of Hazardous Materials, 2010. **183**(1-3): p. 814-822.
- 2911 274. Fathy, N.A., et al., *Free-and Ni-doped carbon xerogels catalysts for wet peroxide oxidation*
2912 *of methyl orange*. Journal of water process engineering, 2017. **16**: p. 21-27.
- 2913 275. Scherdel, C. and G. Reichenauer, *Microporous and mesoporous carbon xerogel having a*
2914 *characteristic mesopore size and precursors thereof and also a process for producing these*
2915 *and their use*. 2012, Google Patents.



276. Duarte, F., et al., *Fenton-like degradation of azo-dye Orange II catalyzed by transition metals on carbon aerogels*. Applied Catalysis B: Environmental, 2009. **85**(3-4): p. 139-147.
277. Catalao, R., et al., *Reduction of NO with metal-doped carbon aerogels*. Applied Catalysis B: Environmental, 2009. **88**(1-2): p. 135-141.
278. Maldonado-Hodar, F.J., *Advances in the development of nanostructured catalysts based on carbon gels*. Catalysis today, 2013. **218**: p. 43-50.
279. Maldonado-Hódar, F., *Metal-doped carbon aerogels as catalysts for the aromatization of n-hexane*. Applied Catalysis A: General, 2011. **408**(1-2): p. 156-162.
280. Moreno-Castilla, C. and F. Maldonado-Hódar, *Carbon aerogels for catalysis applications: An overview*. Carbon, 2005. **43**(3): p. 455-465.
281. Briz-Amate, T., et al., *Growing Tungsten Nanophases on Carbon Spheres Doped with Nitrogen. Behaviour as Electro-Catalysts for Oxygen Reduction Reaction*. Materials, 2021. **14**(24): p. 7716.
282. Ke, Y.-H., et al., *Heterogeneous catalytic oxidation of glycerol over a UiO-66-derived ZrO₂@C supported Au catalyst at room temperature*. RSC advances, 2023. **13**(39): p. 27054-27065.
283. Moreno-Castilla, C., et al., *Group 6 metal oxide-carbon aerogels. Their synthesis, characterization and catalytic activity in the skeletal isomerization of 1-butene*. Applied Catalysis A: General, 1999. **183**(2): p. 345-356.
284. Maldonado-Hódar, F.J., C. Moreno-Castilla, and J. Rivera-Utrilla, *Synthesis, pore texture and surface acid-base character of TiO₂/carbon composite xerogels and aerogels and their carbonized derivatives*. Applied Catalysis A: General, 2000. **203**(1): p. 151-159.
285. Figueiredo, J.L., *Carbon gels with tuned properties for catalysis and energy storage*. Journal of Sol-Gel Science and Technology, 2019. **89**: p. 12-20.
286. Alegre, C., et al., *Sulfurized carbon xerogels as Pt support with enhanced activity for fuel cell applications*. Applied Catalysis B: Environmental, 2016. **192**: p. 260-267.
287. García-Zaragoza, A., et al., *Boosting the catalytic performance of graphene-supported Pt nanoparticles via decorating with-SnBu_n: an efficient approach for aqueous hydrogenation of biomass-derived compounds*. Nanoscale, 2023. **15**(29): p. 12319-12332.
288. Wang, L., et al., *Spatial location and microenvironment engineering of Pt-CeO₂ nanoreactors for selective hydrogenation of cinnamaldehyde to cinnamyl alcohol*. The Journal of Physical Chemistry C, 2021. **125**(41): p. 22603-22610.
289. Zhang, Q., et al., *Sustainable production of high-value gluconic acid and glucaric acid through oxidation of biomass-derived glucose: A critical review*. Journal of Cleaner Production, 2021. **312**: p. 127745.
290. Samant, P.V., M.F. Pereira, and J.L. Figueiredo, *Mesoporous carbon supported Pt and Pt-Sn catalysts for hydrogenation of cinnamaldehyde*. Catalysis today, 2005. **102**: p. 183-188.
291. Xu, H., et al., *Carbon-based bifunctional electrocatalysts for oxygen reduction and oxygen evolution reactions: Optimization strategies and mechanistic analysis*. 2022. **71**: p. 234-265.
292. Rocha, R.P., M.F. Pereira, and J.L. Figueiredo, *Carbon as a catalyst: Esterification of acetic acid with ethanol*. Catalysis Today, 2013. **218**: p. 51-56.
293. Rocha, R., et al., *Nitrogen-doped carbon xerogels as catalysts for advanced oxidation processes*. Catalysis Today, 2015. **241**: p. 73-79.



- 2961 294. Pelech, I., et al., *Oxidative dehydrogenation of isobutane on carbon xerogel catalysts*. Catalysis Today, 2015. **249**: p. 176-183.
- 2962
- 2963 295. Vinchhi, P., S.U. Rawal, and M.M. Patel, *External stimuli-responsive drug delivery systems*, in *Drug Delivery Devices and Therapeutic Systems*. 2021, Elsevier. p. 267-288.
- 2964
- 2965 296. Chen, H., D. Liu, and Z. Guo, *Endogenous stimuli-responsive nanocarriers for drug delivery*. Chemistry Letters, 2016. **45**(3): p. 242-249.
- 2966
- 2967 297. Majumdar, S., et al., *Carbon-dot-coated alginate beads as a smart stimuli-responsive drug delivery system*. ACS applied materials & interfaces, 2016. **8**(50): p. 34179-34184.
- 2968
- 2969 298. Bardajee, G.R., et al., *Synthesis of a novel thermo/pH sensitive nanogel based on salep modified graphene oxide for drug release*. Materials Science and Engineering: C, 2017. **72**: p. 558-565.
- 2970
- 2971
- 2972 299. Kim, H.-J., et al., *Diamond nanogel-embedded contact lenses mediate lysozyme-dependent therapeutic release*. ACS nano, 2014. **8**(3): p. 2998-3005.
- 2973
- 2974 300. Zhang, K., *Lysozyme-triggered nanodiamond contact lens for glaucoma treatment & phenotypically-based combinatorial drug optimization for multiple myeloma treatment*. 2015, UCLA.
- 2975
- 2976
- 2977 301. Molina, M., et al., *Stimuli-responsive nanogel composites and their application in nanomedicine*. Chemical Society Reviews, 2015. **44**(17): p. 6161-6186.
- 2978
- 2979 302. Mazidi, Z., et al., *Smart stimuli-responsive implantable drug delivery systems for programmed and on-demand cancer treatment: An overview on the emerging materials*. Chemical Engineering Journal, 2022. **433**: p. 134569.
- 2980
- 2981
- 2982 303. Shi, Y., et al., *The potential of drug delivery nanosystems for sepsis treatment*. Journal of Inflammation Research, 2021: p. 7065-7077.
- 2983
- 2984 304. Lu, N., et al., *Tunable dual-stimuli response of a microgel composite consisting of reduced graphene oxide nanoparticles and poly (N-isopropylacrylamide) hydrogel microspheres*. Journal of Materials Chemistry B, 2014. **2**(24): p. 3791-3798.
- 2985
- 2986
- 2987 305. Spizzirri, U.G., et al., *Spherical gelatin/CNTs hybrid microgels as electro-responsive drug delivery systems*. International journal of pharmaceutics, 2013. **448**(1): p. 115-122.
- 2988
- 2989 306. Hatakeyama, H., *Recent advances in endogenous and exogenous stimuli-responsive nanocarriers for drug delivery and therapeutics*. Chemical and Pharmaceutical Bulletin, 2017. **65**(7): p. 612-617.
- 2990
- 2991
- 2992 307. Xu, X., et al., *Formation of graphene oxide-hybridized nanogels for combinative anticancer therapy*. Nanomedicine: Nanotechnology, Biology and Medicine, 2018. **14**(7): p. 2387-2395.
- 2993
- 2994
- 2995 308. Fiorica, C., et al., *Double-network-structured graphene oxide-containing nanogels as photothermal agents for the treatment of colorectal cancer*. Biomacromolecules, 2017. **18**(3): p. 1010-1018.
- 2996
- 2997
- 2998 309. Qin, Y., et al., *Near-infrared light remote-controlled intracellular anti-cancer drug delivery using thermo/pH sensitive nanovehicle*. Acta biomaterialia, 2015. **17**: p. 201-209.
- 2999

3000



Data Availability Statement: The data supporting the findings of this study can be obtained from the corresponding author upon request. Due to privacy concerns and other restrictions, the data are not publicly accessible.

